Quantum Hall Wave Functions on the Torus

Mikael Fremling

Doctoral Thesis

Akademisk avhandling
för avläggande av doktorsexamen i teoretisk fysik
vid Stockholms Universitet

Stockholm
University

Department of Physics

Huvudhandledare
Thors Hans Hasson
Stockholms Universitet
Fysikum

Bihandledare
Anders Karlhede
Stockholms Universitet
Fysikum

ISBN 978-91-7649-158-4

Tryck: Holmbergs, Malmö 2015

Omslagsbild: *Fundamentala SL(2,Z) domäner*, Mikael Fremling
Porträttbild: Narit Pidokrajt
Distributör: Department of Physics, Fysikum

Abstract

The fractional quantum Hall effect (FQHE), now entering its fourth decade, continues to draw attention from the condensed matter community. New experiments in recent years are raising hopes that it will be possible to observe quasi-particles with non-abelian anyonic statistics. These particles could form the building blocks of a quantum computer.

The quantum Hall states have topologically protected energy gaps to the low-lying set of excitations. This topological order is not a locally measurable quantity but rather a non-local object, and it is one of the keys to its stability. From an early stage understanding of the FQHE has been facilitate by constructing trial wave functions. The topological classification of these wave functions have given further insight to the nature of the FQHE.

An early, and successful, wave function construction for filling fractions $\nu = \frac{p}{2p+1}$ was that of composite fermions on planar and spherical geometries. Recently, new developments using conformal field theory have made it possible to also construct the full Haldane-Halperin hierarchy wave functions on planar and spherical geometries. In this thesis we extend this construction to a toroidal geometry, *i.e.* a flat surface with periodic boundary conditions.

One of the defining features of topological states of matter in two dimensions is that the ground state is not unique on surfaces with non trivial topology, such as a torus. The archetypical example is the fractional quantum Hall effect. Here, a quantum Hall fluid at filling fraction $\nu = \frac{p}{q}$, has at least a q-fold degeneracy on a torus. This has been shown in a few cases, such as the Laughlin states and the Moore-Read states, by explicit construction of candidate electron wave functions. In this thesis, we construct explicit torus wave functions for a large class of experimentally important quantum liquids, namely the chiral hierarchy states in the lowest Landau level. These states, which includes the prominently observed positive Jain sequence at filling fractions $\nu = \frac{p}{2p+1}$, are characterized by having boundary modes with only one chirality.

Our construction relies heavily on previous work that expressed the hierarchy wave functions on a plane or a sphere in terms of correlation functions in a conformal field theory. This construction can be adapted to the torus when care is taken to ensure correct behaviour under the modular transformations that leave the geometry of the torus unchanged. Our construction solves the long standing problem of engineering torus wave functions for multi-component many-body states. Since the resulting expressions are rather complicated, we have carefully compared the simplest example, that of $\nu = \frac{2}{5}$, with numerically found wave functions. We have found an extremely good overlap for arbitrary values of the modular parameter τ,

that describes the geometry of the torus.

Having explicit torus wave functions allows us to use the methods developed by Read and Read & Rezayi to numerically compute the quantum Hall viscosity. Hall viscosity is conjectured to be a topologically protected macroscopic transport coefficient characterizing the quantum Hall state. It is related to the shift of the same QH-fluid when it is put on a sphere. The good agreement with the theoretical prediction for the $\frac{2}{5}$ state strongly suggests that our wave functions encodes all relevant topological information.

We also consider the Hall viscosity in the limit of a very thin torus. There we find that the viscosity changes as we approach the thin torus limit. Because of this we study the Laughlin state in that limit and see how the change in viscosity arises from a change in the Hamiltonian hopping elements. Finally we conclude that there are both qualitative and quantitative difference between the thin and the square torus. Thus, one has to be careful when interpreting results in the thin torus limit.

Sammanfattning på svenska

Kvanthalleffekten har nu varit känd i över trettio år, och ligger fortfarande i blickfånget för många forskare som arbetar med kondenserad materia (dvs fasta material). Skälen för detta är flera. Till att börja med är kvanthalleffekten det första exemplet på så kallade topologiska isolatorer. En topologisk isolator är ett medium som är isolerande i sitt innandöme (dvs den leder inte ström), men som ändå leder strömmar på utsidan. Det som gör dessa strömmar speciella är att de är ytterst stabila och inte alls är känsliga för orenheter, temperaturvariationer, den exakta geometrin hos materialet och många andra faktorer som skulle kunna spela roll. I fallet med kvanthalleffekten är strömmarna på utsidan så stabila att de kan mätas med en noggrannhet på tolv decimaler. Denna noggrannhet motsvarar att mäta avståndet från Treriksröset till Smygehuk med en noggrannhet på en tusendels millimeter. Detta är med andra ord ett av de mest exakta experimentella mätningar vi kan utföra idag.

En annan anledning till att kvanthalleffekten är intressant att den sker i material som i all väsentlighet är tvådimensionella. Med tvådimensionell menar vi här verkligen att elektronerna i systemet endast kan röra sig i två dimensioner. De är fångade på en yta och han inte förflytta sig höjdled. Detta sker t.ex. i det nya supermaterialet grafen, vilket är ett enda lager av kolatomer, men även i ytskiktet mellan halvledare av gallium-arsenid samt aluminium-arsenid. Denna tvådimensionalitet gör att de excitationer som har lägst energi inte nödvändigtvis måste ha en fermionisk eller bosonisk natur. Fermioner och bosoner utgör det två typerna a fundamentala partiklar som bygger upp vår värld. Elektroner och kvarkar är fermioner medan t.ex. ljus är bosoner. Men ibland, och endast i tvådimensionella system, kan det uppstå partiklar som utgör ett mellanting mellan fermioner och bosoner. Vi kallar dessa exotiska partiklar anyoner – i lös översättning vad-som-helst-ioner – och vi är mycket hoppfulla att dessa inom en snar eller avlägsen framtid kommer kunna utgöra basen för en ny typ av dator som använder kvantmekaniska lagar för att utföra sina beräkningar. En sådan kvantdator skulle effektivt kunna lösa vissa numeriska problem som är mycket svåra att attackera med våra vanliga (klassiska) datorer.

Men innan vi når fram till en fungerande kvantdator har vi många steg på vägen som vi måste först förstå och sedan bemästra. Det är till detta ändamål som denna avhandling lämnar sitt bidrag. I denna avhandling studerar vi olika aspekter av såväl anyoner som de kvantmekaniska grundtillstånden. Vi utför våra studier uteslutande på geometrin för en torus. En torus är en platt yta med periodiska randvillkor i två riktningar, det vill säga en ring, en munk eller en livboj. Vi väljer att studera just en torus då denna inte har någon rand (eller kant). Avsaknaden

av en kant gör att vi inte behöver bekymra oss om de strömmar som skulle har varit närvarande vid en kant. Detta i sin tur gör att det är enklare att studera vad som sker i innandömet.

Vår torus har två axlar L_x och L_y som tillsammans spänner upp en area $A = L_x L_y$. När vi studerar torusen är dess area fixerad av hur många partiklar vi placerar på den, men vi är fria att välja kvoten $\tau_2 = \frac{L_y}{L_x}$ som vi vill. Olika kvoter ger olika geometrier för vår torus. I samtliga undersökningar vi har genomfört – läs publicerade artiklar – har vi varit intresserade av hur förändringar i torusens geometri påverkar hur grundtillståndet ser ut, men också hur spektrat av excitationer ovanför grundtillståndet förändras. Vi har varit speciellt intresserade av vad som händer när vi ändrar geometrin från en kvadratisk $\tau_2 = 1$ torus till en mycket asymmetrisk (tunn) torus $\tau_2 \to 0$.

Vi finner i våra studier att flera kvantiteter överlever övergången till en tunn torus, men inte alla. T.ex. krävs det för samtliga geometrier en ändlig mängd energi för att skapa excitationer. Även laddningen på dessa excitationer är bevarad genom hela geometriförändringen.

Bland de kvantiteter som förändras är (ibland) strukturen på excitationerna samt även grundtillståndets hallviskositet. Hallviskositet är en variant av viskositet som skiler sig från den vanliga viskositeten vi normalt stöter på då den inte är dissipativ. Den dissipativa viskositeten gör att en vätska som rörs om till slut stannar upp av sin egen inre friktion. Hallviscociteten gör inte att vätskan stannar upp utan är snarare ett mått på hur virvlar i vätskan fortplantar sig. I de flesta vätskor är hallviskositeten noll men just i två dimensioner är det möjligt att ha ett ändligt värde. Det är allmänt accepterat att denna viskositet bär information om topologin hos ett kvanthalltillstånd. Att just hallviskositeten förändras är därför extra intressant då det innebär att vi måste vara mycket försiktiga när vi tolkar anyoniska excitationer i på den tunna torusen.

För att sammanfatta kan vi säga att trots att en torus som den vi studerar troligtvis aldrig kommer att kunna existera fysiskt ger det oss ändå värdefull information om vad som händer i en verklig kvanthallvätska i ett riktigt experiment.

Acknowledgements

A thesis is not merely a booklet that ties together a couple of vaguely related research papers. It is a summary of, in my case, five and a half years of toil and sweat. It is a chance for the PhD student to take a step back and look at the bigger picture that one so easily forgets about when the current aim is something as mundane as forcing the bloody Fortran code compile without errors.

But the thesis is also much bigger than the articles that it comprises. It is the result of several people over many years who have either influenced the research directly, or indirectly have helped shape me to the researcher I am today. I would like to thank all of you, co-workers, family and friends that deserve my appreciation. Due to lack of space, here I will only mention a select few:

My two supervisors who called me while on my bike and offered me a position as their PhD student. First **Anders Karlhede**, with whom I also spent more than two years in one of the governing body of the faculty and learned much about the strategic issues that a university has to deal with. Second, and an even bigger thanks to **Thors Hans Hansson**, who introduced me to my coming employer and have shared his wisdom on many occasions on how you navigate in the academic waters. It has been a pleasure to learn from you both!

Eddy Ardonne for acting almost as a third supervisor since he arrived at the group.

My mentor **Fawad Hassan** and **Supriya Krishnamurthy** for keeping a kind eye on me during these years.

My fellow PhD students in the group who I have had the fortune to have as travel companions for summer schools and conferences. **Emma Wikberg**, who is almost always happy and cheering. I hope that your good luck charm Ior found a happy home in the Lake district. **Thomas Kvorning**, whom I can bother with questions high and low. A special thanks for showing how shaky a pair of legs can be, after running 700 meter up and than down a mountain in France. Thank you **Christian Spånslätt**, for pleasant and interesting conversations from one desk to another and for showing what it means to travel like Phileas Fogg. I promise to never again dial 9-1-(1)-800 from an American telephone. One visit from a police officer is more than enough.

My room mate **Fernanda Pinheiro**, for refusing to follow the usual daylight cycle that the rest of us are dependent on.

Astrid de Wijn, for discussions revolving around the everyday life of a researcher; from applying for grants to grading student homework. Unfortunately we have not had the time to play as much go as I would have liked.

Sören Holst, for many thought provoking discussions on philosophy, pedagogics and lately the quality of the course curriculum.

To the many lunch companions over the years, **Maria Hermanns**, **Emma Jakobsson**, **Jonas Larsson** and many others. I have thoroughly enjoyed the chats we have had.

Many thanks to all the other people who are in or have passed through the **condensed matter and quantum optics** group.

My comrade in arms in the PhD council, **Stephan Zimmer**, for a pleasant and fruitful cooperation for the greater good of all the PhD students both at Fysikum and at the faculty of Sciences.

All the helpful people at the administration, especially **Petra Nodler**, **Elisabet Oppenheimer** and **Hilkka Jonsson**, for all your help over the years.

My aunt-in-law **Gertrud Fremling**, for the most thorough read-through of the thesis I could ever have gotten. Not a page unaltered and almost not a sentence untouched, and all for the better.

My former colleagues at Klarna, **Erik Happi Stenman** and **Daniel Luna**, for hiring an inexperienced physicist and showed him that our skills are needed also outside of our own sphere of expertise. The good practices in programming and testing that I learned under your wings have been invaluable during my time as a PhD student.

Denna avhandling hade inte blivit vad den är utan stöd från familj och vänner. En grupp människor som inte alls förstår vad jag pysslar med om dagarna, men som ändå tycker att det är väldigt spännande och är glada att jag gör det jag gör, för det är det jag gillar.

Mina föräldrar, för att ni uppfostrat mig till en balanserad och självständig individ. Tids nog ska vi nog lyckas förklara den där telefonen för dig **Marie Kardell**. **Janne Kardell**, du har berättat att när var ung brukade du och en vän filosofera om andra världar. Jag hoppas jag givit dig inblick i den konstiga men fascinerande världen av kvantmekanik.

Syster **Malin Kardell**, för att du står ut med din disträe bror, som ibland har orsakat översvämningar i ditt rum. Ett speciellt tack för att du tagit dig tid att korrekturläsa avhandlingen.

Mormor **Iva Kardell**, tack för en fin trädgård som inspirerar till att upptäcka hur världen är uppbyggd. Där finns massor av goda hallon, äpplen och plommon.

Tacksamma tankar går till min avlidne svärfar **Lennart Fremling**, för ett genuint intresse och stöd i mitt beslutet att återvända till doktorandstudier från arbetslivet. För att du visade hur vackert det är i svenska fjällen, och för många givande diskussioner om tåg och hur politik skall skötas i praktiken. Jag önskar att du kunde ha varit med till slutet av den här resan.

Svärmor **Margaretha Fremling** för att det finns ett dukat middagsbord, en bäddad gästsäng och en väldigt god drömrulltårta när man inte orkar ta sig hem hela vägen från jobbet.

Moster **Åsa Kardell**, som för länge sedan lät mig praktisera hos henne och gav mig min första kontakt med programmering. Till hennes man **Björn Kardell** riktar jag ett tack för att han inspirerar att cykla till och från jobbet. Bra motion och snabbare än att åka tunnelbana är det.

Till min äldsta kusin **Joakim Kardell**, det har varit roligt att vara din privatlärare i fysik under den här våren. Till min andra kusin **Markus Kardell** skickar jag en uppskattande tanke om de frågor du har för vana att ställa. Det är roligt att se att du är så frågvis, men glöm inte bort att en god portion skepticism inte heller är helt fel ibland.

Min vän sedan lågstadiet **Mattias Gyllsdorff**, för att du med intrese rycker ut och löser mina datorproblem när det har strulat till sig riktigt ordentligt. Hur skall det gå nu när vi flyttar bort från våningen ovanför dig?

Min goda vän och marskalk **Erina Stenholm**, som alltid har ett gott öga för sällskapsspel och aldrig säger nej till en avkopplande spelkväll. Om några år är du också doktor, fast en riktig sådan.

Mina kurskamrater **Simon Molander**, **Disa Åstrand** och **Örjan Wennbom** (fd. Smith), för den vänskap vi inledde på fysiklinjen för snart elva år sedan. Jag antar att denna avhandling får räknas som mitt försök till en Kardell-inveckling. När får jag se en prototyp av en Smith-Molander-apparat?

Studentföreningen **Naturvetenskapliga Föreningen** vid Stockholms Universitet och alla glada **grodor** där, för att det finns en villa man kan gå till när man inte vet vart man annars skall ta vägen. Jag har fått många vänner och lärt mig mycket om administration där som jag kommer nytta av många år framöver.

Min snart ettåriga son **Sebastian Fremling**, för alla saker som vi kommer att göra tillsammans. Det är spännande att upptäcka värden på nytt genom dina ögon.

Till sist, min älskade fru **Karin Fremling**, som finns vid min sida och delar min tillvaro. Det finns så många saker att tacka för att jag har svårt att välja vad jag ska nämna här. Jag tackar dig speciellt för att du har stöttat mig att skriva klart avhandlingen redan under hösten, *innan* jag blev föräldraledig. Jag är övertygad om att det har besparat oss mycket stress. Jag ser fram emot att spendera framtiden med dig, härnäst med tre år på Irland. Vilket äventyr det skall bli!

Contents

Nomenclature

Abbreviations

CFT	Conformal Field Theory
CS	Chern-Simons
FQHE	Fractional Quantum Hall Effect
IQHE	Integer Quantum Hall Effect
LL	Landau Level
LLL	Lowest Landau Level
TI	Topological Insulator

Constants and Variables

N_Φ	Number of Magnetic Flux Quanta
N_e	Number of Electrons
N_s	Number of states in the Hilbert space. On the torus $N_s = N_\Phi$, and $L_x L_y = 2\pi N_s$
R_H	Hall resistance
ℓ	Magnetic length: $\ell = \sqrt{\frac{h}{eB}}$
ν	Filling fraction

The Torus Geometry

L_Δ	Skewness of torus
L_x	Width of torus
L_y	Height of torus
τ	Ratio of the two principal axes $\frac{L_\Delta + \imath L_y}{L_x}$

Translation Operators

$t(\mathbf{L})$	Translation operator: Sends $\mathbf{r} \to \mathbf{r} + \mathbf{L}$ and performs gauge transform
t_1	Finite translation operator in x-direction
t_2	Finite translation operator in τx-direction
$t_{m,n}$	Most general translation operator on the torus. Moves coordinates the finite distance $\frac{L_x}{N_s}(m + \tau n)$

Wave Functions

η_s	Eigenstate of t_1 in LLL on torus
φ_s	Eigenstate of t_2 in LLL on torus

CFT Variables

$K_{\alpha\beta}$	Wen-Zee K-matrix. For $\nu = \frac{2}{5}$, $K = \begin{pmatrix} 3 & 2 \\ 2 & 3 \end{pmatrix}$
N_α	Number of electrons in group α, $\sum_{\alpha=1}^{n} N_\alpha = N_e$
$\mathbf{q}_\alpha$	Charge vector of type α. Contains K-matrix data, $\mathbf{q}_\alpha \cdot \mathbf{q}_\alpha = K_{\alpha\beta}$
$\mathbf{l}_\alpha$	Quasi-particle vector of type α. Dual vector to $\mathbf{q}_\alpha$, $\mathbf{q}_\alpha \cdot \mathbf{l}_\beta = \delta_{\alpha\beta}$
α, β	Label of the differnt groups of electrons, $\alpha = 1, \ldots, n$
i, j	Label of the individual electrons, $i = 1, \ldots, N_e$

Fock Expansions

$\tilde{T}_{ij}$	Momentum contribution to electron pair i, j from the Jastrow factor $\tilde{T}_{ij} = -\tilde{T}_{ji}$
$\mathbb{T}_i$	Total momentum contribution to electron i $\mathbb{T}_i = \sum_{j=1}^{N_e} \tilde{T}_{ij}$
$\mathcal{Z}(\mathbb{T})$	Fock coefficient for the configuration with momentum $\mathbb{T}$
$\tilde{Z}^{(q)}_{\tilde{T}}$	Structure factor for ϑ-functions

List of Accompanying Papers

Paper I **Exclusion statistics for quantum Hall states in the Tao-Thouless limit**
M. Kardell, A. Karlhede
J. Stat. Mech 2011 P02037 (2011)

Paper II **Coherent State Wave Functions on a Torus with a Constant Magnetic Field**
M. Fremling
J. Phys. A 46 275302 (2013)

Paper III **Hall viscosity of hierarchical quantum hall states**
M. Fremling, T. H. Hansson, and J. Suorsa.
Phys. Rev. B 89 125303 (2014)

Paper IV **Analytical Fock coefficients of the Laughlin state on the torus**
M. Fremling
In preparation, arXiv no 1503.08144 (2015)

My Contribution to the Accompanying Papers

Bellow I describe my contribution to the accompanying papers. The reader should be aware that I have changed my last name from **M. Kardell** to **M. Fremling** during my Ph. D. studies and so my first article, **Paper I**, was published under my former name.

In **Paper I**, which was my very first project, I examined the exclusion statistics in the TT-limit. The idea to do this was purely due to Anders Karlhede. I started out by looking at $\nu = \frac{1}{3}$ and $\nu = \frac{2}{5}$ but quite soon I found that there was a generic structure that could be used to characterize the exclusion statistics of any TT-state with a convex interaction. The proofs that the low energy sector in the TT-limit could be written as a permutation of a collection of $\mathfrak{p}$:s and $\mathfrak{h}$:s is also due to me. In the paper there is a numerical study of the TT-limit using exact diagonalization. The program itself was adapted from earlier work by Emil Bergholtz and Anders Karlhede and I extended it in such a way that also Emma Wikberg could use it for some of her work. See *e.g.* Ref. [Wik12]. Regarding the writing of the manuscript, I am responsible for the more technical parts, including the entire appendix.

Both **Paper II** and **Paper III** where initialized by Hans Hanson at around the same time. As I am the single author of **Paper II**, I of course take full credit and responsibility for that work. Nevertheless Hans Hansson came up with the initial idea to compare continuous coherent states to lattice coherent states and was also much involved in discussion of the theory.

As to **Paper III,** it is harder to discern who did what work, especially in regards to the construction of the $\mathbb{D}$-operator. The original construction of the primary torus wave functions is due to Juha Soursa, including the first drafts of Appendix A. I have still made contributions regarding the conformal blocks in the form of working out their modular transformation properties as well as proving the one-dimensional nature of the quotient space $\Gamma/\Gamma^\star$ for the hierarchy states.

In the beginning of the project we where not really thinking in terms of a generalized derivative operator and were only working with different powers of T_1. It was only when I noticed numerically that there was an asymmetry between $\tau \to 0$ and $\tau \to \infty$ that it dawned on us that there should be relations relating the two extreme tori. At this time, Hans construed the first two coefficients $\lambda_{1,0}$ and $\lambda_{0,1}$ by looking at the regularization process when fusing quasi-particles. I strongly argued for the need to respect both $\mathcal{S}$ and $\mathcal{T}$ covariance and extended the ansatz to general $\lambda_{m,n}$.

Further, the completion of the $\mathbb{D}$-operator construction in terms of commuting with T_1 and T_2 is mine and so is the proof that $\left[\mathbb{D}^{(\alpha)}, \mathbb{D}^{(\beta)}\right] = 0$. Regarding the $\mathbb{D}$-operator, there was also initially a discussion regarding which terms where most important, and I argued that the smallest translations should be the best terms and produced the analysis in Section V of that paper to argue for this.

Here too I did all of the numerical work, but this time I built upon a diagonalization program written by Juha for Ref [HSB+08]. Nevertheless this program too has been extended and modified extensively. Thus there is not much left of the original code, except at the very core of building the sparse Hamiltonian before diagonalization.

Finally **Paper IV**, which is still in preparation, was initialized as my own idea. I knew how to expand the Laughlin state in a Fock basis and was interested in using this to analyze the TT-limit of the Hall viscosity.

Chapter 1

Introduction and Outline

This year marks the 30-year anniversary of the first quantum Hall wave function to be written in a toroidal geometry[HR85]. In 1985 Haldane modified the Laughlin wave function by incorporating periodic boundary conditions. In this thesis, I will generalize that construction to a larger class of states that describe many of the experimentally observed fractional quantum Hall plateaus.

The experimental signature of the integer and fractional quantum Hall effect is as striking as it is simple. When a two-dimensional electron gas is subject to a strong magnetic field perpendicular to its surface the longitudinal resistance will sometimes vanish. This phenomenon only happens at particular strengths of the magnetic field. Also precisely at those strengths, the perpendicular resistance – the Hall resistance, R_H – forms plateaus that are insensitive of the strength of the magnetic field. See Figure 2.2 for an experimental example.

In 1983 Laughlin introduced a ground state wave function[Lau83] to explain the fractional quantum Hall effect (FQHE). This ground state contains low energy quasi-particle excitations with both fractional charges[Lau83] as well as fractional statistics[ASW84], the later being a phenomena that only can occur in two spatial dimensions. The theory of the fractional quantum Hall effect is today still an active area of research. The Hall effect was the first example of a topological insulator[KM05], but many other topological insulators have been proposed[Kit09] and realized[KWB$^+$07]. Fractional charges have also been proposed to exist in other types of systems, where fractional Chern insulators[RB11] and polymer chains[SS81] are examples. Extensive research has also been focused on the special state at filling fraction $\nu = \frac{5}{2}$, which is expected to support excitations with non-abelian braiding properties. The non-abelian statistics makes this state of matter an interesting candidate for quantum information storage and processing; in short, a quantum computer.

In quantum mechanics, the existence of a magnetic field drastically alters the structure of the Hilbert space as compared to the case of particles moving in free space. The continuum of energy levels of the free particle, transforms into highly degenerate Landau levels with a degeneracy proportional to the strength of the magnetic field. If the applied magnetic field is strong enough, together with low temperatures and clean samples, the quantum Hall effect is observed. The quantum Hall effect is observed in high quality semiconductor junctions[KDP80,

TSG82] as well as in graphene[NGM+05]. In semiconductors, the temperature has to be very low for the QHE to be manifested, but in graphene the effect is observable even at room temperature[NJZ+07].

The Integer and the fractional quantum Hall effects are examples of Topological Insulators; States of matter that are insulating in the bulk, but has dissipationless transport at the edges. The topological aspect of the QHE is its insensitivity impurities, but also to deformations of a sample as well as to small variations of the applied magnetic field or the precise temperature. Most importantly, the edge currents survive a finite amount of impurities, which is always present in a real system. As a consequence, the electric resistance R_H is quantized to an experimentally very high accuracy[TLAK+10].

The peculiar thing about topological insulators (TI) is that it is locally impossible to know whether or not the ground state is in the interesting phase or the trivial phase. One way to tell is by studying the quasi-particle braiding in the system. A more direct method is by having a shared edge with a system that is in a known topological phase. If the phases are the same then the two systems behaves as one big system. On the other hand, if the systems are different, something dramatic must happen at the edge, as there is now a conflict between the topology of the two sectors. In this case, the energy gap that protects the topological state closes and reopens right at the boundary. This is the reason why there are robust edge states in the first place, since it is only when two TI:s in different topological sectors form an interface that there can be a change in topology.

In this thesis, I am studying the FQHE on the torus, where one of the topological aspects is encoded in the ground state degeneracy on the torus. The torus is also a good testing ground for model trial wave functions coming from Conformal Field Theory (CFT). Trial wave functions for the FQHE have been deduced using correlators from CFT. The CFT wave functions are easily evaluated in a planar geometry, but numerical comparison to exactly diagonalized ground states can be difficult to perform because of boundary effects. The torus as well as the sphere are natural candidates for numerical tests, as they have no boundaries.

I also investigate how to generate trial wave functions on the torus in a self-consistent manner. I rely on the fact that there is more than one way of parametrizing the same torus geometry and that all of these parametrizations are related by modular transformations. By requiring that the physics is unchanged under these modular transformations, I find strong constraints on the possible wave functions on the torus. Further, I propose a trial wave function for the $\nu = \frac{2}{5}$ state that has the correct modular properties.

Using the proposed wave function, I calculate a topological characteristic of the quantum Hall system: the antisymmetric component of the viscosity tensor. Read has demonstrated that this viscosity is proportional to the mean orbital spin of the electron, which is a topological quantity. This transport coefficient can be measured numerically by changing the geometry of the torus[RR11].

This thesis has four accompanying papers. In **Paper I**, I investigated the exclusion statistics of quasi-particles in the Tao-Thouless (TT) limit, an extremely asymmetric torus where the Hamiltonian can be solved exactly for a wide range of potentials. In **Paper II** I constructed coherent states and described some of their properties. As this paper was discussed in detail in my Licentiate thesis[Fre13b] it will be discussed very little in this thesis. In **Paper III** I built upon the work of

Ref [HSB+08] and constructed trial wave functions for all chiral K-matrices. I also computed the viscosity of the $\nu = \frac{2}{5}$ state, both numerically and analytically. In **Paper IV** I expanded the Laughlin state in a Fock basis and used this to deduce the normalization and Hall viscosity in the TT-limit.

The thesis is organized as follows, in **Chapter 2** I briefly describe the history of quantum Hall physics and the basic observations regarding the FQHE. In **Chapter 4** I give mathematical details regarding the torus. **Chapter 3, Chapter 5** and **Chapter 6** deal with he construction of trial wave functions using the CFT machinery. In **Chapter 7** I construct the Fock expansion of the Laughlin state and comment on how it can shed light on the Hall viscosity in the TT-limit. In **Chapter 8** I compute the Hall viscosity, both analytically and numerically, for a selection of wave functions, and comment on the behaviour in the TT-limit. **Chapter 9** presents, as the title suggests, a summary and outlook of this thesis.

Chapter 2

The Quantum Hall Effect

2.1 The classical Hall effect

In 1879 the American physicist Edwin Hall decided to test whether or not electric currents where affected by magnetic forces[Hal79]. He designed an experiment in which he found that a thin metal plate in a magnetic field **B,** perpendicular to the surface of the plate, experiences a voltage drop in a direction perpendicular to **B** and the current **I** flowing through the plate. He concluded that the perpendicular resistance $R_{\mathrm{H}} = \frac{V_{\mathrm{H}}}{I}$ was proportional to the strength and sign of the magnetic field. See figure 2.1 for a schematic set-up of the experiment.

The Hall effect is explained by the behaviour of charged particles in a magnetic field. As the electrons move through the magnetic field, they will be subject to a Lorenz force $\mathbf{F}_B = q\mathbf{v} \times \mathbf{B}$ directed toward one of the edges of the plate. As more and more electrons are diverted toward one side, a charge imbalance builds up inside the plate, generating an electric field across the plate. The existence of a static electric field means that there is a voltage difference, which in this case will be perpendicular to the direction of the current **I**. Eventually the electric field, with the associated electric force $\mathbf{F}_E = q\mathbf{E}$, becomes large enough to balance the magnetic force $\mathbf{F}_B$. This voltage drop is proportional to the total current. A larger current increases the diverting force $\mathbf{F}_B$ so a larger voltage difference will be needed to balance it. The voltage difference is also proportional to the magnetic field as the Lorenz force that deflects electrons is proportional in strength to B. Hence, the Hall resistance, which is the perpendicular resistance R_H, is proportional to the strength of magnetic field $R_{\mathrm{H}} \propto B$. The Hall effect is also inversely proportional to the thickness of the material that the current runs through, and this in turn implies that the Hall effect gets stronger when the plate is thinner. A more detailed analysis demonstrates that the Hall resistance is $R_H = \frac{B}{e\rho_{3D}d}$, where d is the thickness of the plate, ρ_{3D} the electron density and e the electric charge. In the limit of very thin plates, plates that are almost two-dimensional, R_H is better described using the two-dimensional density ρ_{2D}, as $R_H = \frac{B}{e\rho_{2D}}$. It is in this limit of thin plates that quantum mechanical effects can become important, and the Hall effect can be changed into the quantum Hall effect.

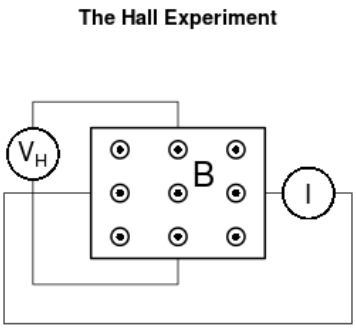

Figure 2.1: The Hall experiment. A current I is driven through a thin metal plate with a perpendicular magnetic field B such that a voltage V_{H} is measured in the transverse direction.

2.2 The quantum Hall effect

In 1980 the German physicist von Klitzing gave the Hall effect a new twist[KDP80] by confining electrons to two dimensions in semiconductor junctions. In his experiments, where he had high quality samples in combination with low temperatures and high magnetic fields, the Hall resistance R_H deviated from the classically predicted linear behaviour and instead started developing kinks and plateaus. Furthermore, these plateaus appeared at regular intervals in such a way that the resistance at the plateaus could be described by the formula $R_H = \frac{1}{\nu} \cdot \frac{h}{e^2}$, where ν is an integer. In addition, at the magnetic fields where the plateaus appeared in the Hall resistance, the longitudinal resistance $\mathbf{R}_{\|}$ dropped to zero. This new phenomena was soon dubbed the Integer Quantum Hall Effect (IQHE)*. The IQHE is so precise that it effectively defines the fundamental unit of resistance, the von Klitzing constant, which can be measured with an accuracy of 10^{-12} to equal $R_K = \frac{h}{e^2} = 25812.807557(18)\ \Omega$[TLAK$^+$10]. Soon, with the revised SI system, R_K will be defined without any experimental uncertainty†.

The key to understanding the IQHE lies in the behaviour of single particles in a magnetic field. From classical physics we know that charged particles are deflected by magnetic fields and therefore move in circles where the radius is proportional to the particle's momentum. The frequency of revolution is therefore independent of the particle momentum. It depends only on the magnetic field $\mathbf{B}$ and on the mass m of the particle, as expressed by the formula $\omega_c = \frac{eB}{mc}$. The oscillatory behaviour is similar to the behaviour of the harmonic oscillator, where the quantum mechanical energy levels are equally spaced as $E_n = \hbar\omega_c \left(n + \frac{1}{2}\right)$ with n being an integer. An analogous calculation for a particle in a magnetic field shows that, here

*The name IQHE was of course used only after the discovery of the FQHE three years later.

†In the near future the SI system will be revised such that R_K is not a measured quantity but rather a fixed constant of nature, just like the speed of light is a fixed quantity and not experimentally measured. The question was under consideration for the 25:th General Conference on Weights and Measures in 2014 but the time was not deemed right[oWM14]. The next conference will likely be held in 2018.

too, the energy levels are equally spaced, with $E_n = \hbar\omega_c\left(n + \frac{1}{2}\right)$. Each energy level is called a Landau level (LL) after Landau[Lan30] who solved the problem in 1930. The LL with $n = 0$ is the lowest energy level and is therefore called the lowest Landau level (LLL). In contrast to the harmonic oscillator, each LL is massively degenerate, as there exists one state for each flux quanta $\Phi_0 = \frac{h}{e}$ of the magnetic field. Thus the density of states in any Landau level is $\frac{B}{\Phi_o} \approx \frac{B}{1\text{ Tesla}} \times 242$ per $(\mu\text{m})^2$. This means that if each electron were confined to a circle, the radius of that circle would be $r = \sqrt{\frac{\Phi_o}{\pi B}} = 363\,\text{Å} \times \sqrt{\frac{1\text{ Tesla}}{B}}$. It is customary to introduce a length scale $\ell = \frac{r}{\sqrt{2}}$, known as the magnetic length, which characterizes the length scale of the Landau problem.

The above mentioned factor ν can be calculated as the filling factor $\nu = \frac{N_e}{N_s}$, which counts the number of filled Landau levels. If ν is an integer, all the Landau levels up to and including level ν are completely filled. Thus there exists a gap of $\hbar\frac{eB}{mc}$ to excite an electron into the next LL[Lau81]. This gap causes the IQH-state to be stable against small variations in the magnetic field as the energy cost of moving an electron to the next LL would be too large.

As samples became cleaner and temperatures lower, new features appeared in the resistance spectrum. New plateaus were observed, together with dips in the longitudinal resistivity. These new plateaus where located at $R_H = \frac{1}{\nu} \cdot \frac{h}{e^2}$, where $v = \frac{p}{q}$ are fractions, such as $\frac{1}{3}$, $\frac{2}{5}$ and $\frac{3}{7}$[TSG82]. The plateaus only developed at fractions with an odd denominator, as can be seen in Figure 2.2. The new effect was named Fractional Quantum Hall Effect (FQHE). Compared to the IQHE, it has more features beyond simply a fractional Hall resistance. One prominent feature is that the minimal excitations do not consist of individual electrons but rather of fractionally charged quasi-particles[Lau83] and these are believed to have statistics different from that of fermions or bosons[ASW84]. This new form of statistics constitutes a generalization of the fermion and boson statistics and can only be obtained in systems with a spatial dimensionality of two or less. Some of these quasi-particles are even conjectured to display non-abelian statistics[MR91]. The experimental verification of the abelian and non-abelian statistics is still lacking despite there having been some new developments during the last few years[WPW10]. The non-abelian nature of the quasi-particles is the reason that people are looking to the FQHE as a possible way to realize a working fault tolerant quantum computer[Kit03]. Since the quasi-particles are topologically protected excitations they would be stable against local de-coherence, which is a problem in many other quantum computational schemes.

For the FQHE, the explanation is not as straightforward as for the IQHE. As ν is no longer an integer, but rather a fraction, such as $\nu = \frac{1}{3}$, one LL will be only partially filled, and the single particle picture of electrons filling one or more entire LL:s no longer works. In order to solve this problem, we* need to go beyond the properties of individual electrons and study the interaction between the particles within a LL. Crudely speaking, the Coulomb repulsion between electrons forces all the electrons to be as far separated in space as possible. This results in a highly correlated fluid where the minimal excitation costs finite energy. The alternative, that can happen for dilute filling fractions, would be a Wigner crystal where the

*From now on I switch to we, as in you and I.

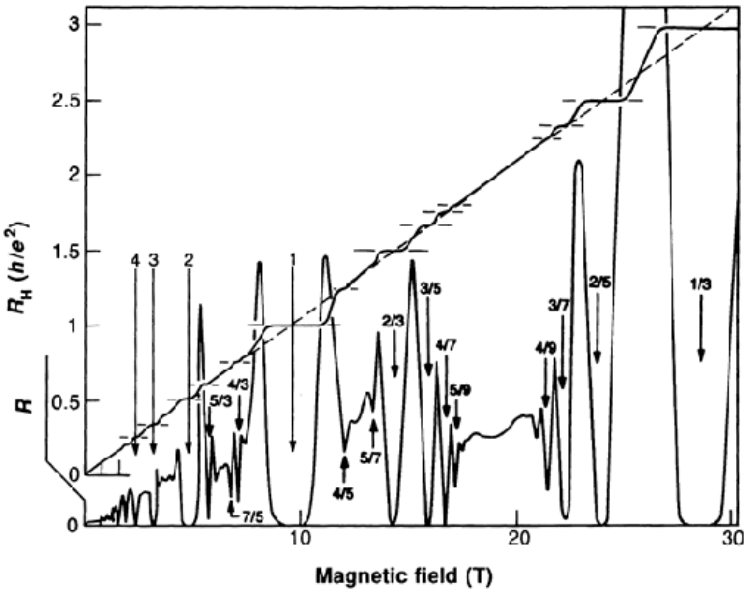

Figure 2.2: Resistance measurements of the FQHE[Sto92]. The transverse resistivity R_H displays plateaus at particular strengths of the magnetic field. These magnetic field strengths correspond to rational filling fractions $\nu = \frac{p}{q}$ of the Landau orbitals. At the same rational filling fractions as where the plateaus are, the longitudinal resistance R drops to zero.

minimal excitations are phonon-like.

Both the IQHE and the FQHE need some amount of impurities to manifest themselves. If the QH-sample would be fully translationally invariant, then Lorentz invariance would imply that no plateaus can be present. Impurities are thus needed to break the Lorentz invariance. However, if the impurities are too strong, then the QHE is not observed if the energy gap is to small, causing some FQHE fractions not to be observable in experiments. In the limit of no impurities, which also means restored Lorentz invariance, all FQHE fractions will be visible, but this will result in a devil's staircase of plateaus in R_H. In that case, FQHE becomes indistinguishable from the classical Hall effect and no plateaus are visible, at least not in simple transport experiments.

2.3 The Laughlin wave function and the hierarchy

In 1983 Robert Laughlin proposed a wave function that would explain the FQHE at $\nu = \frac{1}{q}$[Lau83], where q is an odd integer. The construction was inspired by the realization that in the FQH-states the electrons could minimize their interaction energy by being as far from each other as possible. With that principle in mind,

Laughlin proposed the now famous wave function

$$\Psi_{\frac{1}{q}}(z_1, \ldots, z_{N_e}) = e^{-\frac{1}{4}\sum_j |z_j|^2} \prod_{i<j}^{N_e} (z_i - z_j)^q , \tag{2.1}$$

which is a homogeneous state with well-defined angular momentum. The complex coordinate $z = x + \imath y$ encodes physical coordinates in a convenient manner. This wave function implied that only odd denominator filling fractions could appear, since otherwise the wave function would not be antisymmetric in the electron coordinates. Starting from (2.1), he could also find the elementary excitations, the quasi-particles, that could appear. This was accomplished by inserting an extra quantum of flux into the state at $z = \eta$ and noting that the new wave function contained an extra factor $\prod_j (z_j - \eta)$. By making an analogy with a charged plasma, Laughlin could deduce that the quasi-particles at $\nu = \frac{1}{q}$ had fractional charges $\frac{e}{q}$. The physical explanation for the fractional charge is that the term $(z - \eta)$ does not repel the electron and quasi-particle as strongly as $(z_i - z_j)^q$ repels the electrons from each other. This gives the quasi-particle a smaller correlation hole than the electron which translates into a fractional charge. Later Arovas, Schrieffer and Wilczek deduced that the quasi-particles display fractional exchange statistics[ASW84].

The Laughlin wave function sheds some light on other filling fractions as well since the quasi-particle excitations can be used as building blocks for other states. As the magnetic field B is tuned away from $\nu = \frac{1}{q}$, quasi-particles appear in the state (2.1). As B is tuned still further, these quasi-particles become so numerous that the electrons and quasi-particles condense into a new state, with a new filling fraction. This new state will also support its own quasi-particles with fractional charges and statistics. As the magnetic field is changed further, these 2^{nd} generation quasi-particles can in turn condense into yet another state. By this process, any filling fraction with an odd denominator can be created by repeated condensation of parent quasi-particles[Hal83a, Hal83b]. This idea is called the Haldane-Halperin hierarchy construction since different filling fractions are created at different hierarchical levels of condensation of quasi-particles.

Each level of the hierarchy contains both negatively and positively charged quasi-particles. The negatively* charged excitations are called quasi-holes. Depending on whether the quasi-electrons or quasi-holes are condensed, different technical issues arise. Usually quasi-electron condensation is technically easier to calculate and and quasi-hole condensation more difficult.

In the hierarchy, all quasi-particle excitations are gapped, *i.e.* they cost a finite amount of energy to create. The size of the gap dictates in which order the different fractions should become visible in experiments. To measure the FQHE it is important that the gap to quasi-particle excitation is not closed by thermal fluctuations or impurities. It can be shown that under certain circumstances, the excitation gap of the FQHE at $\nu = \frac{p}{q}$ is monotonically vanishing in the denominator q[BK08]. This explains why the fractions at $\nu = \frac{1}{3}$ and $\nu = \frac{2}{3}$ are observed first, followed by the fractional at $\nu = \frac{2}{5}$, $\nu = \frac{3}{7}$ and $\nu = \frac{4}{9}$ etc.

*Negative charge with respect to the electron charge.

2.4 Composite fermions and conformal field theory

Jain took a different route to explain the FQHE[Jai07]. Inspired by Laughlin's wave function and resistance measurements, he unified the FQHE and the IQHE by introducing the notion of composite fermions. Jain proposed that the electrons could screen parts of the magnetic field by binding vortices to themselves. By binding just enough vortices, reducing the effective magnetic field, the electrons would fill one or more effective LL:s. This construction yielded explicit expressions for wave functions at other filling fractions than $\nu = \frac{1}{q}$, something the hierarchy construction could not achieve. Furthermore, Jain found that the wave functions for composite fermions also displayed remarkably good overlap with those obtained from exact diagonalization of the Coulomb potential.

There now exists an alternative method for deducing trial wave functions for generic FQH-states, one based on the correspondence between the Laughlin wave function and correlators in certain conformal field theories (CFT). These CFT-based wave functions reproduce the wave functions that where constructed by using the composite fermion method. Thus the composite fermion scheme can be seen as a special case of the hierarchy construction. This in turn implies that these two approaches are alternative ways of looking at the same problem.

2.5 Fractional quantum Hall effect on the torus

In this thesis, we will consider the Haldane-Halperin hierarchy wave functions in a toroidal geometry. By construction, the torus lacks a boundary, making it suitable for numerical calculations. The torus is also locally flat, which avoids the trouble that is connected to the curvature of the sphere – another geometry that lacks boundaries. Further, the number of states in the torus Hilbert space is the same as the number of magnetic flux quanta $N_s = \frac{A}{2\pi\ell^2}$, where A denotes the torus area.

The torus does come with its own set of problems. Because of the periodicity, wave functions expressed on the torus consists of rather complicated analytical functions. This includes products of Jacobi ϑ-functions $\vartheta_j(z|\tau)$, making analytical manipulations more complicated. Further, because of the gauge field associated with the magnetic field $\mathbf{B}$, the wave functions are not truly periodic but quasi-periodic.

To make the analytical problems even worse, there is a restriction on which translation operators allowed on the torus. Examining this restriction will form a central part of my thesis as the restriction prohibits the mapping of CFT wave functions formulated on the plane directly to the torus. Technically this is because the planar wave functions in the higher levels of the Haldane-Halperin hierarchy will contain derivative operators ∂_z. We will later show that these derivatives can *not* be interpreted as derivatives on the torus. Instead the derivative can, at best, be mapped onto a linear combination of products of allowed translation operators $t_{m,n}$ as $\prod_i \partial_{z_i} \to \sum_{m,n} \lambda_{m,n} \prod_i t^{(i)}_{m,n}$. The precise meaning of these translation operators will be clarified in Section 4.1 and 6.3.

2.6 Why do we study the torus?

After reading the preceding section the reader might be wondering why we should be studying fractional quantum Hall effect on the torus in the first place. It seems at first glance as a rather artificial place to study physical phenomena and the prospects of constructing any experiment on this geometry are dim. Indeed, there will likely never be possible to design a experiment that actually probes the particular geometry that the torus constitutes.

However, the reason we study the torus has little do to with the feasibility of real life experiments. Instead we use the torus as a theoretical laboratory to infer properties that we believe will also be present in the physical situation, but which might be hard to model there. One major aspect that we are trying to exclude from our analysis is the effect of an edge. A real system will have an edge, but it is often difficult to model properly, and it can be hard in a small system to disentangle which effects come from the bulk and which come from the edge.

It might sound as a rather counter-intuitive approach to study only the bulk, given that it is the edge that carries all of the quantized current. The reason to study the bulk is because of the topological stability of the FQHE. The edge currents are a direct consequence of, and also a mirror of, the physics that takes place in the bulk. By studying the bulk properties, we can thus still make predictions for how the edge of a real system will behave. We call this the bulk-boundary correspondence, and it is an important property of topological insulators.

We should emphasize the aspect of the torus as a theoretical laboratory. As an example, at filling fraction $\nu = \frac{p}{q}$, there is not a unique ground state. Rather, the number of degenerate ground states must be a multiple of the denominator q. It is therefore an important sanity check on any method of generating trial wave functions that it gives us the correct number of degenerate ground states.

The torus also has some advantages that are hard to come by on other geometries. One of these advantages is the possibility to simulate a constant strain rate in the quantum Hall fluid. This is something you can *not* do with a sphere. The force response to a small constant strain rate (or velocity gradient) is encoded in the viscosity of a fluid. Since the quantum Hall fluid has an energy gap there is no ordinary viscous response like that of shear viscosity or bulk viscosity. There is however a non-dissipative viscous response called Hall viscosity. We will learn what this type of viscosity is and why it is interesting Chapter 8.

Chapter 3

Trial Wave Functions from Conformal Field Theory

In this chapter we will construct trial wave functions for the fractional quantum Hall effect on a plane. The construction will be explained in some detail as the same procedure, *mutatis mutandis*, will be applied in Chapter 5 when considering the torus.

As mentioned in Section 2.4, there exists a connection between the FQHE and Conformal Field Theory (CFT). In this chapter we will expand on this connection and present trial wave functions constructed from CFT correlators. This chapter is organized as follows: In Section 3.1 we begin with a few words on how the different pieces CFT, FQHE and Chern-Simons (CS) theory fit together. In Sections 3.2 and 3.3 we introduce the Wen-Zee K-matrix and show how CFT is used to extract wave functions for the chiral Haldane-Halperin hierarchy. Quasi-particle braiding will be discussed in Section 3.4. Section 3.5 discusses derivatives and contains an explicit construction of the $\nu = \frac{2}{5}$ wave function.

3.1 A brief history of CFT, FQHE and CS

It **was** noted by several authors [GJ84, ZHK89, Rea89] that the long range properties of the FQHE could be characterized by an effective field theory of CS type. In the theory, the bosonic scalar fields interacted through a statistical gauge field that would turn the bosons into fermions or anyons, depending on the strength of the coupling to the CS field.

Around the same time, Witten discussed the quantization of a CS theory on manifolds with different topology[Wit89] and showed that the dimension of the resulting finite Hilbert space was the same as the number of conformal blocks in certain CFTs. In the same paper he also calculated expectation values of Wilson loops, which are topological invariants. He further related these to the monodromies of conformal blocks in the CFT containing insertions of local operators related to the loops. Furthermore, for manifolds with boundaries, he found that there are chiral edge modes with dynamics determined by the same CFT.

The relation to physics comes by associating the Wilson loops with the world lines of quasi-particles in a QH-liquid. The conformal blocks can then be interpreted as the wave functions of the quasi-particles, and the monodromies of these blocks as the fractional statistics phases related to braiding them.

The next important step was taken by Moore and Read[MR91], who conjectured that also the *electronic* wave functions could be expressed as conformal blocks of suitably chosen electron operators. They showed that the Laughlin wave function, and its multi-component generalizations[Hal83a, Hal83b] were of this form. They also used this very powerful idea to construct the Moore-Read, or Pfaffian, state. This is an entirely new QH-state with non-abelian fractional statistics. Moore and Read furthermore conjectured that the edge states present in geometries with boundaries should be described by the same CFT that gives the bulk electronic state.

In their original paper, Moore and Read also discussed hierarchy states, but did not propose any explicit wave functions. This was done later in a series of papers[SVH11b, SVH11a] where such wave functions were written as sums of conformal blocks of several kinds of electron operators. The number of distinct electron operators is simply the level in the hierarchy, and the operators differ in the amount of localized (orbital) spin that is carried by the electrons.

In this short review, we will not dwell on the details in this construction, but the results will be explained, since this thesis is focused on generalizing them to a toroidal geometry. In particular, we will need understanding of how the orbital spin is manifested on the torus. To put the CFT hierarchy construction in perspective, we will first review the basic elements of the classification schemes for QH-states developed by Wen and Zee. We will then explain how to go from the topological data that specifies a state in that scheme to a set of CFT operators that will be used to construct explicit wave functions.

3.2 The Wen-Zee classification

The topological properties of a $\nu = \frac{1}{q}$ Laughlin ground state on a flat manifold, can be encoded in the following Chern-Simons Lagrangian

$$\mathcal{L} = \frac{K}{4\pi}\epsilon^{\mu\nu\eta} a_\mu \, \partial_\nu a_\eta + \frac{1}{2\pi}\epsilon^{\mu\nu\eta} A_\mu \, \partial_\nu a_\eta - j^\mu a_\mu, \tag{3.1}$$

where $K = q$, A_μ is the external electromagnetic potential and $\epsilon^{\mu\nu\eta}$ is a Levi-Civita tensor. The field a_μ is a gauge potential that parametrizes the electromagnetic current, as seen from the equation of motion $j^\mu = \frac{1}{2\pi}\epsilon^{\mu\nu\eta}\partial_\nu a_\eta$. By adding extra pieces to this Lagrangian one can also describe the response to curvature in the background manifold. We will comment on this later in the context of the orbital spin of the electrons and Hall viscosity.

The generalization to a general (abelian) quantum Hall state amounts to introducing more Chern-Simons fields $a_\mu^{(\alpha)}$[WZ91] in the Lagrangian (3.1)

$$\mathcal{L} = \frac{1}{4\pi}\sum_{\alpha,\beta} K_{\alpha\beta}\epsilon^{\mu\nu\eta} a_\mu^{(\alpha)} \, \partial_\nu a_\eta^{(\beta)} + \frac{1}{2\pi}\epsilon^{\mu\nu\eta}\sum_\alpha A_\mu \, \partial_\nu a_\eta^{(\alpha)} - \sum_\alpha j^{(\alpha)\mu} a_\mu^{(\alpha)}.$$

In this generalized setting there is one quantized quasi-particle current $j_\mu^{(\alpha)}$ coupled to each CS-field $a_\mu^{(\alpha)}$. Here the K-matrix $K_{\alpha\beta}$ – which has integer entries – encodes the topological properties of the ground state, such as the filling fraction*

$$\nu = \sum_{\alpha,\beta=1}^{n} K^{-1}_{\alpha\beta}. \tag{3.2}$$

The K-matrix also gives the ground state degeneracy d on a manifold of genus g; $d = (\det K)^g$. As explained in Ref. [Wen95], the effective Chern-Simons theory also describes the chiral edge states referred to above.

The hierarchy states are described by a subset of all possible allowed K-matrices. For the part of the hierarchy that is obtained by successively condensing quasi-electrons, but no quasi-holes, the K-matrices are given by

$$K = \begin{pmatrix} K_{11} & K_{11}-1 & K_{11}-1 & \cdots & K_{11}-1 \\ K_{11}-1 & K_{22} & K_{22}-1 & \cdots & K_{22}-1 \\ K_{11}-1 & K_{22}-1 & K_{33} & \cdots & K_{33}-1 \\ \vdots & \vdots & \vdots & \ddots & \vdots \\ K_{11}-1 & K_{22}-1 & K_{33}-1 & \cdots & K_{nn} \end{pmatrix},$$

where n is the level of the hierarchy. All entries $K_{\alpha\beta}$ are integers as with the general K-matrices. A simple example is the level two hierarchy state at $\nu = \frac{2}{5}$ described by $K = \begin{pmatrix} 3 & 2 \\ 2 & 3 \end{pmatrix}$.

3.3 The chiral CFT hierarchy wave functions

As an introductory example, we consider the Laughlin state from (2.1) on a planar geometry. Here the electrons are described by the chiral vertex operator

$$V(z) = e^{\imath\sqrt{q}\phi(z)},$$

which is a primary field with conformal dimension $\frac{q}{2}$ in a very simple CFT. The field ϕ is a compact scalar boson with radius $\sqrt{q}$ defined by the Lagrangian

$$\mathcal{L} = \frac{1}{8\pi}\partial_\mu\phi\partial^\mu\phi. \tag{3.3}$$

As pointed out by Moore and Read, the electronic wave function is given by a correlation function of the electron operators

$$\psi_{\text{Laughlin}} \propto \left\langle \mathcal{O}_{\text{bg}} \prod_{i=1}^{N_e} V(z_i) \right\rangle \propto \prod_{i<j}^{N_e} (z_i - z_j)^q \exp\left\{ -\sum_{i=1}^{N_e} \frac{1}{4\ell_B^2} |z_i|^2 \right\}. \tag{3.4}$$

The angular bracket denotes an expectation value with respect to the action given by (3.3) and $\mathcal{O}_{\text{bg}}$ is a background operator necessary for the correlation function

*The reader familiar with the K-matrix might ask why the charge vectors t_α appearing in the more general equation $\nu = \sum_{\alpha,\beta=1}^{n} t_\alpha K^{-1}_{\alpha\beta} t_\beta$ are missing. In this thesis, we till exclusively work in the basis where $t_\alpha = 1$, and hence we will not mention these charge vectors again.

not to vanish. This background, that physically is related to the magnetic field, is necessary to obtain the correct Gaussian factor* and is discussed in detail in Refs. [Rea09, HSB+08, SVH11b]. There it is also explained how to get quasiparticle excitations by insertion of suitable local, and almost local operators in the correlation functions[SVH11b].

Following Refs. [SVH11b, SVH11a], we construct a general chiral hierarchy wave function at level n, by introducing n distinct electron operators

$$V_\alpha(z) = \partial_z^{\alpha-1} e^{\imath \mathbf{q}_\alpha \cdot \boldsymbol{\phi}(z)}. \tag{3.5}$$

Here $\mathbf{q}_\alpha$ are n-dimensional charge vectors† such that

$$\mathbf{q}_\alpha \cdot \mathbf{q}_\beta = K_{\alpha\beta}, \tag{3.6}$$

and constitute a geometric representation of the information contained in the K-matrix. Because of the definition (3.6) of the vectors $\mathbf{q}_\alpha$, there is an O(n)-freedom in choosing them. Take for instance $\nu = \frac{2}{5}$ with K-matrix $K = \begin{pmatrix} 3 & 2 \\ 2 & 3 \end{pmatrix}$, where we can choose charge lattice vectors as $\mathbf{q}_1 = \left(\frac{3}{\sqrt{3}}, 0\right)$, $\mathbf{q}_2 = \left(\frac{2}{\sqrt{3}}, \frac{5}{\sqrt{15}}\right)$ as depicted in Figure 3.1. However, we could equally well have chosen $\mathbf{q}_\pm = \frac{1}{\sqrt{2}}\left(\sqrt{5}, \pm 1\right)$. The vectors $\mathbf{q}_\alpha$ span a lattice $\Gamma = \{\sum_{\alpha=1}^n n_\alpha \mathbf{q}_\alpha; n_\alpha \in \mathbb{Z}\}$, also depicted in the figure.

The Lagrangian for the CFT is that of n decoupled versions of (3.3), each with a two-point correlation function $\langle \phi(z,\bar{z})\, \phi(w,\bar{w})\rangle = -\ln|z-w|^2$. The wave function corresponding to the K-matrix is

$$\begin{aligned} \Psi_{\text{Hierarchy}} \;=\; & \mathcal{A} \exp\left\{-\sum_{i=1}^{N_e} \frac{1}{4\ell_B^2}|z_i|^2\right\} \prod_{\alpha=1}^{n} \prod_{i_\alpha < j_\alpha \in I_\alpha} \partial_{z_{i_\alpha}}^{\alpha-1} \times \\ & \times \prod_{\alpha=1}^{n} \prod_{i_\alpha < j_\alpha \in I_\alpha} \left(z_{i_\alpha} - z_{j_\alpha}\right)^{K_{\alpha\alpha}} \times \\ & \times \prod_{\alpha<\beta}^{n} \prod_{i_\alpha \in I_\alpha} \prod_{j_\beta \in I_\beta} \left(z_{i_\alpha} - z_{j_\beta}\right)^{K_{\alpha\beta}}, \end{aligned} \tag{3.7}$$

where $\mathcal{A}$ is an operator that antisymmetrizes the electron coordinates between the different groups. Within each group the correlation is automatically antisymmetric because of $V_\alpha(z)\, V_\beta(\eta) = e^{\imath\pi K_{\alpha\beta}} V_\beta(\eta)\, V_\alpha(z)$. Note the presence of the holomorphic derivatives in the operators (3.5). Without them the wave function should vanish under the antisymmetrization $\mathcal{A}$. Physically the derivatives correspond to decreasing the angular momentum of the state, and on a sphere this would manifest itself as a shift in the naïve relation between the number of flux quanta and the number of particles. This will be discussed further in Section 6.4 and Chapter 8.

For simplicity we will abbreviate the notation by writing

*Note the dependence of the magnetic length in the Gaussian factor.

†Note that this is not the same charge vector as t_α, yet we still use the same same.

$$\Psi_{\text{Hierarchy}} = \mathcal{A}\, e^{-\frac{1}{4}\sum_{i=1}^{N_e}|z_i|^2} \times \prod_{i=1}^{N_e} \partial_{z_i}^{s_i} \times \prod_{i<j}^{N_e} (z_i - z_j)^{M_{ij}}\,, \tag{3.8}$$

so that we associate M_{ij} with the $K_{\alpha\beta}$ corresponding to z_{i_α} and z_{j_β}*. In a similar manner we associate s_i with the power $\alpha - 1$ of the derivatives acting on group α. We will employ this kind of abbreviation in many other equations as well and we therefore use Greek indices $\alpha, \beta = 1, \ldots, n$ when considering groups and Roman $i, j = 1, \ldots, N_e$ when considering individual electrons.

The number of particles in the different groups N_α, is determined by demanding that the state is homogeneous, i.e. it has a constant charge density. For this purpose, we study the area covered by each particle group. A single particle wave function of the form $e^{-\frac{1}{2}|z|^2} z^P$ will have its maximum at distance $|z| = \sqrt{2P}$ from the origin. Thus, the highest power of P in a monomial expansion of (3.8) will give the area covered by the quantum Hall liquid. In a homogeneous liquid all groups will cover the same area $P = N_s + \mathcal{O}(1)$, up to corrections of order unity. The highest monomial power for particle z_i is $P_i = \sum_{i \neq j}^{N_e} M_{ij} - s_i = \sum_j^{N_e} M_{ij} - M_{ii} - s_i$. This gives the equation $P_i = N_s + \mathcal{O}(1)$ valid for all i, which in terms of the M-matrix is $N_s = \sum_j^{N_e} M_{ij}$. Since all N_α particles in group α are identical the K-matrix equation is $N_s = \sum_{\beta=1}^{n} K_{\alpha\beta} N_\beta$ with solution $N_\beta = N_s \sum_\alpha K^{-1}_{\beta\alpha}$. The total number of particles is $N_e = \sum_\alpha N_\alpha$ which gives the filling fraction $\nu = \frac{N_e}{N_s}$ of the fluid as (3.2).

3.4 Quasi-particle braidings and monodromies

Although this thesis focuses on ground state properties, we will briefly discuss how to describe quasi-hole excitations in the chiral hierarchy states. For the case of quasi-electrons, we refer to the original articles[HHV09, SVH11a].

Going back to the Wen-Zee classification, just as the electrons are characterized by the $\mathbf{q}$-vectors, the quasi-particles are characterized by the $\mathbf{l}$-vectors. These $\mathbf{l}$-vectors are dual vectors to the electronic $\mathbf{q}$-vectors as

$$\mathbf{q}_\alpha \cdot \mathbf{l}_\beta = \delta_{\alpha\beta}.$$

The quasi-particles have trivial braiding with the electrons and statistical angles given by

$$\theta_{\alpha\beta} = K^{-1}_{\alpha\beta}.$$

The charges of the fundamental quasi-holes are $q_\alpha = -\sum_\alpha K^{-1}_{\alpha\beta}$. The corresponding CFT operators describing the quasi-holes are given by

$$H_\alpha(\eta) = e^{\imath \mathbf{l}_\alpha \vec{\phi}(\eta)}.$$

The simplest example is the Laughlin case where there is a single hole operator $H(\eta) = e^{\imath \frac{1}{\sqrt{q}}\phi(\eta)}$ with statistical phase $\theta = \frac{1}{q}$. Inserting a M of these operators in

*The abbreviation can also the thought of as introducing a larger axillary M-matrix of size $N_e \times N_e$ with one entry for every particle pair $z_i - z_j$.

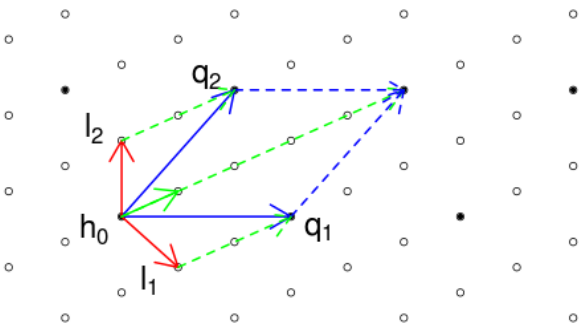

Figure 3.1: The charge lattice Γ of the $\nu = \frac{2}{5}$ K-matrix with $\mathbf{q}_1 = \left(\frac{3}{\sqrt{3}}, 0\right)$ and $\mathbf{q}_2 = \left(\frac{2}{\sqrt{3}}, \frac{5}{\sqrt{15}}\right)$. The figure also displays the dual lattice $\Gamma^\star = \{\sum_{\alpha=1}^{n} n_\alpha \mathbf{l}_\alpha; n_\alpha \in \mathbb{Z}\}$, generated by the vectors $\mathbf{l}_1 = \left(\frac{-1}{\sqrt{3}}, \frac{2}{\sqrt{15}}\right)$ and $\mathbf{l}_2 = \left(0, \frac{3}{\sqrt{15}}\right)$. Duality here means that $\mathbf{q}_\alpha \cdot \mathbf{l}_\beta = \delta_{\alpha\beta}$. Open circles ($\circ$) denote $\Gamma^\star$ and dots ($\bullet$) denote Γ. A unit cell of Γ is spanned by $\mathbf{q}_\alpha$ (blue) and a unit cell of $\Gamma^\star$ is spanned by $\mathbf{l}_\beta$ (red). The quotient group $\Gamma^\star/\Gamma$ is a finite subset of $\Gamma^\star$, constructed by equating all points in $\Gamma^\star$ related by a vector in Γ. The elements in $\Gamma^\star/\Gamma$ are given by the points in the (blue) parallelogram. Note that $\Gamma^\star/\Gamma$ has a finite number of elements that are all proportional to $\mathbf{h}_0 = \mathbf{l}_1 + \mathbf{l}_2$ (green).

(3.4) gives the multi-hole wave function

$$\begin{aligned}\Psi_q(\eta_1 \dots \eta_M; z_1 \dots z_N) &= \\ &= e^{-\sum_{i=1}^{M} \frac{1}{4q}|\eta_i|^2} e^{-\sum_{i=1}^{N} \frac{1}{4}|z_i|^2} \times \\ &\quad \times \prod_{i<j}^{N} (z_i - z_j)^q \prod_{i,j}^{N,M} (z_i - \eta_j) \prod_{i<j}^{M} (\eta_i - \eta_j)^{\frac{1}{q}} . \end{aligned} \tag{3.9}$$

Note that during the interchange of two quasi-holes at η_1 and η_2, a phase $\theta = \frac{1}{q}$ is picked up from the factor $(\eta - \eta)^{\frac{1}{q}}$. As discussed below this *monodromy* has, under certain assumptions, the interpretation of a fractional statistics phase as the particles are braided. Also note that the wave function vanishes at the positions of the holes, reflecting the fractional charge of the excitation.

A simple example: At level 2 are the two hole operators in the $\nu = 2/5$ state with $\mathbf{l}_1 = \left(\frac{-1}{\sqrt{3}}, \frac{2}{\sqrt{15}}\right)$ and $\mathbf{l}_2 = \left(0, \frac{3}{\sqrt{15}}\right)$. As the inverse K-matrix is $K^{-1} = \frac{1}{5}\begin{pmatrix} 3 & -2 \\ -2 & 3 \end{pmatrix}$ the mutual statistics of the two quasi-holes are $\theta_{11} = \theta_{22} = \frac{3}{5}$ and $\theta_{12} = -\frac{2}{5}$. The charges of the two quasi-holes are $q_1 = q_2 = -\left(\frac{3}{5} - \frac{2}{5}\right) = -\frac{1}{5}$. The quasi-particle charge vectors are illustrated in Figure 3.1.

Note that for Ψ_q in (3.9) to constitute a proper electronic wave function we need to add a normalization constant $\mathcal{N}_\eta$. We use the subscript η to emphasize that $\mathcal{N}_\eta$ depends parametrically on the positions η_i of the quasi-particles. This η-dependence of $\mathcal{N}_\eta$ can influence the braiding properties of two quasi-holes in the wave function. There could be an additional Berry phase[Ber84] added to the

monodromy $\theta = \frac{1}{q}$ as η_i is adiabatically dragged around η_j. In the case where $\mathcal{N}_\eta$ really is constant – independent of η_i – the extra berry phase would vanish and the monodromy of adiabatic evolution would equal the true statistics, *i.e.* the *holonomy*.

In his original construction, Laughlin used a plasma analogy to argue that the quasi-holes had fractional charge[Lau83]. The analogy with the charged plasma worked by identifying (3.9) with the partition function of a single component plasma, which was known to be screening. Later, Arovas *et. al.*[ASW84] extended Laughlin's argument. They argued that at large separation of the quasi-holes, there is no η-dependence in the normalization of (3.9). As a consequence they proved that the charge and statistics of the quasi-holes indeed is fractional[ASW84], but the notion of a plasma analogy was still crucial. In the Laughlin case, the plasma analogy can be proven to hold, but for more complicated filling fractions it still remains an hypothesis, albeit very useful. Only in a few other cases can the plasma analogy, or a generalization of it, be proven to hold. However, in all those cases, the description is only of a single component plasma[Rea09]. For multi-component wave functions, where the analogous plasma would be much more complicated, there are indications that the plasma would also be screening[BGN11].

3.5 CFT wave functions from full correlators

In arriving at (3.8) we have swept some details under the carpet. Some of these details will be important when we construct wave functions on torus and we therefore discuss them in this section.

3.5.1 Conformal blocks

When evaluating correlation functions in CFT one must in general consider the full correlation function $\langle \mathcal{O}_{\text{bg}} \prod_i V_i(z_i, \bar{z}_i)\rangle$, instead of only the chiral halves $\langle \mathcal{O}_{\text{bg}} \prod_i V_i(z_i)\rangle$ that where considered earlier in this chapter. On the plane the full correlator decouples into chiral and anti-chiral correlators as

$$\left\langle \mathcal{O}_{\text{bg}} \prod_i^{N_e} V_i(z_i, \bar{z}_i) \right\rangle_{\text{Plane}} = \left\langle \mathcal{O}_{\text{bg}} \prod_i^{N_e} V_i(z_i) \right\rangle \cdot \left\langle \mathcal{O}_{\text{bg}} \prod_i^{N_e} \bar{V}_i(\bar{z}_i) \right\rangle, \tag{3.10}$$

but this is not true in general. Instead the general CFT correlation function will be a sum of products of chiral and non-chiral conformal blocks

$$\left\langle \mathcal{O}_{\text{bg}} \prod_i^{N_e} V_i(z_i, \bar{z}_i) \right\rangle = \sum_i c_i \Psi_i(\{z\}) \bar{\Psi}_i(\{\bar{z}\}). \tag{3.11}$$

Here $\Psi_i(\{z\})$ is a chiral *conformal block*, holomorphic in the coordinates $\{z\}$ and $\bar{\Psi}_i(\{\bar{z}\})$ is an anti-chiral conformal block that depends anti-holomorphically on the coordinates $\{\bar{z}\}$. The number of conformal blocks and the weights c_i depends on the precise type of CFT as well as the genus of the surface the CFT is defined on.

In the simplest cases of abelian hierarchy states on the plane, then there is only one conformal block and the CFT decouples into one chiral and one anti-chiral block as in (3.10). On the torus there is no such decoupling and for the Hierarchy states at $\nu = \frac{p}{q}$ the number of conformal blocks precisely equals q. This is also the expected ground state degeneracy of the torus.

3.5.2 Derivative operators

In the language of CFT, we differentiate between primary operators such as $e^{\imath \mathbf{q}_\alpha \cdot \boldsymbol{\phi}(z)}$ and descendant operators such as $\partial_z e^{\imath \mathbf{q}_\alpha \cdot \boldsymbol{\phi}(z)}$. In the hierarchy, these descendants appear when the quasi-particles condense to form a new filling fraction. Mathematically this is the fusing of a quasi-particle $\mathcal{P}(\eta)$ and an electron $V_1(z)$, which in the limit of $\eta \to z$ has first order poles at $\eta = z$. The resulting, regularized, operator is given by the most singular piece of the operator product expansion around z:

$$\lim_{\eta \to z} \mathcal{P}(\eta) V_1(z) = \frac{\partial_z V_2(z)}{z - \eta} + \text{less singular terms.}$$

For our purposes, this fusing gives rise to extra derivatives that act on the primary operators. In the composite fermions picture[Jai07], the same derivatives are remnants of $\bar{z}$ components as the composite fermions in higher effective Landau level wave functions are projected down to the LLL.

When computing correlation functions of descendant fields the derivatives can be extracted to act on the correlation function of the remaining primary operators. Mathematically this means that we can pull the derivatives to the lefts as $\left\langle \mathcal{O}_{\text{bg}} \prod_i \partial_{z_i}^{s_i} e^{\imath \mathbf{q}_i \cdot \boldsymbol{\phi}(z)} \right\rangle = \prod_i \partial_{z_i}^{s_i} \left\langle \mathcal{O}_{\text{bg}} \prod_i e^{\imath \mathbf{q}_i \cdot \boldsymbol{\phi}(z)} \right\rangle$. The remaining correlation function

$$\psi_{\text{Primary}} = \left\langle \mathcal{O}_{\text{bg}} \prod_i e^{\imath \mathbf{q}_i \cdot \boldsymbol{\phi}(z)} \right\rangle, \tag{3.12}$$

is now identified as a *conformal block* of primary fields. We stress the possibility to first evaluate the primary correlation function, and afterwards act with the derivatives as this approach will be used also on the torus geometry.

To connect the above discussion with FQH wave functions in the LLL we schematically have the procedure

$$\psi_{\text{FQH}} = \mathcal{A} \left\{ \prod_i \partial_{z_i}^{s_i} \psi_{\text{Primary}} \right\}, \tag{3.13}$$

to produce electronic wave functions on any geometry. Note that in the preceding discussion we have been sloppy and have not properly taken the effect of the background operator $\mathcal{O}_{\text{bg}}$ into account. When doing so, the factor $\exp\left(-\frac{1}{4}\sum_i |z_i|^2\right)$ present in ψ_{Primary} will yield terms containing $\bar{z}$. To account for this the true action of the derivatives looks like

$$\psi_{\text{FQH}} = \mathcal{A} \left\{ \prod_i D_{z_i}^{s_i} \psi_{\text{Primary}} \right\},$$

in order to reproduce the result of (3.8). In the above equation $D_z = \partial_z + \frac{1}{4}\bar{z}$ is a covariant derivative as it produces the correct derivative factor when acting on $e^{-\frac{1}{4}|z|^2}$, *i.e.* $D_z e^{-\frac{1}{4}|z|^2} f(z) = e^{-\frac{1}{4}|z|^2}\partial_z f(z)$.

A major theme in this thesis is to find a way to write the planar wave function (3.13) on a toroidal geometry. In doing so we will find that neither ∂_z nor D_z complies with the quasi-periodic boundary conditions of the torus. In Chapter 6 we will therefore construct a torus version of the derivatives. Note that D_z contains an extra term that is not a derivative, but we will refer to this combination as a derivative since that is what remains after it has acted on the exponential factor $e^{-\frac{1}{4}|z|^2}$. For details about the non-commutativity of D_z and the boundary conditions, we refer to Appendix B.

3.5.3 An example, the $\nu = \frac{2}{5}$ state

As a simple concrete example, let us consider the $\nu = \frac{2}{5}$ wave function. This state is reached in the hierarchy scheme by condensing quasi-electrons in the $\nu = \frac{1}{3}$ Laughlin state. The $K-$matrix is $K = \begin{pmatrix} 3 & 2 \\ 2 & 3 \end{pmatrix}$, so there are two groups $\alpha = 1, 2$. We will here refer to them as w and z to keep things explicit and to emphasise that not all electrons are treated equally. The two groups are equal in size and contains $N_z = N_w = \frac{1}{2}N_e$ particles. The charge lattice can be chosen as $\mathbf{q}_z = \left(\frac{3}{\sqrt{3}}, 0\right)$, $\mathbf{q}_w = \left(\frac{2}{\sqrt{3}}, \frac{5}{\sqrt{13}}\right)$, though numerous other choices exist too*. This particular choice of charge lattice gives the electron operators

$$V_w(w) = e^{\imath\sqrt{3}\phi_1(w)} \qquad V_z(z) = \partial_z e^{\imath\frac{2}{\sqrt{3}}\phi_1(z)+\imath\sqrt{\frac{5}{3}}\phi_2(z)}.$$

The derivative in V_z appears though the fusing of quasi-particles in the $\nu = \frac{1}{3}$ state, described by V_w alone. Because of the asymmetry between z ans w, the full many-body wave function needs to be anti-symmetrized at the end of the calculation in accordance with (3.13). When calculating the trial wave functions in a planar geometry, the correlator can be factorized such that the derivatives are outside of the correlator. The trial wave functions are then calculated as

$$\psi_{\frac{2}{5}} = \prod_j D_{z_j} \left\langle \mathcal{O}_{\text{bg}} \prod_{i=1}^{\frac{N_e}{2}} V_w(w_i) \cdot \prod_{j=1}^{\frac{N_e}{2}} \hat{V}_z(z_j) \right\rangle.$$

Here $\hat{V}_z(z)$ is the electron operator without a derivative, such that $V_z(z) = \partial_z \hat{V}_z(z)$. Evaluating the correlation function and acting on it with D_z gives

$$\begin{aligned}\Psi_s(\{z\},\{w\}) = e^{-\frac{1}{4}\sum_{i=1}^{\frac{N_e}{2}}\left(|z|_i+|w|_i+y_{z_i}^2\right)} \times \\ \times \prod_j \partial_{z_j} \cdot \prod_{i<j}(z_i - z_j)^3 \prod_{i,j}(w_i - z_j)^2 \prod_{i<j}(w_i - w_j)^3, \quad (3.14)\end{aligned}$$

*One choice is the more symmetric $\mathbf{q}_z = \left(\frac{5}{\sqrt{10}}, \frac{1}{\sqrt{2}}\right)$, $\mathbf{q}_w = \left(\frac{5}{\sqrt{10}}, -\frac{1}{\sqrt{2}}\right)$.

which is a special case of (3.7). This procedure may seem as overkill since (3.14) can more easily be inferred directly from K. But it is indeed of importance and we show the CFT construction already in the planar setting because on the torus such a construction will be essential. The extra difficulty on the torus comes from a centre of mass piece that is hard to construct from the K-matrix alone.

3.6 CFT wave functions for the full hierarchy

The CFT construction can also be applied to the full hierarchy, where condensations of quasi-holes also are present. In this more general setting the eigenvalues of the K-matrix are not all positive definite and the procedure above will produce non-normalizable wave functions. To handle this, the K-matrix is rewritten as $K = \kappa - \bar{\kappa}$ and the full correlation function is the computed. From the full correlation function the chiral conformal blocks of κ are kept, as well as the anti-chiral conformal blocks of $\bar{\kappa}$. Due of the presence of the anti-holomorphic components the resulting wave function will not reside in the LLL and thus needs to be projected to the LLL. The various methods for projecting will not be the topic of this thesis and we will not discuss it further here.

Chapter 4

Mathematical Details for the Torus

The properties of the torus will be essential for our analysis in the coming chapters and we therefore discuss background mathematical details in this chapter. We will define the magnetic algebra needed in the presence of a magnetic field and discuss the single particle wave functions that diagonalize the Landau Hamiltonian.

4.1 The torus itself

What exactly is a torus? In simple words, a torus means a surface with periodic boundary conditions in two directions. We can think of the torus as a doughnut, such as the one depicted in the right panel of Figure 4.1. Yet, we should remember that our mathematical torus is not only globally, but also locally, flat.

Mathematically the torus is characterized by two lattice vectors $\mathbf{L}_1 = L_x\hat{\mathbf{x}}$ and $\mathbf{L}_2 = L_\Delta\hat{\mathbf{x}} + L_y\hat{\mathbf{y}}$, . This geometry is depicted in the left panel of Figure 4.1. We should think of L_x and L_y as the width and height of the torus respectively, and L_Δ as the skewed distance of the torus. The lattice $\{\mathbf{R}_{nm} = \mathbf{L}_1 n + \mathbf{L}_2 m; n, m \in \mathbb{Z}\}$ that is generated by $\mathbf{L}_1$ and $\mathbf{L}_2$ should be though of as a lattice of identified points. This imposes the constraint on any torus wave function ψ, that $|\psi(\mathbf{r} + \mathbf{R}_{nm})| = |\psi(\mathbf{r})|$. In the equation we only specify the magnitude of the wave functions because the phases at different $\mathbf{R}_{nm}$ will not all be the same, and are related by gauge transformations.

With the identification above, we can reduce all statements regarding the torus to the fundamental domain spanned by $\mathbf{L}_1$ and $\mathbf{L}_2$. We define a dimensionless complex parameter $\tau = \tau_1 + \imath\tau_2$ that encodes the shape of the torus as

$$\tau = \frac{1}{L_x}\left(L_\Delta + \imath L_y\right), \tag{4.1}$$

where $\tau_1 = \frac{L_\Delta}{L_x}$ and $\tau_2 = \frac{L_y}{L_x}$. Since we assume that L_x and L_y are positive lengths, it puts τ in the upper half of the complex plane. We will later, in Section 6.2 find that several values of τ actually describe the same physical torus.

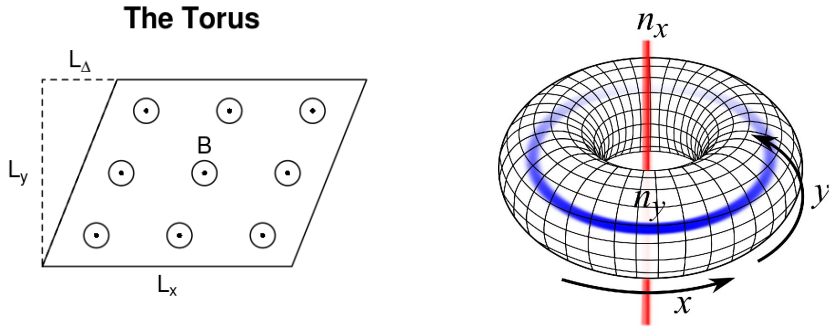

Figure 4.1: *a*) The toroidal geometry: Width L_x, height L_y, skewness L_Δ. All points on the lattice $\mathbf{r} = n\mathbf{L}_1 + m\mathbf{L}_2 = (nL_x + mL_\Delta)\,\hat{\mathbf{x}} + mL_y\hat{\mathbf{y}}$ are identified. *b*) Changing the boundary conditions is equivalent to inserting fluxes through the two cycles of the torus. As fluxes n_x and n_y are inserted, the positions of all the states are transported along the principal directions of the torus. Changing the boundary conditions by 2π is equivalent to adding one unit of flux.

The Landau Hamiltonian will be introduced in the next section and we will find that in order to ensure single-valued wave functions, the area of the torus has to be

$$L_x L_y = 2\pi N_s \ell_B^2.$$

Here N_s is an integer equal to the number of flux quanta that pierce the torus. We can thus express L_x, L_y and L_Δ in terms of the two parameters τ and N_s.

As the torus is a flat two-dimensional surface, we can use complex numbers z as coordinates. We will consider two different parametrizations of the complex number z. The first is the physical Cartesian parametrisation

$$z = \tilde{x} + i\tilde{y},$$

where $0 \le \tilde{x} \le L_x$ and $0 \le \tilde{y} \le L_y$. We put a $\sim$ on x and y to distinguish them from the other set of parameters (τ- coordinates)

$$z = L_x\,(x + \tau y)\,, \tag{4.2}$$

where $0 \le x, y \le 1$ are defined on a unit square. This parametrization is convenient since the range of x and y are independent of the number of fluxes N_s as well as of the geometry τ, in contrast to $\tilde{x}$ and $\tilde{y}$. We will thus mostly be working the τ-coordinates rather than the physical coordinates. In Appendix B we list the basic relations between the different coordinate systems.

4.2 The Landau Hamiltonian and eigenstates in the lowest Landau level

The Hamiltonian of a free particle moving in two dimensions without any confining potential is $H = \frac{1}{2m}p_{\tilde{x}}^2 + \frac{1}{2m}p_{\tilde{y}}^2$. To arrive at the Landau Hamiltonian, which

describes a particle moving in a magnetic field, we employ minimal substitution $p_j \to p_j - eA_j(\tilde{x}, \tilde{y})$ to add a vector potential to the problem. As this should describe a constant magnetic field perpendicular to the $\tilde{x}\tilde{y}$-plane, it should fulfil $\partial_{\tilde{x}} A_{\tilde{y}} - \partial_{\tilde{y}} A_{\tilde{x}} = B$. For later simplicity, we choose a vector potential that is

$$\vec{A} = \frac{\tilde{y}B}{\tau_2}(\tau_2, -\tau_1).$$

This rather odd-looking choice we will refer too as the τ-gauge, as $\vec{A}$ is perpendicular to $\vec{\tau} = (\tau_1, \tau_2)$, which describes the torus geometry through (4.1). We choose this gauge since it is the natural vector potential in the coordinates x and y. The Landau Hamiltonian in the physical coordinates then becomes

$$H = \frac{1}{2m}(p_{\tilde{x}} - eB\tilde{y})^2 + \frac{1}{2m}\left(p_{\tilde{y}} + eB\frac{\tau_1}{\tau_2}\tilde{y}\right)^2. \tag{4.3}$$

Note that $\tau_1 = 0$ corresponds to using the more ordinary Landau gauge $\vec{A} = B(\tilde{y}, 0)$.

To diagonalize the Hamiltonian above, we note that it is quadratic form in the operators $p_{\tilde{y}}$, $p_{\tilde{x}}$, $\tilde{y}$ and $\tilde{x}$. We can therefore introduce a set of ladder operators a and $a^\dagger$ just as is typically done for the harmonic oscillator[Lan30]. The precise choice of a and $a^\dagger$ depends on the vector potential $\vec{A}$ and is

$$\begin{aligned} a &= \sqrt{2}\left(\partial_{\bar{z}} + \frac{\tau}{2}L_x y\right) = \frac{1}{\sqrt{2}}\left(\partial_{\tilde{x}} - \imath\partial_{\tilde{y}} + \frac{\tau}{\tau_2}\tilde{y}\right) \\ a^\dagger &= -\sqrt{2}\left(\partial_z - \frac{\bar{\tau}}{2}L_x y\right) = -\frac{1}{\sqrt{2}}\left(\partial_{\tilde{x}} + \imath\partial_{\tilde{y}} - \frac{\bar{\tau}}{\tau_2}\tilde{y}\right) \end{aligned}$$

for the τ-gauge. By introducing these two ladder operators above, the Hamiltonian is rewritten as

$$H = \hbar\omega\left(a^\dagger a + \frac{1}{2}\right),$$

with $\left[a^\dagger, a\right] = 1$. Hence, all we know about the harmonic oscillator immediately applies to the Landau problem. We have energy eigenstates with energy $E_n = \hbar\omega\left(n + \frac{1}{2}\right)$, where the cyclotron frequency is $\omega_c = \frac{eB}{mc}$. However, since the Landau Hamiltonian is two-dimensional as compared to the one-dimensional harmonic oscillator, there exists an auxiliary set of operators $t_{m,n}$ which commute with a and $a^\dagger$. We will look more closely at t_{mn} in the next section, but for now merely state that they give rise to a degeneracy at each energy level. An energy level is called a Landau level (LL), and the degeneracy is the same as the number of magnetic fluxes N_s.

By studying the destruction operator a, it is possible to show that all wave functions in the lowest Landau level (LLL) – where $n = 0$ – will have the structure

$$\psi_{\mathrm{LLL}} = e^{\imath\pi\tau N_s y^2} f(z). \tag{4.4}$$

Here $f(z)$ is a purely holomorphic function subject to the boundary conditions of the torus.

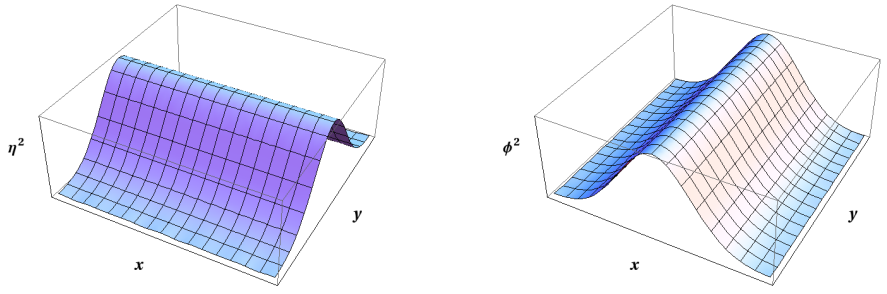

a) *b)*

Figure 4.2: Density profiles for lowest Landau level eigenstates of the $t_1$and t_2 translation operators. *a)* The t_1 eigenstates are Gaussian in the y-direction whereas *b)* the t_2 eigenstates are Gaussian in the x-direction.

As will be explained in detail in Section 4.3, there are two translation operators t_1 and t_2 that generate all the other operators. The first, t_1, moves a coordinate one N_s:th step in the $\mathbf{L}_1$ direction whereas t_2 moves similarly in the $\mathbf{L}_2$-direction. We can choose to express the LLL wave functions as eigenfunctions of t_1, and arrive at the wave functions

$$\begin{aligned}\eta_s(z) &= \frac{1}{\sqrt{L_x\sqrt{\pi}}}\sum_t e^{-\imath 2\pi(s+N_s t)x} e^{\imath\pi\tau N_s\left(y-t-\frac{s}{N_s}\right)^2} \\ &= \frac{e^{\imath\pi\tau N_s y^2}}{\sqrt{L_x\sqrt{\pi}}}\vartheta\begin{bmatrix} -\frac{s}{N_s} \\ 0 \end{bmatrix}\left(\frac{N_s}{L_x}z\middle|N_s\tau\right). \end{aligned} \tag{4.5}$$

In equation (4.5), the generalized quasi-periodic Jacobi ϑ-function is introduced, as it has the correct quasi-periodicity for the torus. The definition of ϑ is found in equation (A.1) in the Appendix, which contains a collection of useful formulae related to the Jacobi ϑ-functions. We have chosen the definition of η_s such that the support of the wave function is centred over the coordinate $y = \frac{s}{N_s}$. This can be seen in Figure 4.2. As η_s is an eigenfunction of t_1, it forms a (discretized) standing wave in the x-direction with eigenvalues $t_1^n\eta_s = e^{-\imath 2\pi\frac{ns}{N_s}}\eta_s$. With t_2 we cycle through the basis as $t_2^n\eta_s = \eta_{s-n}$. From equations (4.5) and (A.3), it is easy to see that there are N_s linearly independent basis states, as $\eta_{s+N_s} = \eta_s$.

The basis η_s consists of eigenfunctions of t_1, but it is also possible to instead construct eigenfunctions of t_2. Since we know that the phase that accompanies commutation of t_1^m and t_2^n is $e^{\imath 2\pi\frac{mn}{N_s}}$, the eigenfunctions of t_2 can formally be written as $\varphi_l(z) = \frac{1}{\sqrt{N_s}}\sum_s e^{-\imath 2\pi\frac{ls}{N_s}}\eta_s(z)$. Using the transformation property (A.10) of the ϑ-function under Fourier sums, the eigenfunctions of t_2 can immediately be expressed as

$$\varphi_l(z) = \frac{e^{\imath\pi\tau N_s y^2}}{\sqrt{N_s L_x\sqrt{\pi}}}\vartheta\begin{bmatrix} 0 \\ \frac{l}{N_s} \end{bmatrix}\left(\frac{1}{L_x}z\middle|\frac{\tau}{N_s}\right). \tag{4.6}$$

A graph of the φ_l states are shown in Figure 4.2. A more physical approach to constructing φ_l can be taken by noticing that all the physics should be invariant under the identification $\mathbf{L}_1 \to \mathbf{L}_2$ and $\mathbf{L}_2 \to -\mathbf{L}_1$. This is equivalent to a rotation of the coordinate system. Seen from this point of view, φ_l can be obtained from η_s with the use of (A.9) and without the need to explicitly utilize the Fourier summation. This is done by performing the modular transformation $\tau \to -\frac{1}{\tau}$, while letting $z \to \frac{|\tau|}{\tau} z$, and applying the appropriate gauge transformation connected with the rotation described above.

4.3 Magnetic translation operators

When constructing the operators a and $a^\dagger$ to diagonalize the Hamiltonian (4.3), we mentioned that there exists a set of operators $t_{m,n}$ that act within each degenerate LL. In this section we describe these translation operators.

We seek a set of operators that commute with H, *i.e.* commutes with a and $a^\dagger$. These operators are called guiding centre coordinates R_x, R_y and are given by

$$\begin{aligned} R_x &= -\imath \frac{\partial_y}{2\pi N_s} + x \\ R_y &= \imath \frac{\partial_x}{2\pi N_s}. \end{aligned}$$

We call these "guiding centre coordinates" as R_x and R_y give the position expectation value of a wave function. To illustrate this, we look at the t_1 and t_2 basis functions (4.5) and (4.6) again. This time we approximate the torus by the infinite plane and only keep the leading terms, giving

$$\begin{aligned} \eta_s(z) &\approx \mathcal{N}_\eta e^{\imath\pi\tau N_s\left(y-\frac{s}{N_s}\right)^2} e^{-\imath 2\pi s x} \\ \varphi_l(z) &\approx \mathcal{N}_\varphi e^{-\imath\pi\frac{N_s}{\tau}\left(x+\frac{l}{N_s}\right)^2} e^{-\imath 2\pi N_s y\left(x+\frac{l}{N_s}\right)} \end{aligned}$$

where we used (A.8) to obtain the expression for $\varphi_l(z)$. Note that η_s contains $y - \frac{s}{N_s}$ and φ_l contains $x + \frac{l}{N_s}$ which means that η_s is centred around $y = \frac{s}{N_s}$ and φ_l is centred around $x = -\frac{l}{N_s}$. We can also extract this informations using R_x and R_y since $R_y\eta_s(z) \approx \frac{s}{N_s}\eta_s(z)$ and $R_x\varphi_l(z) \approx -\frac{l}{N_s}\varphi_l(z)$. Thus, on the infinite plane η_s is an eigenstate of R_x and φ_l is an eigenstate of R_y. The guiding centre coordinate expectation values are

$$\begin{aligned} \langle \eta_s | R_y | \eta_s \rangle &\approx \frac{s}{N_s} \\ \langle \varphi_l | R_x | \varphi_l \rangle &\approx -\frac{l}{N_s}, \end{aligned}$$

where the approximate-sign can be made into an equal-sign if the integration region is chosen wisely*. Note that $[R_y, R_x] = \frac{\imath}{2\pi N_s}$, which reflects that position in x and y can not simultaneously be defined with arbitrary precision within a LL. This is

*The appropriate integration bounds for η_s are $-\frac{1}{2} < y - \frac{s}{N_s} < \frac{1}{2}$ and for φ_l they are

nothing more than a real space version of the Heisenberg uncertainty principle, but this time it is x and y that are non-commuting within a LL instead of x and p_x.

From R_x and R_y, we may define a magnetic translation operator as $t(\mathbf{l}) = \exp\left[\imath 2\pi N_s \left(l_y R_x - l_x R_y\right)\right]$ that commutes with H and moves $(x, y) \to (x + l_x, y + l_y)$ while also performing an appropriate gauge transformation. For the Hamiltonian without a magnetic field $H_{B=0} = \frac{\mathbf{p}^2}{2m}$, the translation operator in the real space coordinates $(\tilde{x}, \tilde{y})$ is the ordinary $t_{B=0}(\mathbf{r}) = e^{\mathbf{r}\cdot\nabla}$, that has the effect $t_{B=0}(\mathbf{r})\,\psi(\mathbf{x}) = \psi(\mathbf{x}+\mathbf{r})$. In a magnetic field $[H, t_{B=0}] \neq 0$, and the operator $t(\mathbf{r})$ that translates a wave function in some direction $\mathbf{r}$ is more complicated

$$t(\mathbf{r}) = \exp\left[\mathbf{r}\cdot\nabla + \imath\frac{r_y}{\ell_B^2}\left(\tilde{x} - \frac{\tau_1}{\tau_2}\tilde{y}\right)\right] = \exp\left[\mathbf{r}\cdot\nabla + \imath\frac{r_y}{\ell_B^2}L_x x\right],$$

where for clarity the magnetic length ℓ has been restored.

The first part of $t(\mathbf{r})$ is the same as for the free Hamiltonian. The second part of $t(\mathbf{r})$ encodes the gauge transformation that is needed for $t(\mathbf{r})$ to commute with H. When convenient, the complex notation $t(r_x + \imath r_y) \equiv t(r_x\hat{\mathbf{x}} + r_y\hat{\mathbf{y}})$ will be used, and the magnetic length ℓ_B will be set to $\ell_B = 1$. For translations in the $\tilde{x}$ and $\tilde{y}$ directions, we may evaluate the effect of the translation operator as

$$\begin{aligned} t(r_x\hat{\mathbf{x}})\,f(\tilde{x},\tilde{y}) &= f(\tilde{x}+r_x,\tilde{y}) \\ t(r_y\hat{\mathbf{y}})\,f(\tilde{x},\tilde{y}) &= f(\tilde{x},\tilde{y}+r_y)\exp\left[\imath r_y\left(\tilde{x}-\frac{\tau_1}{\tau_2}\tilde{y}\right)\right]\exp\left[-\imath\frac{1}{2}r_y^2\frac{\tau_1}{\tau_2}\right]. \end{aligned}$$

Just as $\tilde{x}$ and $p_{\tilde{x}}$ do not commute for a particle in the absence of a magnetic field, neither do magnetic translations in different directions commute. We rather have a magnetic algebra

$$t(\gamma)\,t(\delta) = t(\delta)\,t(\gamma)\,e^{\frac{\imath}{2}\Im\left(\gamma\bar{\delta}\right)}, \tag{4.7}$$

such that when translating around a closed loop, we pick up a phase equal to the area enclosed by the loop, in units of ℓ_B^2. Since the torus has a closed surface, and there should be no ambiguity in the phase depending on which side of the loop we choose as the interior, there is a constraint on the area of the torus to be $A_{\text{torus}} = L_x L_y = 2\pi N_s \ell_B^2$.

The periodic boundary conditions are implemented as

$$\begin{aligned} t(L_x)\,\psi(z) &= e^{\imath\phi_1}\psi(z) \\ t(\tau L_x)\,\psi(z) &= e^{\imath\phi_2}\psi(z), \end{aligned} \tag{4.8}$$

where $\psi(z)$ is a wave function and the phase angles ϕ_i have the physical interpretation of fluxes threading the two cycles of the torus. This is illustrated in Figure 4.1b. The physical effects of changing ϕ_j is that all states on the torus will

$-\frac{1}{2} < x + \frac{l}{N_s} < \frac{1}{2}$. The integration region should thus be chosen to be symmetric around the naïve guiding centre expectation value. The fact that the expectation value depends on the precise integration domain over the torus is a refection of the fact that R_x and R_y do not respect the periodic boundary conditions of the torus, a common theme in this thesis. The effect of changing the integration region was discussed in **Paper II**.

shift their positions a distance $(x,y) \to \left(x + \frac{\phi_2}{2\pi N_s}, y + \frac{\phi_1}{2\pi N_s}\right)$. Even though ϕ_j and $\phi_j + 2\pi$ represents the same boundary conditions, there is a flow of the single particle orbitals as $\eta_s \to \eta_{s+1}$ under the change $\phi_2 \to \phi_2 + 2\pi$. In the case of $\phi_1 \to \phi_1 + 2\pi$, the corresponding statement is true for $\varphi_l \to \varphi_{l+1}$.

As a direct consequence of the imposed boundary conditions on the torus, not all translation operators $t(\mathbf{r})$ preserves these boundary conditions. If we wish to stay within a sector defined by specific of boundary conditions, then by necessity $[t(\mathbf{r}), t(L_x)] = [t(\mathbf{r}), t(\tau L_x)] = 0$ and only a subset of $t(\mathbf{r})$ satisfy this condition. These translation vectors fall on the lattice $\Gamma = \frac{L_x}{N_s}(n + \tau m)$, for integers n and m, and provide one reason why the τ-coordinates in (4.2) are useful. In terms of these, the sub-lattice of translations that preserve the boundary conditions (4.8) are parametrized simply as $(x,y) = \frac{1}{N_s}(m,n)$. The operators that map out this lattice are

$$t_{m,n} = e^{\frac{1}{N_s}(\partial_x m + \partial_y n + \imath 2\pi N_s n x)}, \tag{4.9}$$

which translate in the two main directions on the sub-lattice. For future reference, we also introduce the shorthand notation

$$\begin{aligned} t_1 &\equiv t_{1,0} \\ t_2 &\equiv t_{0,1} \end{aligned}$$

for the elementary translation operators. These operators have η_s and φ_l from equations (4.5) and (4.6) as their eigenstates. These finite translation operators form a simple commutator algebra

$$t_{m,n} t_{m',n'} = t_{m',n'} t_{m,n} e^{\imath 2\pi \frac{1}{N_s}(mn' - m'n')}, \tag{4.10}$$

which form a subset of (4.7). From this, it is clear that $t_1^{N_s}$and $t_2^{N_s}$ which correspond to translations along the full cycles of the torus, commutes with any $t_{m,n}$.

As we will later use translation operators that operate on all particles, we introduce the many-body translation operators

$$T_{m,n} = \prod_{i=1}^{N_e} t_{m,n}^{(i)}, \tag{4.11}$$

which acts on all particles with coordinates z_i. On a torus where the filling fraction $\nu = \frac{N_e}{N_s}$ is $\nu = \frac{p}{q}$ with p and q relatively prime, the commutation relations (4.10) translate into

$$T_{m,n} T_{m',n'} = T_{m',n'} T_{m,n} e^{\imath 2\pi \frac{p}{q}(mn' - m'n')},$$

showing that the degeneracy of the many-body state on the torus is a multiple of q[Hal85]. This is because $T_{m,n}$ will commute with not only the single particle Hamiltonian but any translationally invariant interaction, and can therefore be used to label the different many-body states. We define the two minimal many-body operators as

$$\begin{aligned} T_1 &= T_{1,0} \\ T_2 &= T_{0,1}, \end{aligned}$$

and note that $[T_1, T_2^q] = [T_1^q, T_2] = 0$. In Chapter 5 we till construct wave functions that are eigenfunctions of T_1 and we will see that T_2 transforms these wave functions into each other.

Chapter 5

The CFT Approach to QH-states on the Torus

In this chapter and the next, we will construct the torus version of the hierarchy states. This first chapter deals with finding the primary wave function ψ_{Primary}. The next chapter explains how to handle the derivatives ∂_z that appear in (3.8).

Let us repeat the strategy to compute ψ_{Primary} using the CFT machinery. We first define the vertex operators V_α that carry the information contained in K-matrix. We also define a background operator $\mathcal{O}_{\text{Bg}}$ with the opposite total charge as all the V_α:s. The correlation function $\langle \mathcal{O}_{\text{Bg}} \prod_i V_i(z_i, \bar{z}_i) \rangle$ containing the vertex operators and the background operators is then evaluated. From the correlator we extract the chiral functions $\Psi_{\mathbf{F}}$. These function are the building blocks of the chiral primary blocks $\Psi_{\mathbf{h},\mathbf{t}}$. The $\Psi_{\mathbf{h},\mathbf{t}}$ are constructed as linear combinations of $\Psi_{\mathbf{F}}$ that satisfy all the single particle boundary conditions. As a final step we identify $\Psi_{\mathbf{h},\mathbf{t}}$ with the primary electronic wave function ψ_{Primary}.

5.1 Primary correlation functions on the torus

We are now in a position to construct primary quantum Hall wave functions on the torus. These will be constructed from the sums of products of conformal blocks that make up the correlation function of primary fields. On the torus, the factorization into holomorphic and anti-holomorphic primary fields, with corresponding factorization of the correlation functions can however not be accomplished because the zero-modes in $\phi(z, \bar{z})$. These zero-modes may wind around the torus handles and hence couples the holomorphic and anti-holomorphic pieces together. We will therefore be considering the full primary field

$$V_\alpha(z, \bar{z}) = e^{\imath \mathbf{q}_\alpha \cdot \boldsymbol{\phi}(z, \bar{z})} \tag{5.1}$$

instead of the chiral (3.5) that we used on the plane.

On the torus, we use the τ-gauge where the LLL wave functions can be written as

$$\psi_{\text{LLL}} = \exp\left\{ \imath \pi \tau N_s \sum_{i=1}^{N_e} y_i^2 \right\} \cdot f(\{z_i\}).$$

Note that the Gaussian pre-factor differs from the one on the plane. Also, we now have a ground state degeneracy that can be divided by the denominator q, of the filling fraction $\nu = \frac{p}{q}$[Hal85]. For the simplest abelian FQH states such as $\nu = \frac{1}{3}, \frac{2}{5}, \frac{3}{7}, \ldots$, the degeneracy exactly equals q. On the torus the CFT approach will be essential to regain proper wave function properties, such as the ground state degeneracy. The ground state degeneracy makes the analysis of the CFT construction outlined in Chapter 3 more involved but the basic set-up is still the same. There are vertex operators given by (5.1) that together with a suitable neutralizing background make up the correlator. As the geometry is different from the plane, the correlation function for the boson is however different and is given by

$$\langle \phi(z,\bar{z})\,\phi(0,0)\rangle = -\ln\left|\frac{L_x\vartheta_1\left(\frac{z}{L_x}\middle|\tau\right)}{\vartheta_1'(0|\tau)}e^{\imath\pi\tau y^2}\right|^2. \tag{5.2}$$

This two-point correlator takes into account the periodicity of the torus. The extra factors of $\frac{L_x}{\vartheta_1'(0|\tau)}$ are chosen such that in the limit of $z \to 0$, the two-point function reduces to the planar one $\langle \phi(z)\,\phi(0)\rangle = -\ln|z|^2$*. Details can be found in Appendix A of **Paper III**.

Just as on the plane, a background operator is needed on the torus to make the correlator charge neutral. The natural choice for such an operator is a as homogeneous background. We use the same operator as in Ref. [HSB+08]

$$\mathcal{O}_{\mathrm{Bg}} = e^{\frac{\imath}{2\pi N_s}\int d^2z\,\mathbf{Q}\cdot\vec{\phi}(z,\bar{z})},$$

which can be thought of as a charge homogeneously smeared out over the torus. All in all this gives the correlator

$$\begin{aligned}&\left\langle \mathcal{O}_{\mathrm{Bg}}\prod_\alpha\prod_{i_\alpha\in I_\alpha}V_\alpha\left(z_{i_\alpha},\bar{z}_{i_\alpha}\right)\right\rangle \propto\\ &e^{-2\pi\tau_2 N_s\sum_{i=1}^{N_e}y_i^2}\prod_{i<j}\left|\vartheta_1\left(\frac{z_i-z_j}{L_x}\middle|\tau\right)\right|^{2M_{ij}}\sum_{\mathbf{F},\bar{\mathbf{F}}}\mathcal{F}_{\mathbf{F}}(\mathbf{Z},\tau)\,\bar{\mathcal{F}}_{\bar{\mathbf{F}}}\left(\bar{\mathbf{Z}},\bar{\tau}\right)\end{aligned} \tag{5.3}$$

where $\mathbf{Z} = \sum_i^{N_e}\mathbf{q}_i z_i = \sum_\alpha \mathbf{q}_\alpha Z_\alpha$ is a centre of mass coordinates (CoM). In the definition of $\mathbf{Z}$ we have also introduced the centre of mass coordinates $Z_\alpha = \sum_{i_\alpha\in I_\alpha} z_\alpha$ for group α.

Before we further investigate the different pieces of the correlator, two remarks are in order. First, the correlator (5.3) is not really in the form given by (3.11), as the sums over $\mathbf{F}$ and $\bar{\mathbf{F}}$ are infinite sums. Only when we impose periodic boundary conditions will we extract the conformal blocks, and they will be our quantum Hall wave functions.

Second, the CoM coordinate $\mathbf{Z} = \sum_\alpha \mathbf{q}_\alpha Z_\alpha$ is not CoM coordinate in the sense of being the equal sum of all the coordinates $\sum_{i=1}^{N_e} z_i$. This can be seen by multiplying with an arbitrary element of Γ, $\mathbf{q} = \sum_\alpha m_\alpha \mathbf{q}_\alpha \in \Gamma$, to get $\mathbf{q}\cdot\mathbf{Z} = \sum_{\alpha,\beta} m_\alpha K_{\alpha\beta} Z_\beta$ such that clearly the different groups come with different weights. In spite of this, we will still refer to $\mathbf{Z}$ as a CoM coordinate.

Let us now examine the different pieces of (5.3) one by one. The Gaussian is the square of the gauge factor needed in the LLL, but since we will be using the

*In a Taylor expansion around $z = 0$ then $\vartheta_1(z|\tau) = z\vartheta_1'(0|\tau) + \mathcal{O}(z^2)$ since $\vartheta_1(0|\tau) = 0$.

τ-gauge on the torus, it is not the factor from (3.4) but rather the one from (4.4). If the background operator would not have been present, the Gaussian piece would also be lacking.*

Next is the square of the Jastrow factor

$$|\psi_{\text{Jastrow}}|^2 = \prod_{i<j} \left| \vartheta_1 \left(\frac{z_i - z_j}{L_x} \middle| \tau \right) \right|^{2M_{ij}},$$

which is a periodic version of the planar Jastrow factor present in (3.8). Just as for the two-point function (5.2) the Jastrow factor reduces to the planar one when $z_i \to z_j$.

The last piece, $\sum_{\mathbf{F},\bar{\mathbf{F}}} \mathcal{F}_{\mathbf{F}}(\mathbf{Z},\tau)\, \bar{\mathcal{F}}_{\bar{\mathbf{F}}}\left(\bar{\mathbf{Z}},\bar{\tau}\right)$, is the new object that appears on the torus as compared to plane. This is a centre of mass piece as it takes as argument the CoM coordinate $\mathbf{Z}$ of all the particles. It is the CoM function that is difficult to construct without the CFT formalism, and it is

$$\mathcal{F}_{\mathbf{F}}(\mathbf{Z},\tau) = e^{\imath\pi\tau\mathbf{F}^2} e^{2\pi\imath\mathbf{F}\cdot\frac{\mathbf{Z}}{L_x}}.$$

The sum over $\mathbf{F}$ and $\bar{\mathbf{F}}$ is really a sum over the integer vectors $\mathbf{e}$ and $\mathbf{m}$ such that $\mathbf{F} = \frac{\mathbf{e}}{\mathbf{R}} + \frac{\mathbf{mR}}{2}$ and $\bar{\mathbf{F}} = \frac{\mathbf{e}}{\mathbf{R}} - \frac{\mathbf{mR}}{2}$, where the vector multiplication and vector division is to be performed 0e10lement by element. Note that $\sum_{\mathbf{F},\bar{\mathbf{F}}} \mathcal{F}_{\mathbf{F}}(\mathbf{Z},\tau)\, \bar{\mathcal{F}}_{\bar{\mathbf{F}}}\left(\bar{\mathbf{Z}},\bar{\tau}\right)$ is real since the correlation function has to be real.

5.2 Primary electronic wave functions

In order to arrive at a physical wave-function from (5.3), the correlator has to be split in a sum of chiral and anti-chiral parts. We do this using the structure of the LLL in (4.4) and get the sum

$$\left\langle \mathcal{O}_{\text{Bg}} \prod_{\alpha} \prod_{i_\alpha \in I_\alpha} V_\alpha\left(z_{i_\alpha}, \bar{z}_{i_\alpha}\right) \right\rangle \propto \sum_{\mathbf{F},\bar{\mathbf{F}}} \Psi_{\mathbf{F}}\left(\{z\},\tau\right) \Psi_{\bar{\mathbf{F}}}\left(\{\bar{z}\},\tau\right).$$

The chiral half we will be working with is given by

$$\Psi_{\mathbf{F}}\left(\{z\},\tau\right) = \mathcal{N}(\tau)\, e^{\imath\pi\tau N_s \sum_{i=1}^{N_e} y_i^2} \prod_{i<j} \vartheta_1\left(\frac{z_i - z_j}{L} \middle| \tau\right)^{M_{ij}} \mathcal{F}_{\mathbf{F}}(\mathbf{Z},\tau), \tag{5.4}$$

where we can identify the Gaussian pre-factor, the Jastrow factor, and a CoM piece. Just as with the planar CFT construction, the absolute normalisation is not known, but the CFT construction provides us with a candidate for the normalization. Later, in Chapter 8, we will use the knowledge of this normalization to compute the viscosity of the quantum Hall state that we have constructed.

The chiral half in (5.4) do not form a proper basis for single particle wave functions since they are not eigenfunctions of the translation operators $t_1^{N_s}$ and $t_2^{N_s}$. Thus the physical wave functions are linear combinations of the chiral conformal

*Actually the whole correlation function would vanish identically since the neutrality condition $\sum_i \mathbf{q_i} = \mathbf{0}$ would not be fulfilled.

blocks in such a way that proper boundary conditions are met. The boundary conditions are determined by two n-dimensional vector quantities $\mathbf{h}$ and $\mathbf{t}$, such that the physical wave function $\Psi_{\mathbf{h},\mathbf{t}}(\{z\},\tau)$ is given by

$$\Psi_{\mathbf{h},\mathbf{t}}(\{z\},\tau) = \sum_{\mathbf{q}\in\Gamma} e^{\imath 2\pi \mathbf{t}\cdot\mathbf{q}} \Psi_{\mathbf{h}+\mathbf{q}}(\{z\},\tau).$$

Depending on the choice of $\mathbf{h}$ and $\mathbf{t}$, the many-body wave function $\Psi_{\mathbf{h},\mathbf{t}}(\{z\},\tau)$ can be made to exhibit not only arbitrary boundary conditions but also to be in different momentum sectors for a given set of boundary conditions. The physical wave functions are

$$\Psi_{\mathbf{h},\mathbf{t}}(\{z\},\tau) = \mathcal{N}(\tau)\, e^{\imath\pi\tau N_s \sum_{i=1}^{N_e} y_i^2} \prod_{i<j} \vartheta_1\left(\frac{z_i - z_j}{L_x}\middle|\tau\right)^{M_{ij}} \mathcal{F}_{\mathbf{h},\mathbf{t}}(\mathbf{Z},\tau), \tag{5.5}$$

where the CoM function with proper boundary properties is

$$\mathcal{F}_{\mathbf{h},\mathbf{t}}(\mathbf{Z},\tau) = \sum_{\mathbf{q}\in\Gamma} e^{\imath\pi\tau(\mathbf{q}+\mathbf{h})^2} e^{\imath 2\pi(\mathbf{q}+\mathbf{h})\cdot(\mathbf{Z}+\mathbf{t})}. \tag{5.6}$$

With no other guidance that proper electronic boundary conditions it might seem that deducing the correct form for the centrer of mass pieces should be difficult. Indeed only the simplest case, which gave rise to the Laughlin wave function, was constructed the intuitive way[Hal85]. This simplest example of a wave function on the torus only has one component, so $n = 1$ and the charge lattice is one-dimensional; $\mathbf{q}_\alpha = \sqrt{q}$. The charges all lie on the line $\mathbf{q} \in \sqrt{q}\cdot\mathbb{Z}$, giving the Laughlin wave function

$$\Psi_{h,t}(\{z\},\tau) = \mathcal{N}(\tau)\, e^{\imath\pi\tau N_s \sum_{i=1}^{N_e} y_i^2} \prod_{i<j} \vartheta_1\left(\frac{z_i - z_j}{L_x}\middle|\tau\right)^{q} \vartheta\begin{bmatrix} h \\ qt \end{bmatrix}(qZ|q\tau), \tag{5.7}$$

where we have parametrised $\mathbf{h} = \sqrt{q}h$ and $\mathbf{t} = \sqrt{q}t$. Periodic boundary conditions are obtained for $t = h = \frac{N_e-1}{2} + \frac{1}{q}\mathbb{Z}$.

The first wave functions for the chiral hierarchy were constructed using an explicit hierarchical CFT construction computed by Hermanns et. al. in Ref. [HSB$^+$08] but with a different form for the CoM functions $\mathcal{F}_{\mathbf{h},\mathbf{t}}$. By studying the structure of the charge lattice Γ for the chiral hierarchies, it can be shown that the two formulations in Ref. [HSB$^+$08] and Ref. [FHS14] are equivalent.

Note that in a physical LL wave function, all electrons should be indistinguishable. However, for the constructed electronic wave functions in (5.5) with $n > 1$, this is not true. The very CFT construction builds in the notion of partitioning the different particles into groups that have certain braiding properties. Thus an anti-symmetrization will be necessary in order to obtain a wave function with indistinguishable particles. Unfortunately, under this anti-symmetrization the wave function (5.5) will vanish identically. The solution in the CFT construction, on the plane, is to apply the derivatives before the anti-symmetrization takes place. The only problem is that on the torus, these derivatives are not well defined. We will show how to solve this problem in next chapter.

As a final remark it should be noted that the primary electronic wave functions in (5.5) are perfectly valid wave functions if we drop the requirement of indistinguishably of the electrons. For instance, with *e.g.* $K = \begin{pmatrix} 3 & 1 \\ 1 & 3 \end{pmatrix}$ then (5.5) is a torus version of a bilayer state; the Halperin 331-state[Hal83b] where electrons in the two layers (or with different spin) *can* be distinguished from each other.

Chapter 6

Derivatives Generalized to the Torus

In this chapter we will address the question of how to construct the torus counterpart of holomorphic derivatives. Regardless of which state in the hierarchy we wish to construct, the method is the same, *i.e.* we construct the trial wave function (5.5) from the conformal blocks building up the correlation functions of electron vertex operators. For the Laughlin state (5.7), this is sufficient. However, for the rest of the hierarchy there is additional complexity needed. The main difference from the Laughlin state is that not all electrons are equivalent. This means: 1) there usually exists more than one type of electron operator V_α; 2) there are external derivatives ∂_z acting on the correlator; and 3) the whole wave functions needs to be anti-symmetrized explicitly, since all electrons are not treated on an equal footing. Taking all of the above considerations into account, the Hierarchy wave functions on the plane may be written as

$$\psi_{\text{Hierarchy}} \propto \mathcal{A}\left\{\prod_i \partial_{z_i}^{s_i} \psi_{\text{Primary}}\right\}, \tag{6.1}$$

where ψ_{Primary} is extracted by evaluating the correlation function of primary fields (3.12). In this equation, $\mathcal{A}$ denotes anti-symmetrization over electrons, and s_i records how many derivatives that act on particle i. The derivatives arise since some of the electron operators $V^{(\alpha)}(z)$ are describing the hierarchical fusing of quasi-particles and electrons. This manifests itself through the appearance of derivatives in the vertex operators $V_\alpha(z) = \partial_z^{s_\alpha} \hat{V}_\alpha(z)$.

Before delving too deeply into the business of derivatives, let us ask what would happen if we just ignored them altogether. The answer is, that the anti-symmetrized wave functions would vanish identically. For the hierarchy states, this can be understood in the framework of composite fermions, where the removal of derivatives amounts to placing more electrons in the LLL than there are single particle orbitals. Thus, some analogue of derivatives must exist to prevent the anti-symmetrization from killing the trial wave function.

Physically, the derivatives also change the orbital angular momentum of the primary wave function. This change in momentum occurs as a consequence of the

derivatives lowering the maximum monomial power of the holomorphic polynomial in (3.8). This change of angular momentum has measurable consequences that we will explore in Chapter 8. Further, it will also yield a physical constraint when the derivatives are generalized to the torus.

Thus, on the torus as well as on the plan we run into problems after constructing the primary wave function in (5.5) if we naively just anti-symmetrize. Hence, external derivatives are needed. It turns out that the derivatives do not respect the periodic boundary conditions imposed for the single particle states by $t(L_x)$ and $t(\tau L_x)$ since $[\partial_z, t(\tau L_x)] \neq 0$.

6.1 How *not* to implement derivatives

An appealing alternative to handle the derivatives, would be to project them on the LLL. This would yield an operator $\mathcal{D}$ that has all the right properties, and equation (6.1) could be implemented with the modification $\partial_z \to \mathcal{D}$. Doing this for one particle – as was investigated in **Paper II** – we find the projected derivative to be

$$\mathcal{P}_{\text{LLL}}\partial_z\psi(z) = \sum_{l=1}^{N_s} a_l t_1^l \psi(z), \tag{6.2}$$

if $\psi(z)$ is a LLL wave function[Fre13a]. We can thus express the projected derivative ∂_z as an operator

$$\mathcal{D} \equiv \mathcal{P}_{\text{LLL}}\partial_z\mathcal{P}_{\text{LLL}} = \sum_l a_l t_1^l. \tag{6.3}$$

Since derivatives on different particles commute, the projection of a product of derivatives on different particles would be

$$\mathcal{P}_{\text{LLL}} \prod_i \partial_{z_i} \mathcal{P}_{\text{LLL}} = \prod_i \mathcal{D}_i.$$

The problem with the coefficients a_l in (6.2) is that they depend on how the torus is parametrized. That is to say, when integrating over the torus we have to choose where to start and stop the integration $\int_{-\frac{1}{2}+\delta}^{\frac{1}{2}+\delta} dy$, where the parameter δ controls the integration region used. The fact that a_l has dependence on δ shows that something is pathological in (6.3), as the result should not depend on a non-physical parametrization of the projection. For the moment, setting aside this caveat about the proper choice of δ*, it is easy to believe that we at least have obtained a method that translates derivatives ∂_z to a well defined operator

*In writing this we should admit that we are oversimplifying when we use the word "derivatives", since the operator that we really mean on the plane is $D_S = \partial_z + \frac{1}{4}\bar{z}$, in symmetric gauge. The corresponding operator on the torus in τ-gauge is $D_\tau = \partial_z - \frac{L_x}{2}x$, see Appendix C. In **Paper II** only ∂_z was considered and not the full D_τ which lead to a projection on the form $\mathcal{P}_{\text{LLL}}\partial_z = \sum_l a_l t_1^l$. A more thorough analysis using D_τ would yield $\mathcal{P}_{\text{LLL}}D_\tau\mathcal{P}_{\text{LLL}} = \sum_{m,n} a_{m,n}t_{m,n}$ and thus restoring the symmetry between the x and y directions. Unfortunately the problem with δ would still remain.

$\mathcal{D} = \sum_{l=1}^{N_s} a_l t_1^l$ on the torus. Applying the recipe $\partial_z \to \mathcal{D}$ on (6.1) would then give us the many-body wave function

$$\begin{aligned}\psi_{\text{Physical}} &= \mathcal{A}\prod_{\alpha}\prod_{i_\alpha}\mathcal{D}_{i_\alpha}^{s_\alpha}\psi_{\text{Primary}} \\ &= \mathcal{A}\prod_{\alpha}\prod_{i_\alpha}\left(\sum_{l=1}^{N_s} a_l t_{1,z_{i_\alpha}}^l\right)^{s_\alpha}\psi_{\text{Primary}}.\end{aligned}$$

Formally we have managed to obtain a LLL wave function, *but*, it is still pathological. The problem is the many-body operator $D_\alpha = \prod_{j_\alpha}\mathcal{D}_{j_\alpha}$ itself. It is straightforward to verify that D_α only in general commutes with $T_2^{N_s}$, rather than T_2^q. This non-commutativity is disastrous since it means that D_α changes the quantum numbers of ψ_{Physical} and takes it out of the desired q-fold subspace of trial wave functions. Thus, we can *not* use equation (6.2), even if we can find a proper choice of δ. From this example, we conclude that it is not sufficient to have operators that preserve the boundary conditions. They must also preserve the q-fold set of trial wave functions that we expect.

Let us introduce yet another operator

$$T_{m,n}^{(\alpha)} = \prod_{i_\alpha \in I_\alpha} t_{m,n}^{(i_\alpha)},$$

which is the translation operator that moves all the electrons that are in group α a distance $z_{i_\alpha} \to z_{i_\alpha} + \frac{L_x}{N_s}(m + \tau n)$. From the definition (4.11) of $T_{m,n}$ we see that $T_{m,n} = \prod_\alpha T_{m,n}^{(\alpha)}$. This new operator is needed because the only parts of D_α that will commute with T_2^q are precisely the parts that can be written as $T_{k,0}^{(\alpha)}$, for some integer k. These are the terms that were used in Ref. [HSB+08] which first addressed this problem.

A related problem is connected with the description of hole-condensates, briefly mentioned in Section 2.3, where terms that include powers of $\bar{z}$ are generated. These anti-holomorphic terms cause the wave function to occupy higher Landau levels, such that it has to be projected down to the lowest LL. In the symmetric gauge, this is readily done by the substitution $\bar{z} \to \partial_z$. On the torus, the prescription $\bar{z} \to \partial_z$ will not work, and it is not clear what should replace it. In the summary in Chapter 9 we will comment on a possible solution based on the use of coherent states as a way to project the wave functions to the LLL. This is done by interpreting the primary wave functions as coefficients for coherent state wave functions[SVH11b, SVH11a].

6.2 Modular transformations of the torus

To set the stage for later sections, we here make a minor technical digression to focus on the modular transformations of the torus. The torus geometry defined in Chapter 4 is parametrized by τ. However, there are several τ that describe the same geometry as τ only states which lattice points are identified. For instance, if the points z, $z + L_x$ and $z + \tau L_x$ are identified, then so are the

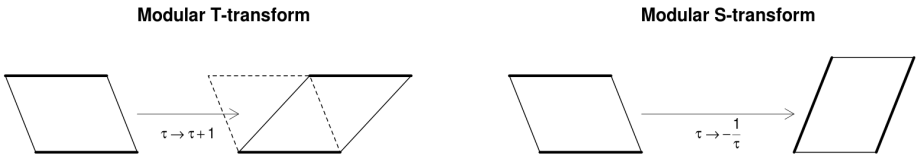

a) *b)*

Figure 6.1: *a)* The geometric interpretation of a $\mathcal{T}$-transform, $\tau \to \tau + 1$. Both L_x and L_y are unchanged but the torus is tilted such that $L_\Delta \to L_\Delta + L_x$.
b) The geometric interpretation of an $\mathcal{S}$-transform, $\tau \to -\frac{1}{\tau}$. The torus is effectively rotated such that $L_x \to |\tau|\, L_x$, $L_y \to \frac{1}{|\tau|} L_y$ and $L_\Delta \to -\frac{1}{|\tau|} L_\Delta$.

points $z + L_x\,(m + \tau n)$, where $n, m \in \mathbb{Z}$. We see that there is redundancy in the parametrization of the lattice $L_x\,(m + \tau n)$, as we can for instance let $m \to m - n$ and $\tau \to \tau + 1$, which explicitly will leave this lattice invariant. The change in τ that we make is called a $\mathcal{T}$-transform. Its effect upon the torus is to skew it by one lattice constant. This can be seen in Figure 6.1a.

Note that if we rotate the entire torus such that τL_x points along the real axis, we will have a physically equivalent torus but with a different parametrization. This second operation we perform is more complicated since it involves a rotation. It is done as follows: The two principal directions for the torus are $L_1 = L_x$ and $L_2 = \tau L_x$, but now they are considered to have switched places. Thus we let $L_1 \to L_2$ and $L_2 \to -L_1$, where the minus sign is present to preserve the orientation of the surface $L_1 \times L_2$. This causes $\tau = \frac{L_2}{L_1}$ to change as $\tau \to \frac{-L_1}{L_2} = \frac{-L_x}{\tau L_x} = -\frac{1}{\tau}$. We call this transformation an $\mathcal{S}$-transformation and its effect on the torus is seen in Figure 6.1b. In terms of the lattices of identified points, by letting $\tau \to -\frac{1}{\tau}$ and simultaneously renaming $m \to n$ and $n \to -m$, we obtain

$$L_x\,(m + \tau n) \to \frac{|\tau|}{\tau} L_x\,(m + \tau n)\,,$$

which has exactly that same shape as the original lattice, only rotated by $\frac{|\tau|}{\tau}$. The absolute value in the equation above arise because of the fixed area of the torus $\tau_2 L_x^2 = 2\pi N_s$, which forces $L_x \to |\tau|\, L_x$.

To summarize, we have two transformations

$$\begin{aligned} \mathcal{T}: &\quad \tau \to \tau + 1 \\ \mathcal{S}: &\quad \tau \to -\frac{1}{\tau}, \end{aligned} \tag{6.4}$$

which generate all equivalent parametrisations of a torus in terms of τ. This partitions the upper complex half plane into an infinite set of regions, some of which are depicted in Figure 6.2. The fundamental region can be taken to be $-\frac{1}{2} < \Re(\tau) < \frac{1}{2}$ and $|\tau| > 1$, where all values of τ corresponds to a unique geometry realization.

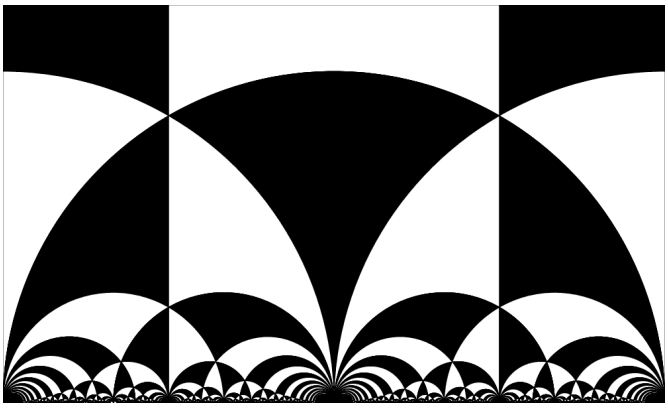

Figure 6.2: The modular space generated by $\mathcal{S}$ and $\mathcal{T}$ from the fundamental domain at $-\frac{1}{2} < \Re(\tau) < \frac{1}{2}$ and $|\tau| > 1$, here depicted in the white upper region. The black and white regions are merely a visual guide. All black (white) regions can be reached from the fundamental domain with an odd (even) number of modular transformations.

The modular transformations affects the structure of the wave functions and particularly the translation operators $t_{m,n}$ as these depend on the precise geometry of the torus. The translation operators transform in much the same way as the lattice $L_x(m + \tau n)$, under modular transformations, which is

$$\begin{aligned} \mathcal{T}: \quad & t_{m,n} \to t_{m+n,n} \\ \mathcal{S}: \quad & t_{m,n} \to t_{-n,m}. \end{aligned} \tag{6.5}$$

For the purpose of clarity, we have in the above equation suppressed the gauge transformations $U_{\mathcal{S}}$ and $U_{\mathcal{T}}$, which are needed to account for the change in coordinates the modular transforms induce. Under the $\mathcal{T}$-transform, $\tau \to \tau + 1$, the different powers of t_1 and t_2 will thus transform into each other, such that $t_2^n \to t_1^n t_2^n$. This is easily seen, since what was a translation in the τ-direction will now be a translation in the $(\tau + 1)$-direction. Likewise, for the $\mathcal{S}$-transform, effectively $t_1 \leftrightarrow t_2$, which is natural as the two torus axes have traded places.

By performing the relabelling

$$\begin{aligned} \mathcal{T}: \quad & (m,n) \to (m-n,n) \\ \mathcal{S}: \quad & (m,n) \to (n,-m) \end{aligned} \tag{6.6}$$

we can cancel the effect in (6.5). Figure 6.3a depicts some examples of transformations of (m,n). The relabelling induced in (6.6) is interesting since not all pairs (m,n) can be connected to each other using (6.6). In fact, two pairs (m,n) and (m',n') can only be connected if $\gcd(m,n) = \gcd(m',n')$. For this reason, the lattice of modularly connected pairs (m,n) splits into an infinite set of self-similar lattices, labelled by $\gcd(m,n)$, as seen in Figure 6.3b.

We choose to focus on the $\mathcal{S}$ and $\mathcal{T}$ transformations because the geometry of the torus is equivalent under these modular transformations. If two different geometries are equivalent, then all the physics on those geometries should also be

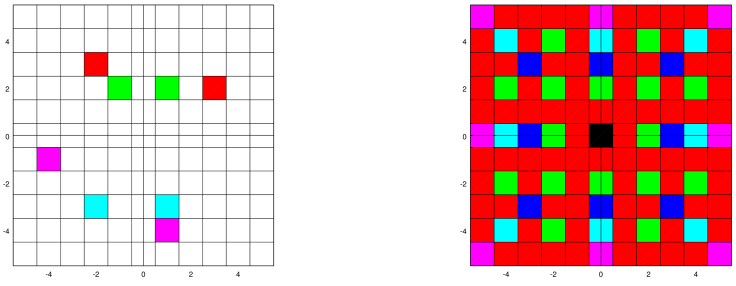

a) *b)*

Figure 6.3: *a)* Examples of modular transformations on the translation lattice the red and purple are $\mathcal{S}$-transformations whereas the green and cyan are $\mathcal{T}$-transformations.
b) The infinite set of self similar lattices generated by $\mathcal{S}$ and $\mathcal{T}$. Each colour corresponds to a particular grid type and value of $\gcd(m,n)$, as $\gcd(m,n) = 1, 2, 3, 4, 5$.

equivalent. Requiring that the physics to be unchanged under these transformations gives us constraints that will fix the form of the generalized ∂_z operator on the torus.

6.3 How to treat the derivatives in many-particle states

As seen in the previous chapters, we can write electronic trial wave functions for hierarchy states using conformal blocks. We have also seen how the hierarchical fusing of quasi-particles and electrons gives rise derivatives that that on the primary electronic wave functions. In this section we will outline the numerical and analytical clues that will lead to the general ansatz for the torus derivatives that will appear (6.12).

For concreteness we will use the $\nu = \frac{2}{5}$ state as an illustrative example. The construction of this state on the plane was described in section 3.5.3. Since the strategy on the torus will parallel the planar construction in many respects we only point out the important differences in what follows.

The K-matrix, as well as the number of particles in each group $\alpha = z, w$, is the same on the torus as on the plane. We choose the same charge lattice as on the plane, but now we consider the full boson operators $\phi(z, \bar{z})$ instead of simply the chiral ones. As a result the two electron operators are

$$V_w(w, \bar{w}) = e^{\imath\sqrt{3}\phi_1(w,\bar{w})} \qquad \hat{V}_z(z) = e^{\imath\frac{2}{\sqrt{3}}\phi_1(z,\bar{z})+\imath\sqrt{\frac{5}{3}}\phi_2(z,\bar{z})}.$$

Note that we only consider the primary operators – without derivatives.

We now consider the full correlation function

$$\left\langle \mathcal{O}_{\text{bg}} \prod_{i=1}^{\frac{N_e}{2}} V_w\left(w_i, \bar{w}_i\right) \cdot \prod_{j=1}^{\frac{N_e}{2}} \hat{V}_z\left(z_j, \bar{z}_j\right) \right\rangle, \tag{6.7}$$

which is factorized into chiral and anti-chiral components according to equation (5.3). As always, a background charge is inserted to make the whole correlator charge neutral. On the torus, as we mentioned in Chapter 3, the correlator can not directly be factorized in a holomorphic and an anti-holomorphic component.

The treatment of the derivatives is somewhat obscure as these should now be acting within the full correlator. The approach taken here is to ignore the derivatives when computing the correlation function (6.7) and apply their torus generalizations at the end of the calculation. To be specific, the insertion takes place after the conformal blocks have been extracted, but before the anti-symmetrization, just like in (6.1). The correlator can now be calculated and for $\nu = \frac{2}{5}$, the conformal blocks that fulfills the boundary conditions are

$$\begin{aligned}\Psi_s\left(\{z\},\{w\}\right) &= e^{-\imath\pi\tau N_s \sum_i \left(y_{w_i}^2 + y_{z_i}^2\right)} \mathcal{F}_s\left(W, Z\right) \times \\ &\times \prod_{i<j} \vartheta_1\left(\frac{z_i - z_j}{L_x}\middle|\tau\right)^3 \prod_{i,j} \vartheta_1\left(\frac{w_i - z_j}{L_x}\middle|\tau\right)^2 \prod_{i<j} \vartheta_1\left(\frac{w_i - w_j}{L_x}\middle|\tau\right)^3.\end{aligned}$$

The details of the center of mass function $\mathcal{F}_s\left(W, Z\right)$ are given in (5.6), with a suitable choice of $\mathbf{t}$ and $\mathbf{r}$. However, for our purposes they are not particularly important. The explicit formulation of the $\nu = \frac{2}{5}$ CoM piece was first given in Ref. [HSB+08] but in a slightly different form than (5.6). In the case of $\nu = \frac{2}{5}$, as in general for hierarchy states, all electronic coordinates are not equivalent in the CoM function. We emphasize this by giving $\mathcal{F}_s\left(W, Z\right)$ the arguments $W = \sum_i w_i$ and $Z = \sum_i z_i$.

We now turn to the derivatives: There is *à priori* no method telling us what should replace the derivatives, when on the torus. Nevertheless there exists constraints that limit the possible alternatives: 1) The wave function should, in the planar $N_s \to \infty$ limit, reduce to the planar wave functions. 2) The wave function should transform "nicely" under modular transformations. 3) The $q-$fold degeneracy should not be changed. We will return to precisely what we mean by "nicely" in Section 6.4.

Based on the conclusions from Section 6.1, we begin with an ansatz where we use the operator $T_{l,0}^{(z)}$ as the torus derivative. This will preserve the q-fold degeneracy. The ansatz wave functions is

$$\psi_s^{(x)} = \sum_{l=1}^{N_s} D_{l,0} \Psi_s = \sum_{l=1}^{N_s} \lambda_{l,0}^{N_w} T_{l,0}^{(w)} T_{2l,0} \Psi_s, \tag{6.8}$$

where the parameters $\lambda_{l,0}$ are unspecified for the time being. We write the parameter $\lambda_{l,0}$ to the power N_w to emphasize that each of the N_w particles in group w contribute the same amount to the weight. The additional operator $T_{2l,0}$ only contributes with a phase, but is included such that $T_{l,0}^{(w)} T_{2l,0}$ will commute with $T_{m,n}$. This ansatz is exactly what was used by Hermanns *et.al.* in Ref. [HSB+08]. In their work, they found that as $L_x \to 0$, the first term $\lambda_{1,0}$ becomes increasingly

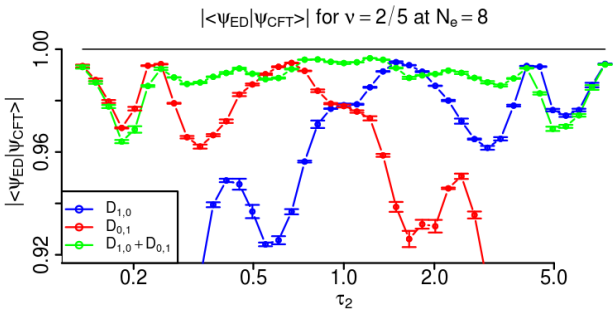

Figure 6.4: Overlap between the exact Coulomb ground and $D_{1,0}$ (Blue), $D_{0,1}$ (Red) and $D_{1,0}+D_{0,1}$ (Green), with $\lambda_{m,n}$ given in (7.10). The number of electrons are $N_e = 8$. Cross section of $\Re(\tau) = 0$ for $0.13 < \Im(\tau) < 7.4$. Notice that the overlap with $D_{1,0}$ drastically vanishes as $\Im(\tau) \to 0$. The mirrored behaviour is seen for $D_{0,1}$ as $\Im(\tau) \to \infty$. The combination $D_{1,0} + D_{0,1s}$ is good for all values of $\Im(\tau)$.

dominant when fitted to the exact ground state for the Coulomb potential. Suggestively, and for future convenience, we call the combination $D_{l,0} = \lambda_{l,0}^{N_w} T_{l,0}^{(w)} T_{2l,0}$.

We are now faced with a problem. When L_x is changed in the opposite direction, such that $L_y \to 0$, *no* combination of $D_{l,0}$ allows for a good overlap with the Coulomb ground state. This result can be understood physically by considering the torus geometry. When $L_x \to 0$, the operator $t_1^{(w)} \approx 1 + \frac{L_x}{N_s}\partial_{\tilde{x}}$ approximates a derivative well, as the torus is thin in the $\tilde{x}$ direction. Remember that the wave function vanishes under anti-symmetrization if there are no derivatives, so in practice $\mathcal{A}\prod_i t_1^{(w_i)} \approx \mathcal{A}\prod_i \left(1 + \frac{L_x}{N_s}\partial_{\tilde{x}_i}\right) = \mathcal{A}\frac{L_x}{N_s}\prod_i \partial_{\tilde{x}_i}$. When $L_y \to 0$, such that $L_x \to \infty$, the torus is thin in the opposite direction, and the $t_1^{(w)}$ operator does no longer resemble a derivative. We can remedy this by generalizing the ansatz (6.8) and simply trade $T_{l,0}$ for $T_{0,l}$. These two operators do *not* commute, so $T_{0,l}$ will change the momentum sector of the Ψ_s wave function. This is easily accounted for by adding an extra operator $T_{0,2l}$ just as in (6.8). We thus get an alternative wave function

$$\psi_s^{(y)} = \sum_{k=1}^{N_s} \lambda_{0,k}^{N_w} T_{0,k}^{(w)} T_{0,2k,} \Psi_s.$$

The numerical overlap with this function and the ground state of the Coulomb potential is bad when $L_x \to 0$, and good when $L_y \to 0$. This is the mirrored behavior from $\psi_s^{(x)}$, as can be seen in Figure 6.4.

It is also possible to imagine translation operators of the form $T_{m,n}^{(w)} T_{2m,2n}$ as these constructions also commute with T_2^5. Studying the overlap as we alter the value of τ_1 instead of τ_2, we see that as τ_1 go from $\tau_1 = 0$ to $\tau_1 = 1$, the good overlaps found with $\psi_s^{(x)}$ and $\psi_s^{(y)}$ are both diminishing. Especially the $\psi_s^{(y)}$ terms loose their good overlap. The general trial wave function ansatz for $\nu = \frac{2}{5}$ can

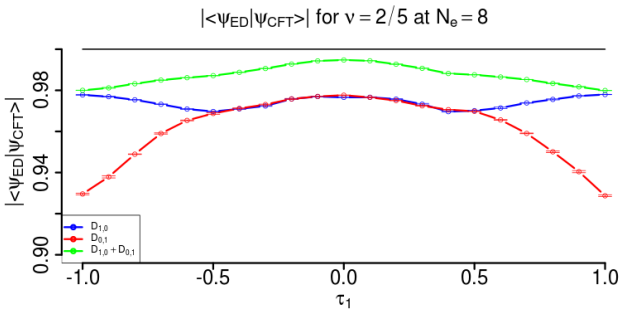

Figure 6.5: Overlap between the exact Coulomb ground and $D_{1,0}$ (Blue), $D_{0,1}$ (Red) and $D_{1,0}+D_{0,1}$ (Green), with $\lambda_{m,n}$ given in (7.10). The number of electrons are $N_e = 8$. Cross section of $\Im(\tau) = 1$ for $-1 < \Re(\tau) < 1$. The combination $D_{1,0}+D_{0,1}$ is still good even though non-trivial phases enter through the coefficients $\lambda_{m,n}$.

thus be extended to

$$\psi_s = \sum_{m,n=1}^{N_s} \lambda_{m,n}^{N_w} T_{m,n}^{(w)} T_{2m,2n} \Psi_s. \tag{6.9}$$

Note that $\left[T_{m,n}^{(w)} T_{2m,2n}, T_{m',n'}\right] = 0$, implying that the quantum numbers are preserved for both T_1^5 and T_2^5. We will schematically write the ansatz (6.9) as $\psi_s = \mathbb{D}\Psi_s$, where

$$\mathbb{D} = \sum_{m,n} D_{m,n} = \sum_{m,n=1}^{N_s} \lambda_{m,n}^{N_w} T_{m,n}^{(w)} T_{2m,2n}.$$

The purpose of this formulation is to emphasize that the operator $\mathbb{D}$ should be capable of acting on any state $\psi_s^{\left(\frac{2}{5}\right)}$ – even those that are eigenstates of the T_2 operator instead of the T_1.

How can we find some guiding principle that can fix the values of $\lambda_{m,n}$? To answer this question, we need to study the modular behaviour of the wave function (6.9). I will turn out that the mixed terms $D_{m,n}$ are essential for the ansatz.

6.4 The requirement of modular covariance

In this section we draw inspiration from our knowledge of how the Laughlin state (5.7) transforms under modular transformations. In these transformations, the conformal weight h_ψ of the CFT operators V_α shows up. For the general primary electronic wave function Ψ_s the same weight is also present. The assumption that we make is that when $\mathbb{D}$ acts on Ψ_s the conformal nature of the wave function is retained. That means that Ψ_s and $\mathbb{D}\Psi_s$ transforms in exactly the same way up to a change the conformal weight h_ψ. This change in h_ψ should mirror the change – on the plane – in angular momentum that happens to ψ_{Primary} when the derivatives act on it.

The modular properties are important since they tell us about how ψ_s transforms under changes in τ. As we wrote in Section 6.2, there are two transformations of τ that should not affect the physics, namely the $\mathcal{S}$- and $\mathcal{T}$-transforms of (6.4). We will take the requirement of modular covariance as a physical constraint on the operator $\mathbb{D}$. We thus require that if Ψ_s transforms in a specific way under $\mathcal{S}$- and $\mathcal{T}$-transforms, then $\psi_s = \mathbb{D}\Psi_s$ should transform in the very same way, up to a possible phase.

To be precise, we note that if we perform modular transformations on Ψ_s, it will transform as

$$\begin{aligned} \mathcal{S}\Psi_s &= \sum_{s'} S_{s,s'}\Psi_{s'} \left(\frac{\tau}{|\tau|}\right)^{h_\psi} \\ \mathcal{T}\Psi_s &= \sum_{s'} T_{s,s'}\Psi_{s'}, \end{aligned}$$

where the transformation matrices are the modular S and T matrices $S_{s,s'} = e^{\imath 2\pi \frac{ss'}{q}}$ and $T_{s,s'} = \delta_{s,s'} e^{\imath\pi\left(\frac{s^2}{q}+\frac{c}{12}\right)}$. The appearance of there matrices under modular transformations provides yet another check that we have managed to extract the correct conformal blocks from the CFT correlation function. Even more interesting than the modular matrices is the phase factor $\left(\frac{\tau}{|\tau|}\right)^{h_\psi}$. It measures the total conformal weight of the primary vertex operators V_α in the correlation function as is $h_\psi = \frac{1}{2}\sum_j M_{jj} = \frac{1}{2}\sum_\alpha N_\alpha K_{\alpha\alpha}$.

We now impose the constraint on $\mathbb{D}$ that $\mathbb{D}\Psi_s$ should transform exactly like Ψ_s, but with the important difference that the conformal weight of the transformation should be $h_\psi + N_\alpha$ instead of just h_ψ. This change to the conformal weight is a reflection of the change in the angular momentum that $\prod_{i=1}^{N_\alpha}\partial_{z_i}$ gives rise to on the plane. The required transformation properties are therefore

$$\begin{aligned} \mathcal{S}\mathbb{D}_{(\alpha)}\Psi_s &= \sum_{s'} S_{s,s'}\mathbb{D}_{(\alpha)}\Psi_{s'} \left(\frac{\tau}{|\tau|}\right)^{h_\psi+N_\alpha} \\ \mathcal{T}\mathbb{D}_{(\alpha)}\Psi_s &= \sum_{s'} T_{s,s'}\mathbb{D}_{(\alpha)}\Psi_{s'}, \end{aligned}$$

for the $\mathbb{D}_{(\alpha)}$ operator that acts on group α. This constraint can also be formulated without any reference to Ψ_s as

$$\begin{aligned} \mathcal{S}\mathbb{D}_{(\alpha)}\mathcal{S}^{-1} &= \mathbb{D}_{(\alpha)} \left(\frac{\tau}{|\tau|}\right)^{N_\alpha} \\ \mathcal{T}\mathbb{D}_{(\alpha)}\mathcal{T}^{-1} &= \mathbb{D}_{(\alpha)}. \end{aligned} \tag{6.10}$$

Since $\mathbb{D}$ contains $T_{m,n}$ operators and the modular transformations will map these onto each other according to (6.5), it has to exist τ-dependent relations between the different $\lambda^{(\tau)}_{m,n}$. If there where none, $\mathbb{D}$ would not be able to transform according to (6.10). Using the $\mathcal{S}$-transform, we obtain relations between the coefficients $\lambda_{m,n}$ and $\lambda_{n,-m}$ in (6.9). In the same way under the $\mathcal{T}$-transform, we generate relations between $\lambda_{m,n}$ and $\lambda_{m+n,n}$.

The modular properties of $\lambda_{m,n}$ imposed by condition (6.10) can be summarized as

$$\begin{aligned} \lambda_{m,n}(\tau+1) &= e^{\imath\phi_S}\lambda_{m+n,n}(\lambda) \\ \lambda_{m,n}\left(-\frac{1}{\tau}\right) &= e^{\imath\phi_T}\lambda_{-n,m}(\lambda), \end{aligned} \tag{6.11}$$

such that $\lambda_{m,n}$ co-varies with $T_{m,n}$, but with the added possibility of a constant phase ϕ_S. Note the possibility of a solution to (6.11) where $\lambda_{m,n} = \lambda$ is a τ-dependent constant. However, such a solution fits poorly with the data from Figure 6.4 since different terms seem to be dominant at different values of τ. Quite the contrary, the relations (6.11) between the different $\lambda_{m,n}$, in conjunction with the overlap results – as presented in Figure 6.4 and Figure 6.5 – indicate that $\lambda_{n,m}$ does indeed display (n,m)-dependent τ-dependence.

To fix the τ-dependence of $\lambda_{m,n}(\tau)$ requires a more extensive analysis, one that studies the modular transformation properties of the conformal blocks that make up ψ_s. A detailed description of that procedure can be found in **Paper III**, and we here only limit the discussion to an heuristic argument about the general behaviour of $\lambda(\tau)$. The numerical results in Figure 6.4 imply that $\frac{\lambda_{1,0}(\tau)}{\lambda_{0,1}(\tau)} \to 0$ as $\tau \to 0$ and that $\frac{\lambda_{0,1}(\tau)}{\lambda_{1,0}(\tau)} \to \infty$ as $\tau \to \infty$. The parameters $\lambda_{m,n}$ must thus depend on τ and possess the limiting behaviour mentioned above. From (6.5) we know that $\lambda_{0,1}$ and $\lambda_{0,1}$ must transform into each other under $\mathcal{S}$, such that ψ_s has proper modular behaviour. A similar analysis will give us relations between the generic $\lambda_{m,n}$-values.

The modular $\mathcal{S}$-transformation does however only connect the coefficients $\lambda_{m,n}$, $\lambda_{n,-m}$,$\lambda_{-m,-n}$ and $\lambda_{-n,m}$. To shed light on the relative sizes of the different $\lambda_{m,n}$ we need another mechanism. The alternative $\mathcal{T}$-transform introduces further constraints on $\lambda_{m,n}$. From Figure 6.5, we can see that as $\tau \to \tau+1$, the term $D_{0,1}$ becomes less important as the overlap declines. There must thus be another term that plays the role of $D_{0,1}$ at $\tau+1$. This term is $D_{-1,1}$, as can bee seen in Figure 6.6. This means that $|\lambda_{0,1}(\tau)| = |\lambda_{-n,1}(\tau+n)|$ to make different terms dominant at different τ.

The last piece of the puzzle comes from a full analysis of how the quasi-particle operators should be regularized in the toroidal geometry, which gives us insight in to the form of $|\lambda_{m,n}|$. Putting all the pieces together gives us the coefficients $\lambda_{m,n}$ as

$$\lambda_{m,n}(\tau) = \sqrt{\tau_2}\eta^3(\tau)\frac{e^{-\imath\pi\tau\frac{n^2}{N_s^2}}e^{-\imath\pi\frac{nm}{N_s^2}}}{\vartheta_1\left(\frac{1}{N_s}(m+\tau n)\middle|\tau\right)}. \tag{6.12}$$

At this point in the analysis, it is unclear whether (6.12) provides the unique solution that respects (6.11). We can now go back to Figures 6.4, 6.5 and 6.6 and investigate the result of adding two or more $D_{m,n}$ terms. In all of these figures we see that for almost any τ, the combined result is better than that of any individual term $D_{m,n}$. This means that the phases and sizes of the weight $\lambda_{m,n}$ must be correct. After all, we are adding terms with complex coefficients and similar magnitude and even a small phase error could destroy the good overlap.

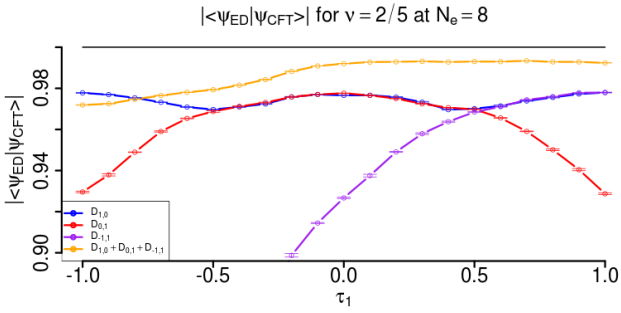

Figure 6.6: Overlap between the exact Coulomb ground and $D_{1,0}$ (Blue), $D_{0,1}$ (Red), $D_{-1,1}$ (Purple) and $D_{1,0} + D_{0,1} + D_{-1,1}$ (Orange), with $\lambda_{m,n}$ given in (7.10). The number of electrons are $N_e = 8$ and cross section of $\Im(\tau) = 1$ for $-1 < \Re(\tau) < 1$, the same as in Figure 6.5. The role of $D_{0,1}$ has been taken by $D_{-1,1}$ as $\tau_1 \to 1$. The combination $D_{1,0} + D_{0,1} + D_{-1,1}$ is excellent considering that non-trivial phases enter through the coefficients $\lambda_{m,n}$.

The entire τ-plane as in Figure 6.7, can be scrutinized, too. Reasonable overlap can be obtained in the entire τ-plane even if only one $D_{m,n}$ is used. The $D_{m,n}$ term in question has to be chosen wisely though and the most relevant term constitutes the smallest translation distance. The overlap becomes better for all values of τ, when we introduce more $D_{m,n}$ terms, provided we add them in the order of most importance. Most importantly, there are no variational parameters in the overlap calculations presented in 6.7 and the whole τ-dependence of $\mathbb{D}$ is fixed by its modular properties!

Because of the good overlap, we can be fairly confident that (6.9) faithfully reproduces the qualitative features of the Coulomb ground state. As a second check that the state (6.9) is properly describing a quantum Hall fluid we will later, in Chapter 8, calculate the viscosity of that state.

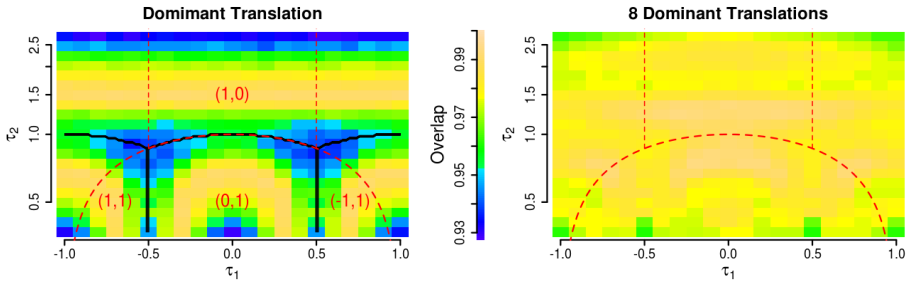

a) *b)*

Figure 6.7: Overlap with the exact Coulomb ground state in a region $-1 < \tau_1 < 1$ and $0.37 < \tau_2 < 2.72$ of the τ-plane, for $N_e = 8$ particles. In *a)* the thick black lines mark the boundaries of regions with different minimal translation steps $\delta_{m,n}$. Note the logarithmic scale of τ_2 for a more symmetric plot. *a)* Only the dominant term is included in the sum (6.9). The overlap with the exact Coulomb state is good everywhere. *b)* The eight most dominant terms at $\tau = \imath$, with (m,n)=(1,0), (1,0), (2,0), (0,2), (-1,1), (1,1), (-2,2), (2,2), are included in the sum (6.9). Overlap with the Coulomb state is better or equal in most parts of the τ-plane; at the edges, other terms than the eight used here are dominant. This shows that our ansatz is valid in the entire τ-plane.

Chapter 7

Fock Expansions

The Laughlin state constructed in (5.7) is the simplest quantum Hall wave function. Nevertheless, there are still fundamental questions left to be answered. One such question regards the normalization of the Laughlin state. The normalization is important as it affects the braiding statistics of the fractionally charged quasi-particles. On the plane, it is possible to add quasi-particles at positions w_i by modifying the Laughlin wave function as

$$\begin{aligned}\psi_{\text{Laughlin}}^{(N_e,N_{\text{qp}})} &= \mathcal{N}_{\text{Laughlin}} e^{-\frac{1}{4}\sum_i |z_i|^2} e^{-\frac{1}{4q}\sum_i |w_i|^2} \times \\ &\quad \times \prod_{i<j}^{N_e} (z_i - z_j)^q \cdot \prod_{i=1}^{N_e}\prod_{i=1}^{N_{\text{qp}}} (z_i - w_j) \cdot \prod_{i<j}^{N_{\text{qp}}} (w_i - w_j)^{\frac{1}{q}} .\end{aligned}$$

This is the same wave function that was given in (3.9). There is a conjecture attributed to Laughlin himself[Lau83] that the normalization constant $\mathcal{N}_{\text{Laughlin}}$ will be independent of w_i provided the different w_i are separated well enough. This conjecture goes under the name *plasma analogy* because of the analogy Laughlin made with charged particles in the screening phase of a one-component plasma. Physically, if the plasma is screening, the total energy of the plasma will be independent of the positions of the particles at w_i as long as they do not come to close together. The connection between the plasma and $\mathcal{N}_{\text{Laughlin}}$ is that $\mathcal{N}_{\text{Laughlin}}$ is related to the partition function and therefore the energy of the plasma.

On the torus, we can formulate a version of the plasma analogy that does not concern quasi-particles at positions w_i, but rather deals with the geometry of the torus and its parametrization τ. The analogy with the plasma is still valid but this time the question concerns of how the energy depends on distortions in the geometry. The intuitive picture remains the same: if the plasma is screening, the partition functions should not depend on how the torus edges are identified. The corresponding statement for the Laughlin wave function is that $\mathcal{N}(\tau)$ in (5.7) should be independent of τ, up to a very specific factor given by (8.4). For the Laughlin state, this factor is

$$\mathcal{N}(\tau) = \mathcal{N}_0 \frac{\left[\tau_2 \eta(\tau)^4\right]^{\frac{qN_e}{4}}}{\eta(\tau)^{q\frac{N_e(N_e-1)}{2}+1}},$$

and the assumption is as that $\mathcal{N}_0$ is independent of τ. If this assumption is true, we can analytically compute such quantities as the anyonic statistics of the quasi-particles[ASW84] as well as the viscosity of the quantum Hall fluid[Rea09, FHS14]. We will return to this in Chapter 8.

There are two distinct alternative procedures for normalizing the Laughlin state, or any other state. The first direct approach is to simply integrate over the modulus squared of the wave functions and obtain the normalization as

$$\mathcal{N}_{\text{Laughlin}}^{-2} = \int d^2 z \, |\psi_{\text{Laughlin}}|^2 .$$

Unfortunately these integrals are hard to evaluate analytically and one must resort to Monte Carlo evaluation in order to estimate $\mathcal{N}_{\text{Laughlin}}$.

In this chapter, we will investigate the alternative approach and construct the Fock expansion of the state as

$$\psi_{\text{Laughlin}} = \sum_{\{k_i \in \mathbb{Z}_{N_s}\}} \mathcal{Z}_{\{k\}} \prod_i \eta_{k_i}(z_i) . \tag{7.1}$$

Here η_k are the single particle orbitals defined in (4.5), and $\mathcal{Z}_{\{k\}}$ is the weight of the configuration $\{k\}$*. For a state with N_s fluxes and single particle periodic boundary conditions, $k_i \in \mathbb{Z}_{N_s}$ and the total momentum of the state is $k_{\text{tot}} = \sum_i k_i = \frac{q}{2} N_e (N_e - 1) + m N_e \mod N_s$. Here $m \in \mathbb{Z}_q$ label the q-fold degeneracy of the Laughlin state on the torus.

The normalization coefficient of the Laughlin state is given by

$$\mathcal{N}_{\text{Laughlin}}^{-2} = \sum_{\{k_i \in \mathbb{Z}_{N_s}\}} \left| \mathcal{Z}_{\{k\}} \right|^2 .$$

On the plane, the coefficients for the Laughlin states are known as the coefficients of Jack polynomials[BH08]. These coefficients can be constructed recursively[LLM00] by starting at the root partition of the Laughlin state[RGJ08].

Before we compute the values of $\mathcal{Z}_{\{k\}}$ analytically, it should be noted that there exists a third option, specific to the Laughlin state. This option uses the fact that the Laughlin state is the exact zero energy state of the Haldane pseudo-potential interaction[Hal83a]. This means that by diagonalizing the pseudo-potential Hamiltonian, we are actually computing $\mathcal{N}_{\text{Laughlin}} \mathcal{Z}_{\{k\}}$. By sampling the exactly diagonalized wave function and comparing this with the real space wave function (5.7), it is possible to numerically deduce $\mathcal{N}_{\text{Laughlin}}$ up to the usual $U(1)$ freedom. We will use this short-cut in Section 8.3 where we investigate the viscosity in the TT-limit.

7.1 The Laughlin state

The key to constructing the Fock expansion is to isolate the Fourier components $e^{\imath 2\pi k_i \frac{z_i}{L_x}}$ in (5.7). Since the LLL is holomorphic in its structure, these factors map

*Note that $\prod_i \eta_{k_i}(z_i)$ is not a Slater determinant so $\mathcal{Z}_{\{k\}}$ needs to be fully antisymmetric under the interchange of any two k_i,k_j for the above expression to represent a fermionic many-particle state.

directly onto the Fourier components of the basis states (4.5). These components need to be extracted from the Jastrow factors as well as the CoM factor. Once the components $e^{\imath 2\pi \sum_i k_i z_i}$ have been extracted, the Slater determinant can be reconstructed by re-indexation of the sums over k_i. As, by construction, the Laughlin state is fully antisymmetric, the Slater determinant should also be manifest in the Fock expansion. We summarize the main steps here and details of the procedure can be found in **Paper IV**.

To Fourier-expand the Jastrow factors, we make the Fourier factors explicit. We use that the generalized ϑ-function to the power N has an expansion that is

$$\vartheta\begin{bmatrix} a \\ b \end{bmatrix}(z|\tau)^N = \sum_{\tilde{T}\in\mathbb{Z}+aN} e^{\imath\pi\tau\frac{1}{N}\tilde{T}^2} e^{\imath 2\pi\tilde{T}(z+b)} \tilde{Z}^{(N)}_{\tilde{T}}. \tag{7.2}$$

The factor $\tilde{Z}^{(N)}_{\tilde{T}}$ encodes all the information about the N^{th} power of ϑ. The most important properties of $\tilde{Z}^{(N)}_{\tilde{T}}$ is $\tilde{Z}^{(N)}_{\tilde{T}+N} = \tilde{Z}^{(N)}_{\tilde{T}}$ and $\tilde{Z}^{(N)}_{\tilde{T}} = \tilde{Z}^{(N)}_{-\tilde{T}}$. A selection of other properties, as well as an explicit expression for $\tilde{Z}^{(N)}_{\tilde{T}}$ are listed in the Appendix of **Paper IV**. In the trivial case of $N = 1$, then $\tilde{Z}^{(1)}_a = 1$. Applying the expansion (7.2) to each of the ϑ_1-functions in the Jastrow factor (5.7) yields the form

$$\prod_{i<j}\vartheta_1(z_{ij}|\tau)^q = \sum_{\{\tilde{T}_{ij}\in\mathbb{Z}+\frac{q}{2}\}} e^{\imath\pi\tau\sum_{i<j}\frac{\tilde{T}^2_{ij}}{q}} e^{\imath\pi\sum_{i<j}\tilde{T}_{ij}} e^{\imath 2\pi\sum_i \mathbb{T}_i\frac{z_i}{L_x}} \prod_{i<j}\tilde{Z}^{(q)}_{\tilde{T}_{ij}}. \tag{7.3}$$

Here each pair z_{ij} has been associated with a summation index $\tilde{T}_{ij}$. As z_{ij} is antisymmetric in its indexes $z_{ij} = -z_{ji}$ so is $\tilde{T}_{ij}$. In other words $\tilde{T}_{ij}$ has the property $\tilde{T}_{ij} = -\tilde{T}_{ji}$. Since the Jastrow factor consists of ϑ_1-functions (where $a = b = \frac{1}{2}$) there exists an offset of $\tilde{T}_{ij}$ from being integer, that is $\tilde{T}_{ij} \in \mathbb{Z} + \frac{q}{2}$. We put the $\sim$ on top of T_{ij} to remind us of this. Note that the Jastrow expansion (7.3) can be generalized to the more generic Jastrow factor in (5.5).

The variable $\mathbb{T}_i$ is used for bookkeeping as it counts the total momentum contribution to particle z_i as

$$\mathbb{T}_i = \sum_{j=1}^{N_e} \tilde{T}_{ij}.$$

Due to the antisymmetry of $\tilde{T}_{ij}$,

$$\sum_{i,j} T_{ij} = 0,$$

such that there is a balance condition on $\mathbb{T}_i$ yielding

$$\sum_i \mathbb{T}_i = 0. \tag{7.4}$$

We can visualize the object $\tilde{T}_{ij}$ as forming an $N_e \times N_e$ antisymmetric matrix. In the table below we have added both a special column and row showing $\mathbb{T}_i$ as the sum of each row and column of $\tilde{T}_{ij}$:s

$$\begin{array}{ccccc|c} 0 & \tilde{T}_{12} & \tilde{T}_{13} & \cdots & \tilde{T}_{1N_e} & \mathbb{T}_1 \\ -\tilde{T}_{12} & 0 & \tilde{T}_{23} & \cdots & \tilde{T}_{2N_e} & \mathbb{T}_2 \\ -\tilde{T}_{13} & -\tilde{T}_{23} & 0 & \cdots & \tilde{T}_{3N_e} & \mathbb{T}_3 \\ \vdots & \vdots & \vdots & \ddots & \vdots & \vdots \\ -\tilde{T}_{1N_e} & -\tilde{T}_{2N_e} & -\tilde{T}_{3N_e} & \cdots & 0 & \mathbb{T}_{N_e} \\ \hline -\mathbb{T}_1 & -\mathbb{T}_2 & -\mathbb{T}_3 & \cdots & -\mathbb{T}_{N_e} & 0 \end{array}$$

With the expression (7.3), the Fourier modes $e^{\imath 2\pi \mathbb{T}_i \frac{z_i}{L_x}}$ are written for each coordinate z_i separately. The price paid is the introduction of the $\tilde{T}_{ij}$, labelling the interdependence of the different momentum components. The balance condition (7.4) ensure that the wave function will be in a well defined momentum sector.

Next, we also Fourier-expand the Laughlin CoM function. This procedure is straight forward as we deal with just a single ϑ-function with expansion (A.1). By individually, for each y_i, completing the squares over y_i that come from the Gaussian factor, we reconstruct the terms

$$\zeta_k = e^{-\imath 2\pi k x} e^{\imath \pi \tau N_s \left(y - \frac{k}{N_s}\right)^2}.$$

These terms make up the basis states in (4.5) as $\eta_k = \sum_t \zeta_{k+tN_s}$. Putting these expansion together gives the total expanded Laughlin state

$$\psi_{h,t} \quad = \quad \sum_{\left\{\mathbb{T}_i \in \mathbb{Z} + q\frac{N_e-1}{2}\right\}} \sum_m \mathcal{Z}\left(\mathbb{T}\right) e^{\imath 2\pi m t} \prod_{i=1}^{N_e} \zeta_{k_i}\left(z_i\right), \tag{7.5}$$

with the weight

$$\mathcal{Z}\left(\mathbb{T}\right) = \sum_{\left\{\tilde{T}_{ij} \in \mathbb{Z} + \frac{q}{2}\right\}} e^{\imath \pi \tau \frac{1}{q} \sum_{i<j<k} \left(\tilde{T}_{ij} + \tilde{T}_{jk} + \tilde{T}_{ki}\right)^2} e^{\imath \pi \sum_{i<j} \tilde{T}_{ij}} \prod_{i<j} \tilde{Z}^{(q)}_{\tilde{T}_{ij}}. \tag{7.6}$$

Here $t = h = q\left(N_e - 1\right)\frac{1}{2} + \mathbb{Z}$ is chosen as half-integers to ensure periodic boundary conditions. The formula above works for both fermions and bosons, and the momenta are now

$$k_i = \mathbb{T}_i + mq + h,$$

such that $\sum_i k_i = N_e h \bmod N_s$. From this expression we see why h is required to be a half integer if N_e is even. Because of the periodic boundary conditions, k_i is an integer, but the $\tilde{T}_{ij}$ are $\frac{q}{2}$-integers, such that $\mathbb{T}_i$ is a $q\frac{N_e-1}{2}$-integer. In order to ensure that k_i is integer, then $t = h$ has to be given as $q\left(N_e - 1\right)\frac{1}{2}$-integers.

The weight $\mathcal{Z}\left(\mathbb{T}\right)$ is the Fock coefficient in (7.1), but some massaging is required to arrive at that conclusion: the sums over ζ_{k_i} need to be extended to make them sums over η_{k_i}. For this purpose, we shift all the coordinates as $\mathbb{T}_i \to \mathbb{T}_i - qm$,

except for $\mathbb{T}_{N_e}$ which by the constraint (7.4) is shifted as $\mathbb{T}_{N_e} \to \mathbb{T}_{N_e} + (N_e - 1)\, qm$. This transforms $\mathcal{Z}(\mathbb{T}) \to \mathcal{Z}(\mathbb{T})\, e^{\imath\pi(N_e-1)qm}$ which cancels the $e^{\imath 2\pi mt}$ present in (7.5). The momenta of η_{k_i} can now be written as

$$k_i = \begin{cases} \mathbb{T}_i + h & i \neq N_e \\ \mathbb{T}_i + N_s m + h & i = N_e \end{cases}.$$

We can now perform the sum over m to transform $\zeta_{k_{N_e}}$ into $\eta_{k_{N_e}}$. To accomplish the same thing for the rest of the k_i, we split $\mathbb{T}_i$ as $\mathbb{T}_i \to \mathbb{T}_i + r_i N_s$ where now $\mathbb{T}_i \in \mathbb{Z}_{N_s}$ and $r_i \in \mathbb{Z}$. The r_i also obey the balance condition $\sum_i r_i = 0$. Hence, the momentum equals

$$k_i = \begin{cases} \mathbb{T}_i + N_s r_i + h & i \neq N_e \\ \mathbb{T}_i + h & i = N_e \end{cases},$$

such that it will be natural to sum over r_i to obtain η_{k_i}. It can be shown that $\mathcal{Z}(\mathbb{T}_i + r_i N_s) = \mathcal{Z}(\mathbb{T}_i)$ which means that the only place where r_i appears is precisely in k_i. This allows us to reconstruct all the basis functions (4.5). We obtain the expression (7.1), where now $k_i = \mathbb{T}_i + h \mod N_s$. With this, we have managed to extract the Fock coefficients (7.6) of the Laughlin state. Given this analytic form of the Fock expansion, we can study such things as the asymptotic normalization of the Laughlin state in the TT-limit.

7.2 Recursive construction of $\mathcal{Z}(\mathbb{T})$

Equation (7.6) enables us to compute the Fock coefficients of the Laughlin state. Nevertheless, the question remains whether it is numerically feasible to actually compute them. The sum (7.6) contains $\mathcal{O}\left(N_e^2\right)$ infinite sums, that can not be factorized and need to be evaluated as one big sum. Consequently, the number of operations needed to estimate any coefficient will scale as $\sim e^{\#\mathcal{O}\left(N_e^2\right)}$, with some number $\#$ depending on the number of terms needed for each variable $\tilde{T}_{ij}$.

But we can do better than this, and with some manipulation given in **Paper IV,** we can rewrite $\mathcal{Z}(\mathbb{T})$ on a recursive form as

$$\mathcal{Z}_{\mathbb{T}}^{(N_e)} = \sum_{\left\{\mathbb{T}_i^{(N_e-1)} \in \mathbb{Z}\right\}} e^{\imath\pi\tau q(N_e-1)N_e\, \pi(N_e)} e^{\imath\pi \sum_i^{N_e-1} \mathbb{T}_i^{(N_e)}} \times \\ \times \mathcal{Z}_{\mathbb{T}}^{(N_e-1)} \cdot \prod_i^{N_e-1} Z^{(q)}_{\mathbb{T}_i^{(N_e)} - \mathbb{T}_i^{(N_e-1)}}.$$

Each coefficient for N_e particles $\mathcal{Z}_{\mathbb{T}}^{(N_e)}$ now depends on the coefficients for $N_e - 1$ particles $\mathcal{Z}_{\mathbb{T}}^{(N_e-1)}$, the structure factors $Z^{(q)}_{\mathbb{T}_i^{(N_e)} - \mathbb{T}_i^{(N_e-1)}}$, and the weight

$$\pi(N) = \sum_{i=1}^{N-1} \left(\frac{\mathbb{T}_i^{(N-1)}}{q(N-1)} - \frac{\mathbb{T}_i^{(N)}}{qN} \right)^2 - \frac{1}{N-1} \left(\frac{\mathbb{T}_N^{(N)}}{qN} \right)^2. \tag{7.7}$$

We have introduced the notation $\mathbb{T}_i^{(k)} = \sum_{j=1}^{k} \tilde{T}_{ij}$ to keep track of what momentum components correspond to what number of electrons. With this new notation, the $\mathbb{T}_i^{(N)}$ are the fixed parameters for a given configuration $\{k\}$ whereas $\mathbb{T}_i^{(N-1)}$ are indexes summed over.

As the Fock components for smaller systems can be computed and then stored, this formulation reduces the computational complexity of computing $\mathcal{Z}_{\mathbb{T}}^{(N_e)}$ from $\mathcal{O}\left(e^{\#\mathcal{O}\left(N_e^2\right)}\right)$ to $\mathcal{O}\left(e^{\#\mathcal{O}(N_e)}\right)$. The drawback here is that in a computation, extra storage is required to hold the roughly $\sum_{N=1}^{N_e-1} \frac{1}{qN}\binom{qN}{N}$ states at previous iterations.

But we can do even better still. The sums over $\mathbb{T}_i^{(N-1)}$, intertwined in (7.7), can be partially separated. To reduce the notational complexity, we use $M = N-2$ to enumerate the number of independent components of $\mathbb{T}_i^{(N-1)} = \mathbb{T}_i^{(M+1)}$. The problem with (7.7) is that for the M independent variables $\mathbb{T}_i^{(M+1)}$ that are summed over, there are $M+1$ squares in (7.7). Looking only at the $\mathbb{T}_i^{(N-1)} = \mathbb{T}_i^{(M+1)}$ terms and ignoring the $\mathbb{T}_i^{(N)} = \mathbb{T}_i^{(M+2)}$ terms, the sum can be rewritten in a form containing only M squares:

$$\sum_{i=1}^{M+1} \mathbb{T}_i^2 = \sum_{i=1}^{M} \mathbb{T}_i^2 + \left(\sum_{i=1}^{M} \mathbb{T}_i\right)^2 = \sum_{n=1}^{M} w_n \left(\sum_{j=1}^{M} v_j^{(n)} \mathbb{T}_j\right)^2 . \tag{7.8}$$

For notational simplicity, we have removed the superscript on $\mathbb{T}_i^{(M+1)}$ and thus write simply $\mathbb{T}_i$. The vector $v^{(n)}$, with components

$$v_j^{(n)} = \begin{cases} 1 & j \le n \\ -n & j = n+1 \\ 0 & j > n+1 \end{cases},$$

is the orthogonalized eigenvectors of the $M \times M$ matrix $\mathcal{M}_{ij} = 1 + \delta_{ij}$ describing $\sum_{i=1}^{M+1} \mathbb{T}_i^2 = \sum_{i=1}^{M} \mathbb{T}_i \mathcal{M}_{ij} \mathbb{T}_j$. This matrix has eigenvalues $\lambda_n = 1 + n\delta_{n,M}$. The $w_n = \frac{\lambda_n}{s_n} = \frac{(1+n\delta_{n,M})^2}{n(n+1)}$ appearing in (7.8) is the eigenvalue λ_n divided by the squared norm of $v^{(n)}$, namely $s_n = n + n^2\left(1 - \delta_{n,M}\right)$.

When also incorporating the contribution from $\mathbb{T}_i^{(N)} = \mathbb{T}_i^{(M+2)}$ into (7.8), then (7.7) can be rewritten to yield

$$\begin{aligned} \mathcal{Z}_{\mathbb{T}}^{(N_e)} \quad = \quad & \sum_{\left\{\mathbb{T}_i^{(N_e-1)} \in \mathbb{Z}_{q(N_e-1)+\frac{q}{2}(N_e-2)}\right\}} \Lambda\left(\mathbb{T}^{(N_e)}, \mathbb{T}^{(N_e-1)}\right) \\ & \times e^{\imath\pi \sum_i^{N_e-1} \mathbb{T}_i^{(N_e)}} \mathcal{Z}_{\mathbb{T}}^{(N_e-1)} \cdot \prod_i^{N_e-1} Z^{(q)}_{\mathbb{T}_i^{(N_e)} - \mathbb{T}_i^{(N_e-1)}} . \end{aligned} \tag{7.9}$$

The introduced weight

$$\Lambda\left(\mathbb{T}^{(N_e)}, \mathbb{T}^{(N_e-1)}\right) =$$

$$\sum_{\{q_n \in \mathbb{Z}_n\}} \prod_{n=1}^{N_e-2} \vartheta\begin{bmatrix} \frac{q_n}{n} - \frac{q_{n+1}}{n+1} - \frac{D_n}{n(n+1)} \\ 0 \end{bmatrix}\left(0 \middle| (N_e-1)\, N_e\, (n+1)\, nq\tau\right) \tag{7.10}$$

is a sum of products of ϑ-functions that depends on $\mathbb{T}_j^{(N_e-1)}$ and $\mathbb{T}_i^{(N_e)}$ through

$$D_n = -\sum_{j=1}^{N_e-2} v_j^{(n)} \frac{\lambda_n \mathbb{T}_j^{(N-1)}}{q(N_e-1)} + \sum_{i=1}^{N_e-1} v_j^{(n)} \frac{\mathbb{T}_j^{(N_e)}}{qN_e}.$$

This way of formulating $\mathcal{Z}_{\mathbb{T}}^{(N_e)}$ should improve the convergence, as for each set of $\mathbb{T}_i^{(N_e-1)}$, a finite set of strongly converging ϑ-functions now can be computed. There is strong convergence on many of these terms as they take the form $\exp(\imath\pi\tau qn(n+1)N_e(N_e-1))$ in the TT-limit. In this limit the sum can be truncated to only contain a few dominant terms.

The reader should be aware that even though (7.10) is much more efficient than (7.6) for numerical purposes, it is still inferior to an option we mentioned earlier in this chapter. That option is to diagonalize the Haldane pseudo-potential Hamiltonian. Using the exact diagonalization we can compute the Fock coefficients for at least 12 electrons, depending on computational resources. As comparison, our current numerical implementation of (7.9) and (7.10) can *not* do more than 6 electrons. We have numerically compared the two ways for computing the Fock coefficients of the Laughlin state, and in all cases tested, we have perfect agreement. This option enables us to verify that our numerical implementation of (7.10) – and thus likely (7.10) itself – is correct.

Note also that the method outlined above can just as well be applied to all the chiral Haldane-Halperin states in (5.5). The crucial difference is; these states are *not* the exact zero energy eigenstates of any pseudo-potential Hamiltonian. Because of that, our method is the only one we know of that can exactly compute the Fock coefficients of these states.

Chapter 8

Topological Characterization and Hall Viscosity

As mentioned, there are novel difficulties when analysing the torus, as compared to the plane. After all, the wave functions are more complicated and there exists no clear analogy of what the derivatives are. So why bother with the torus? The answer is that some things are more easily computed on the torus than on other geometries. The antisymmetric component of the viscosity tensor is one such example. We will soon return to the antisymmetric viscosity and how it is calculated.

For the moment, let us consider single particle orbitals on the sphere. If you imagine a single particle on a sphere that is pierced by N_Φ fluxes, you will find that there are $N_\Phi + 1$ single particle orbitals. This extra "effective flux" is present because electrons carry a non-zero orbital spin $\bar{s}_{\text{SP}} = \frac{1}{2}$*. On the sphere, which has a curved surface, this spin will pick up a Berry phase as the electrons move over the curved surface; a Berry phase, which will show up as an extra effective magnetic flux.

This extra flux is also present when considering many-body states. It will be important for the Hall viscosity. Let us start with the example of the filled LLL, where due to the single particle properties, we need $N_e = N_\Phi + 1$ electrons to fill the LLL for N_Φ fluxes. Anticipating what will come, we can write this relation between N_e and N_Φ as

$$N_e = \nu \left(N_\Phi + \mathcal{S} \right). \tag{8.1}$$

For the filled LLL, which describes the state responsible for the IQHE at $\nu = 1$, $\mathcal{S} = 1$ as argued above. The point in writing (8.1) is that $\mathcal{S}$ represents a topologically protected number which will not depend on N_e, for a fixed ν. As an example, for ν filled LL:s then $\mathcal{S} = \nu$.

We now ask the question; what happens when a LL is only partially filled, *i.e.*when ν is not integer? The naive answer we might get; obtained by extrapolating from the filled LL:s, is that in general $\mathcal{S} = \nu$. This can however not be the whole truth, as (8.1) does not have integer solutions for all ν. Indeed, requiring

*SP = Single Particle

N_e and N_Φ to be integers and $\nu = \frac{p}{q}$, constrains $\mathcal{S}$ to be $\mathcal{S} = \frac{\mathbb{Z}}{p}$, which does not work if $q \neq 1$.

What happens is that interactions between the electrons invalidates the non-interacting picture of single electrons and induces extra average orbital spin $\bar{s}$ to the electrons. As a result, $\mathcal{S}$ will change. As examples, the Laughlin state at $\nu = \frac{1}{q}$ has $\mathcal{S} = q$ whereas the first level sates in the Haldane-Halperin hierarchy[Hal83a, Hal83b] at $\nu = \frac{2}{5}$, has $\mathcal{S} = 4$. As such, the shift contains information about the average orbital spin of the electrons $\bar{s}$, such that $\mathcal{S} = 2\bar{s}$. Since $\mathcal{S}$ is a topologically protected number, different quantum Hall states at the same filling fraction can have different shifts, which can be used to distinguish these states from each other.

On the torus, there is no curvature, thus N_e is proportional to N_Φ, so that $N_e = N_s\nu$ instead of (8.1). At first glance it looks as if the shift is a purely geometrical effect unrelated the torus, but this conclusion would be incorrect. The shift is a topological characteristic of the quantum Hall system and must thus be observable on all geometries. This means that there must exist a quantity on the torus that carries the same topological information as the shift $\mathcal{S}$. However, since the torus has a flat surface, the orbital spin does not manifest itself in the filling fraction equation (8.1). Instead it is manifest through a transport coefficient. This particular coefficient is the antisymmetric component of the viscosity tensor η^A. The connection between η^A and $\mathcal{S}$ is actually quite non-trivial and bellow we will give some heuristic arguments why the two are related.

The viscosity tensor η relates the strain-rate $\dot{u}$ to the stress σ in an analogues way that the elastic modulus λ relates σ to the strain u in a system. As σ, u and $\dot{u}$ are 2-tensors, λ and η are 4-tensors and

$$\sigma_{\alpha\beta} = \sum_{\gamma,\delta=1}^{d} \left(\lambda_{\alpha\beta,\gamma\delta} u_{\gamma\delta} + \eta_{\alpha\beta,\gamma\delta}\dot{u}_{\gamma\delta}\right),$$

where d is the dimensionality of space. The viscosity tensor may be split into two pieces as

$$\eta = \eta^S + \eta^A,$$

where η^S is symmetric under the exchange of the first and second pair of indexes whereas η^A is antisymmetric under the same exchange

$$\begin{aligned} \eta^S_{\alpha\beta,\gamma\delta} &= \eta^S_{\gamma\delta,\alpha\beta} \\ \eta^A_{\alpha\beta,\gamma\delta} &= -\eta^A_{\gamma\delta,\alpha\beta}. \end{aligned}$$

In an isotropic system, η^S only possesses two independent components, the *shear viscosity* and *bulk viscosity*. The antisymmetric viscosity however has peculiar properties and for isotropic systems only exists in two dimensions[ASZ95]. We seek to calculate this particular type of viscosity, sometimes called the Hall viscosity, which is unique for two-dimensional systems. If the fluid is isotropic – as in our case – there is only one independent component of the tensor η^A. The symmetric viscosity components, the bulk and shear viscosity η^S are related to dissipation and can be thought of as the *thickness* of a fluid. In contrast, the antisymmetric component is related to a dissipationless response of the fluid and can not the thought of in terms of a thickness. That the response would be dissipationless is explained by the gap to excitations that exists in FQH fluids. This

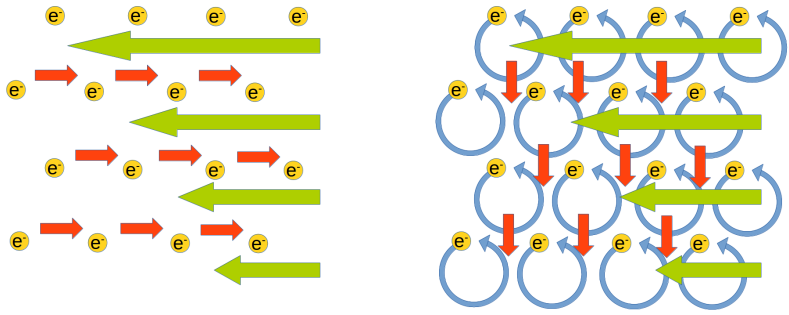

Figure 8.1: A physical interpretation of ordinary viscosity vs. antisymmetric viscosity.
a) In a symmetric viscous response, the particles experience a force ⟵ in the opposite direction of the direction of motion ⟵, and as a result dissipate energy due to friction.
b) In an anti-symmetric viscous response, the experienced force ⟵ is perpendicular to the direction of motion ⟵, and no energy is dissipated. For isotropic systems this can only happen in two dimensions when time reversal symmetry is broken. The quantum Hall system fulfil these criteria.

means that the viscous response is area preserving as the fluid is incompressible. A way to visualize this response is to consider the semi-classical picture of electrons undergoing cyclotron motion. When a velocity gradient is set up in the system, the cyclotron motion will make the fluid experience a force to the side. Because the force is perpendicular to the direction of motion, no work is done and no energy is dissipated. This difference between the ordinary symmetric viscosity and the antisymmetric viscosity is illustrated in Figure 8.1.

Avron *et al.* computed the Hall viscosity for filled Landau Levels[ASZ95] where $\nu \in \mathbb{Z}$. They found it to be

$$\eta_{\text{LL}} = \frac{1}{2}\hbar\bar{n}\bar{s}.$$

Here $\bar{n}$ stands for the number density of electrons, and is thus given by $\bar{n} = \frac{N_e}{L_x L_y} = \frac{N_e}{2\pi N_s \ell_B^2} = \frac{\nu}{2\pi\ell_B^2}$. $\bar{s} = \frac{\nu}{2}$ is the mean orbital spin for ν filled LL:s. We write the viscosity in this suggestive form to make contact with the topological shift $\mathcal{S} = 2\bar{s}$. Even though the Avron calculation involved a many-particles state, it boiled down to computing the contributions from each single particle orbital in (4.5). From that analysis it follows that $\bar{s}_{SP} = \frac{1}{2} + n$, where n is the LL index. The many-particle result is obtained by taking the mean value of all the $\bar{s}_{\text{SP}}$ contributions as $\bar{s}_{\text{LL}} = \frac{1}{\nu}\sum_{n=0}^{\nu-1}\bar{s}_{\text{SP}} = \frac{1}{2} + \frac{1}{\nu}\frac{\nu(\nu-1)}{2} = \frac{\nu}{2}$.

In the case of a partially filled LL, the analysis is more complicated as the electrons are now interacting. Nevertheless is has been performed by Read and Read & Rezayi for the Laughlin state and the Moore-Read state[Rea09, RR11]. Read demonstrated that the mean orbital spin is related to the antisymmetric viscosity of the quantum Hall system[Rea09] as

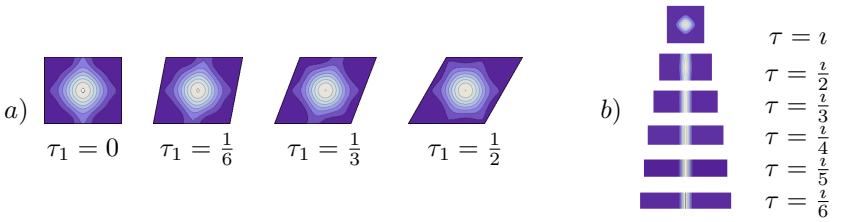

Figure 8.2: Single particle orbital density as a function of τ in the euclidean coordinates $\tilde{x}$ and $\tilde{y}$. *a)* A continuous coherent state (**Paper II**) reshapes itself to account for the skewness introduced when $\tau = \imath\frac{\sqrt{3}}{2} \to \tau = \tau_1 + \imath\frac{\sqrt{3}}{2}$. *b)* A lattice coherent state (**Paper II**) becomes increasingly anisotropic as the TT-limit is approached. All deformations of τ are area preserving. This graphically explains why there exists a Berry curvature associated with changes in τ. As τ is altered, the shape of the single particle orbitals changes to account for the new geometry, which gives rise to a Berry phase.

$$\eta^A = \frac{1}{2}\hbar\bar{n}\bar{s}. \tag{8.2}$$

The average orbital spin need however *not* be $\bar{s} = \frac{\nu}{2}$ any more. In the Laughlin case, where $\nu = \frac{1}{q}$ then $\bar{s} = \frac{q}{2} = \frac{1}{2\nu}$, which means that interactions can modify the mean orbital spin away from the non-interacting value. Read conjectured that the general relation between average orbital spin and viscosity should always be given by (8.2).

However, the viscosity computations by Read & Rezayi where only made for single component wave functions. It is not clear that the relation (8.2) will hold for multicomponent constructions too, such as the $\nu = \frac{2}{5}$ wave function. It is important to calculate the viscosity for the $\nu = \frac{2}{5}$ trial wave function, both to make sure that it is in the expected topological phase as well as to check whether it corresponds to the Read conjecture (8.2) or not.

8.1 How to compute the viscosity

Viscosity is calculated by computing the Berry phase that arises as a response to changes in the torus geometry, τ. But why should we look at adiabatic changes in τ in order to compute η? Consider a semi-classical picture of electrons confined to cyclotron orbits. Because of the Coulomb repulsion, the electron orbits will attempt to lie as far apart from each other as possible. As the geometry is changed, the electron orbitals adjust themselves ever so slightly to reach an optimal distribution in the new geometry. This change in geometry is in a sense an adiabatic version of setting up a strain rate. This is because the change in geometry induces strain in the system. As viscosity is the response to a strain rate, the adiabatic change in geometry will capture this through the Berry phase. Figure 8.2 provides a graphical illustration of how this Berry phase appears.

Another way to understand why the viscosity would be associated with the change in geometry parameter τ is by considering what happens for instance when

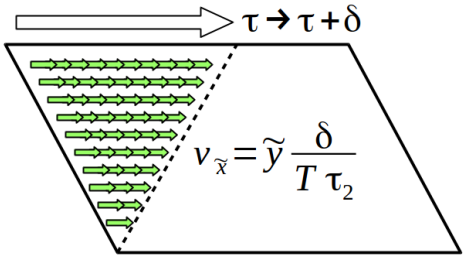

Figure 8.3: The physical intuition why a changing τ would probe a viscous response. If $\tau(t) = \tau_0 + t\frac{\delta}{T}$, the velocity for a point fixed at $z = L_x(x + \tau y)$ has a horizontal speed ($\Longrightarrow$) $v_{\tilde{x}} = \frac{\delta L_x}{T} y = \frac{\delta}{\tau_2 T}\tilde{y}$. This creates a velocity gradient in the $\tilde{y}$-direction. In this sense, changing τ really simulates a constant velocity gradient.

$\tau \to \tau + \delta$. If we assume that τ changes with time, such that $\frac{\partial \tau}{\partial t} = \frac{\delta}{T}$ is constant, then the real space velocity of a point at $z = L_x(x + \tau y)$ will change by $v_{\tilde{x}} = \frac{\partial z}{\partial t} = L_x y \frac{\partial \tau}{\partial t} = \frac{\delta L_x}{T} y$ so that there is a constant velocity gradient in $\tilde{y}$ direction that is $\partial_{\tilde{y}} v_{\tilde{x}} = \frac{\delta L_x}{T}\partial_{\tilde{y}} y = \frac{\delta}{T\tau_2}$. With this in mind, changing τ simulates the application of a constant velocity gradient as illustrated in Figure 8.3.

Analytically it is really the Berry curvature $\mathcal{F} = \imath\partial_{\bar{\tau}} A_\tau - \imath\partial_\tau A_{\bar{\tau}}$ that captures the viscosity information through the relation

$$\eta^H = -\frac{2\tau_2^2}{A_{\text{Torus}}}\mathcal{F}, \tag{8.3}$$

where $A_{\text{Torus}} = L_x L_y = 2\pi N_s \ell_B^2$ is the area of the torus. The Berry curvature is computable from the Berry connection $A_\mu = \imath\langle\varphi|\partial_\mu\varphi\rangle$, where $\mu = \tau, \bar{\tau}$. Here $|\varphi(\tau)\rangle$ represents the wave function as a function of τ.

For the trial wave function (6.9), we can compute the viscosity analytically if we make use of the plasma analogy. A careful computation of the primary correlation function (5.4) yields a candidate for the normalization $\mathcal{N}(\tau)$. This normalization, where we know the full τ-dependence is

$$\mathcal{N}(\tau) = \mathcal{N}_0 \frac{\left[\tau_2 \eta^4(\tau)\right]^{\frac{1}{4}\sum M_{ii}^2}}{\eta(\tau)^{\sum_{i<j} M_{ij}}\,\eta^n(\tau)}. \tag{8.4}$$

In this setting, the plasma analogy implies that (8.4) contains the full τ-dependence so that $\mathcal{N}_0$ is a constant. Under these circumstances, it can be shown that

$$\bar{s} = \frac{1}{N_e}\sum_\alpha N_\alpha\left(\frac{1}{2}K_{\alpha\alpha} + \alpha - 1\right),$$

which coincides with the result obtained by Kvorning on the sphere[Kvo13].

To numerically evaluate $\mathcal{F}$ at a specific point $\tilde{\tau} = \tilde{\tau}_1 + \imath\tilde{\tau}_2$, we use the procedure of Read & Rezayi[RR11], and compute the mean Berry curvature $\bar{\mathcal{F}}$ in a region Ω by integrating the Berry connection around a closed loop following the contours of Ω. The mean Berry curvature $\bar{\mathcal{F}}$ is obtained from the Berry connection as

$\bar{\mathcal{F}} = \frac{1}{A_\Omega} \oint_{\partial\Omega} A_\mu(\lambda)\, d\lambda_\mu$. If the area of Ω is small enough, then $\mathcal{F}$ is approximately constant, and the path $\partial\Omega$ may be discretized into straight segments. As a result, $\bar{\mathcal{F}}$ can approximately be evaluated as

$$W = e^{\imath A_\Omega \bar{\mathcal{F}}} = e^{\imath \oint A_\mu(\lambda)\, d\lambda_\mu} \approx \prod_j \langle \varphi_j | \varphi_{j+1} \rangle, \tag{8.5}$$

where $|\varphi_j\rangle$ is the state at point j along the curve $\partial\Omega$. We typically use a radius of $r = 0.005$ and $N = 200$ steps, as in Ref. [RR11]. The area A_Ω of Ω is calculated as

$$A_\Omega = \int_\Omega \frac{d\tau_1\, d\tau_2}{\tau_2^2} = 2\pi \left[\frac{1}{\sqrt{1 - \left(\frac{r}{\tilde{\tau}_2}\right)^2}} - 1 \right] \approx \pi \left(\frac{r}{\tilde{\tau}_2}\right)^2,$$

where $\tilde{\tau}_2$ is the imaginary τ coordinate for the centre of Ω, r the radius of Ω. In terms of W, the viscosity is

$$\eta^H = -\frac{2\tilde{\tau}_2^2}{A_{\text{Torus}}} \frac{\Im(W)}{A_\Omega},$$

where (8.5) was inserted into (8.3). We take the imaginary part of W – $\Im(W)$ – since for small area of Ω, $W \approx 1 + \imath A_\Omega \bar{\mathcal{F}}$ and we are solely interested in the real component of $\bar{\mathcal{F}}$. Using (8.2), we can express the average orbital spin as

$$\bar{s} = -\frac{\tilde{\tau}_2^2}{N_e} \frac{\Im(W)}{A_\Omega}, \tag{8.6}$$

where we use that $\bar{n} = \frac{N_e}{A_{\text{Torus}}}$.

Note that when computing the viscosity using exact diagonalization, the overlap is computed using the Fock expansion coefficients as $\langle \varphi_j | \varphi_{j+1} \rangle = \sum_{\mathbf{k}} \alpha_{\mathbf{k}}^{\star(j)} \alpha_{\mathbf{k}}^{(j+1)}$, where $\alpha_{\mathbf{k}}$ expands the state $|\varphi_j\rangle = \sum_{\mathbf{k}} \alpha'_{\mathbf{k}} |\mathbf{k}; \tau_j\rangle$. This way of computing the overlap would imply that $\langle \mathbf{k}'; \tau' | \mathbf{k}; \tau \rangle = \delta_{\mathbf{k},\mathbf{k}'}$, which is not true. The consequence is that the non-interacting contribution from the Slater determinant $|\mathbf{k}; \tau(j)\rangle$ is not accounted for in (8.6). Fortunately the non-interacting result can be simply added to the interacting one and gives the modified equation

$$\bar{s}_{\text{ED}} = -\frac{\tilde{\tau}_2^2}{N_e} \frac{\Im(W)}{A_\Omega} + \frac{1}{2},$$

for viscosity computed through exact diagonalization. From this equation, it is obvious that any state that is only a single Slater determinant, will have $\bar{s} = \frac{1}{2}$. After all, $\Im(W)$ identically vanishes for these states since $W = 1$.

8.2 Viscosity in the $\nu = \frac{2}{5}$ state

We now have two systems at $\nu = \frac{2}{5}$ for which we may compute the viscosity: the exact Coulomb ground state and the Hierarchy state given by (6.9). We shall compute viscosity for both the exactly diagonalized state and the trial wave

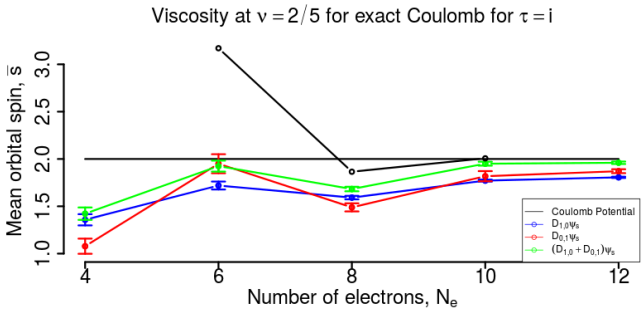

Figure 8.4: Viscosity, in units of the mean orbital spin $\bar{s}$, for the exact Coulomb ground state and CFT wave functions for $N = 4, 6, 8, 10, 12$ electrons. The torus geometry is $\tau = \imath$. The value of $\bar{s}$ depends on N_e. This is likely a finite size effect since $\bar{s}$ converge on $\bar{s} = 2$ as N_e increases.

functions. This is a sanity-check as overlaps are not always a good characterization on if two states are the same.*

Considering the $\nu = \frac{2}{5}$ state, given by (6.9), three objectives needs to be met in order to declare (6.9) a good trial wave function. First, the overlap with the exact Coulomb ground state has to be high. We have already showed this to be the case in Section 6.4, in particular with Figure 6.7. Second, we need establish that the trial wave function and Coulomb wave function have the same $\bar{s}$, which is a natural test that the two wave functions are in the same topological sector. Third, the numerical value of $\bar{s}$ should correspond to the analytically predicted value $\bar{s} = 2$, which is really a test that the above mentioned plasma analogy holds.

In Figure 8.4 we compute $\bar{s}$ for $\tilde{\tau} = \imath$ as a function of system size with $N_e = 4, 6, 8, 10, 12$ particles. We find that $\bar{s}$ asymptotically approaches $\bar{s} = 2$ for both the trial wave function and the Coulomb ground state. There are however still noticeable finite size effects. We can compute the viscosity only for $N_e = 10$ exactly diagonalized particles but the trial wave function can be evaluated for at least $N_e = 12$ particles. Note that using only $D_{1,0}$ or $D_{0,1}$ on their own yields a result further from $\bar{s} = 2$ than if the two terms where added together. This is only to be expected since the same behaviour was observed for the overlap in Figure 6.4. We expect that when two terms are equally dominant, both terms may be needed.

In Figure 8.5, we choose a system of N_e particles and study how $\bar{s}$ depends on τ as we go away from the square torus of $\tau = \imath$. We see that even for moderate deviations from $\tau = \imath$, the values of $\bar{s}$ are significantly different from $\bar{s} = 2$. We believe this τ-dependence of $\bar{s}$ to be a finite-size effect† since it becomes less

*There are examples of wave functions that have very good overlap, but still have very different symmetries. A case in point is the Gaffnian[SRCB07], which has good overlap with the exact Coulomb ground state, but also possesses several pathological properties. One of these properties is the existence of gapless excitations, such that the Gaffnian does not represent a stable gapped topological phase of matter.

†It should be noted that for $\tau \to \imath 0$ and $\tau \to \imath\infty$, we expect $\bar{s} \to \frac{1}{2}$. In this limit, which is the thin torus limit, all dynamics are frozen out. Thus the problem becomes one-dimensional

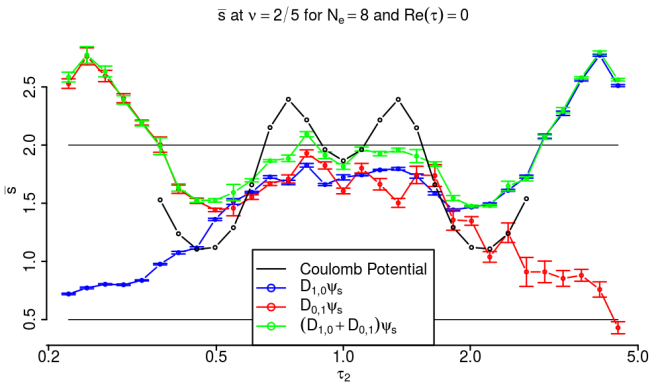

Figure 8.5: Viscosity, in units of the mean orbital spin $\bar{s}$, for the Hierarchy wave functions $D_{1,0}\Psi_s$ (Blue), $(D_{1,0}+D_{0,1})\,\Psi_s$ (Green) and $D_{0,1}\Psi_s$ (Red) defined in (6.9). The torus has the parameters $\Re(\tau) = 0$ and $0.2 < \Im(\tau) < 5$. In the region $\Im(\tau) \approx 1$ both $D_{0,1}$ and $D_{1,0}$ has viscosity near $\bar{s} = 2$. For $\Im(\tau) \to 0$ and $\Im(\tau) \to \infty$ the value of $\bar{s}$ drops to $\bar{s} = \frac{1}{2}$, which is related to the torus becoming thin. It is clear that the different weights in (6.9) are kicking in, as $D_{0,1} + D_{0,1}$ follows either $D_{1,0}$ or $D_{0,1}$ depending on τ.

pronounced for larger values of N_e. Both the trial wave functions and exactly diagonalized Coulomb ground state behave in qualitatively the same way as a function of τ, but the trial wave function seems to be more stable as $\bar{s} \approx 2$ in a wider region around $\tau \approx \imath$. This might not be too surprising as (6.9) is intended to realize a particular topological sector.

We also compute the viscosity for the different terms making up the hierarchical wave function (6.9). The $\bar{s}$-values for the various pieces differ substantially as τ is tuned away far from $\tau = \imath$. This is clearly seen in Figure 8.5, where as expected, the coefficients entering in (6.9) single out one viscosity value over the other.

Numerically it is time consuming to evaluate the viscosity. For the exact diagonalization, we are as usual limited by the exponential growth of the Hilbert space, meaning that it is not tractable to look at systems larger than $N_e = 12$ without resorting to super computers. Also, the number of steps that discretize the path Ω should be on the order of $N = 200$ steps. This reduces the largest systems size to $N_e = 10$.

For the Hierarchical states, there exists a different problem. Although we do not need to perform an exact diagonalization, the overlap in (8.5) has to be evaluated using Monte Carlo methods. This introduces statistical noise into the viscosity calculation, necessitating the error bars on $\bar{s}$ for the trial wave functions but not for the diagonalized state.

To summarize: The Hierarchy states appear to have the mean orbital spin $\bar{s} = 2$. This result is consistent with the expected result given by shift $\mathcal{S} = 4$. Nevertheless, there still remain large numerical errors.

---

and electrostatic.

8.3 Tao-Thouless limit – where the plasma analogy fails

In this section we will briefly discuss what should be expected of the viscosity in limit of a thin torus (TT-limit). The thin torus limit is approached when the aspect ratio τ_2 of the torus becomes so large that one of the two principal axes are comparable with the magnetic length $L_{\{1,2\}} \approx \ell_B$. In this limit all the hopping elements in the Hamiltonian vanish and only the electrostatic terms remain. Since only electrostatic terms remain in the TT-limit, the ground state is in the simplest cases given by only a single Slater-determinant[BK08]. The Coulomb interaction in the LLL has this particular property in the TT-limit. The thin torus limit is also sometimes called the Tao-Thouless limit as the single Slater-determinant state was an early proposal by Tao and Thouless to explain the fractional conductivity in the FQHE[TT83]. The acronym TT can thus interchangeably stand for *thin torus* or *Tao-Thouless*. For a detailed description of the TT-limit we refer to Ref. [BK08].

The TT-limit is interesting since it is adiabatically connected to the physical geometry at $\tau \approx \imath$, in the sense that the gap to the lowest excitations is always open, as τ is changed from $\tau \approx \imath$ to $\tau \to 0$[BK08]. Thus, results obtained in the TT-limit can shed light on the more physical quadratic geometry. It is especially easy to compute the fractional charge of the quasi-particles in this limit.

As there are no hopping terms in this limit, the problem is in a sense classical* and it is practical to describe the physics in terms of momentum (or Fock) configurations such as 001001001001001 or 001010010100101. The n:th digit labels the number of electrons that occupy the n:th orbital. The two configurations give the TT-states for the filling fractions $\nu = \frac{1}{3}$ and $\nu = \frac{2}{5}$ respectively.

8.3.1 Exclusion statistics in the TT-limit

In **Paper I** we investigated the TT-limit with focus on the excitation spectrum of the quasi-particles. We introduced quasi-particle configurations $\mathfrak{p}$ and quasi-hole configurations $\mathfrak{h}$. For $\nu = \frac{1}{3}$ the configurations are $\mathfrak{p} = 01$ and $\mathfrak{h} = 0$, whereas for $\nu = \frac{2}{5}$ they are $\mathfrak{p} =01$ and $\mathfrak{h} = 001$. We showed that the ground state was given by the configuration $\mathfrak{php}\mathfrak{php}\mathfrak{php}\mathfrak{h}$ and the low energy sector was described by all the possible permutations of the $\mathfrak{p}$ and $\mathfrak{h}$ configurations. As an example, the minimal particle hole excitation was given by the configuration $\mathfrak{php}\mathfrak{h}\underline{\mathfrak{hp}}\mathfrak{php}\mathfrak{h}$. Here, the underscore marks the $\mathfrak{h}$ and $\mathfrak{p}$ that have been permuted to generate the excitation.

Using the language of $\mathfrak{h}$ and $\mathfrak{p}$ we computed the exclusion statistics[Hal91] g for the quasi-particles in the TT-limit. Exclusion statistics is a generalization of the Pauli exclusion principle. It measures how many single particle states are occupied by adding an extra particle. For fermions this number is $g_f = 1$ due to the Pauli exclusion principle, whereas for bosons it is $g_b = 0$ since several bosons can be in the same single particle state. Exclusion statistics is closely tied to the phase two particles pick up when they are exchanged; Two fermions pick up a phase $e^{\imath\pi g_f} = -1$ when exchanged and two bosons pick up the phase $e^{\imath\pi g_b} = 1$.

*In the sense that the Hamiltonian is diagonal.

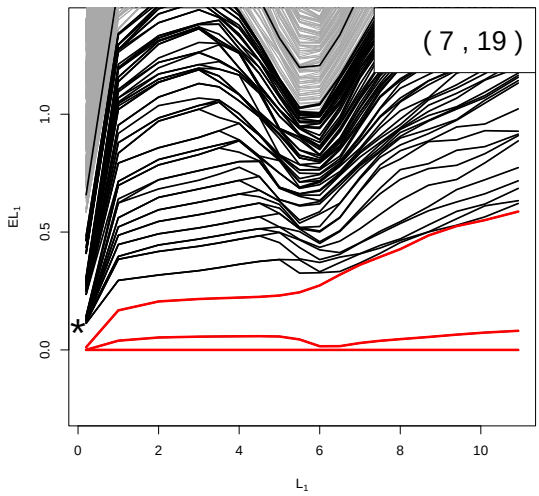

Figure 8.6: Energy spectra for a screened Coulomb potential at $\nu = \frac{1}{3}$ as L_1 (L_x) is changed from the TT-regime $L_1 = 0$ to the physical regime. The state contains a configuration with 5 electrons and two extra quasi-particles making up a total of $N_e = 7$ electrons and $N_s = 19$ flux quanta. One of the low energy states (red) leaves the lowest band of states and joins the band of higher energy. This change of band signifies a change of exclusion statistics for the quasi-particles.

Several other authors (see references in **Paper I**) have discussed exclusion statistics and our conclusions concur with the literature for the quasi-holes. However, our results differ from the other authors in the case of the quasi-particles. Numerical studies performed in **Paper I** indeed show – as τ develop from the TT-regime to the physical regime at $\tau \approx \imath$ – that the exclusion statistics do change from our result to the values proposed by other authors. See Figure 8.6.

That the exclusion statistics change between the TT-regime and the physical regime is a signature that not all quantities in the TT-limit are adiabatically connected with the physical state at $\tau \approx \imath$. It is thus interesting to see how deep into the TT-regime the viscosity remains a meaningful quantity.

8.3.2 Viscosity in the TT-limit

Figure 8.7 illustrates why we should be careful then studying viscosity in the TT-limit. The mean orbital density drops to $\bar{s} = \frac{1}{2}$ and will do so for a large enough value of τ for any system size. In this sense, the TT-limit regime will persist even in the thermodynamic limit, given that the system is sufficiently thin. That there is a well defined region where $\bar{s} = \frac{1}{2}$, is clear from the right hand plot of Figure 8.7: there is universal behaviour that only depends on the shorter physical size – L_x in this case – of the torus. Note that the onset takes place at about $L_x \approx 5\ell_B$, just as the system changes from a simple TT-state to a more correlated state[BK06].

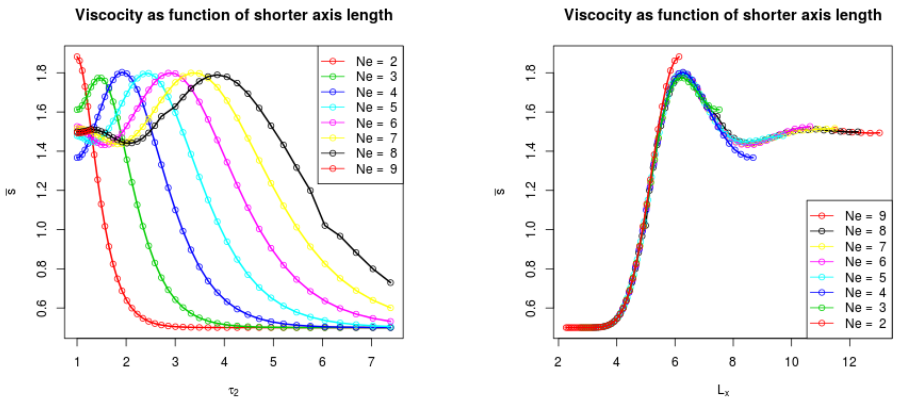

a) *b)*

Figure 8.7: Viscosity of the Laughlin state at $\nu = \frac{1}{3}$ for $N_e = 2, \ldots, 9$ particles. *a)* $\bar{s}$ as a function of τ_2. *b)*$\bar{s}$ as function of $L_x = \sqrt{\frac{2\pi N_s}{\tau_2}}$. Notice that the curves are almost independent of system size if $\bar{s}$ is plotted as a function of L_x. The curves for larger system sizes extends to larger L_x as the system size increases. This is since the square torus is at $L_x = \sqrt{2\pi N_s}$.

The physical intuition is this: if L_x is small enough, the overlaps between neighbouring electron wave functions is exponentially suppressed. Because of this suppression all hopping terms except the electrostatic terms – which do not contain any hopping – vanish in the TT-limit. This is illustrated in Figure 8.8. As a result of the vanishing hopping terms, the electrons have no knowledge of how long ($\tau_2 L_x$) the system is, and are thus only sensitive to the short length-scale L_x.

We now return to the Fock expansion of the Laughlin state in (7.1) and consider what happens in the TT-limit. Since the Laughlin wave function reduces to a single Slater determinant for the root partition $\ldots 001001001001\ldots$, it follows that only one element of $\mathcal{Z}(\mathbb{T}_i)$ remains non-zero as $\tau \to \infty$. From this we can deduce that the viscosity in the TT-limit really is $\bar{s} = \frac{1}{2}$ since the entire contribution comes from this single Slater determinant.

We may now compute the correction to the CFT normalization $\mathcal{N}(\tau)$ by studying $\mathcal{Z}(\mathbb{T}_i)$. The TT-limit behaviour of $\mathcal{Z}(\mathbb{T}_i)$ by extracted by keeping only the leading factors of (7.6), which are

$$\mathcal{Z}(\tau) \approx \sqrt{\tau_2}^{-\frac{N_e}{2}} e^{-\pi\tau_2 \frac{q}{24}\left(N_e^2 - 3N_e + 2\right)}.$$

The factor $\sqrt{\tau_2}$ comes from the normalization of the single particle wave functions, the exponential from all the ways of ordering $1 \leq i < j < k \leq N_e$. Further, leading behaviour of $\mathcal{N}(\tau)$ can be extracted from (8.4) and is

$$\mathcal{N}(\tau) \approx \frac{\sqrt{\tau_2}^{\frac{qN_e}{2}}}{e^{\imath\pi\tau\frac{1}{12}\left[\frac{N_s}{2}(N_e-3)+1\right]}}.$$

Since only one Fock state is present in the expansion (7.1), the properly normalized

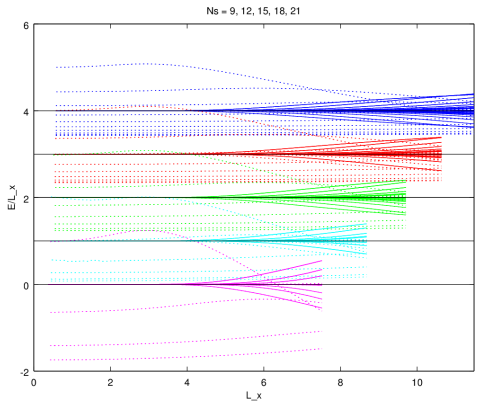

Figure 8.8: Hopping elements of the Coulomb Hamiltonian at $\nu = \frac{1}{3}$ and $N_e = 3, 4, 5, 6, 7$ particles. The range of L_x is from $L_x \approx 0$ to $L_x = L_y$ ($\tau = \imath$) which is why the curves for larger system sizes extends further to the right. Dotted lines represents electrostatic terms, *i.e.* where no hopping occurs. Solid lines represent all other hopping terms. Notice that the hopping terms have all vanished at $L_x \approx 4\ell_B$. This is also the point where the viscosity diverges from $\bar{s} = \frac{1}{2}$. See Figure 8.7.

state then has the property $\mathcal{N}_0 \mathcal{N}(\tau)\, \mathcal{Z}(\tau) = 1$. However, since

$$\mathcal{N}_0 = \frac{1}{\mathcal{N}(\tau)\, \mathcal{Z}(\tau)} = \left[\sqrt{\tau_2}\eta^2(\tau)\right]^{\frac{(q-1)N_e}{2}},$$

there is an asymptotic correction to the normalization $\mathcal{N}(\tau)$ when $\tau \to \infty$. From the non-trivial correction $\mathcal{N}_0$ we draw the conclusion that the viscosity in the TT-limit does *not* carry any information about the topological aspects of the wave functions. As a consequence, there is no generalized plasma analogy in this limit. We must thus take case to ensure that we are sufficiently far from the TT-limit when interpreting the viscosity data. Fortunately, the universality behaviour of the viscosity seems to be present also in other systems than the Laughlin state. Hence, it is fruitful to use L_x as the control parameter instead of τ when studying viscosity.

Chapter 9

Summary and Outlook

In this thesis we have focused mainly on the construction of quantum Hall wave functions on the torus. The construction consists of two different pieces, first the conformal blocks that are extracted from correlators of vertex operators, and second, the modular invariant derivatives that distinguish different particle groups under anti-symmetrization and thus prevent the wave functions from vanishing under anti-symmetrization.

In the first step, we have computed the correlation function of a string of vertex operators, one for each particle. The correlation function can be expressed as a sum over chiral and ant-chiral conformal blocks, which are glued together. The wave functions with proper single particle boundary conditions are constructed as linear combinations of the chiral blocks.

The second step of constructing modular covariant derivatives is inspired by the short range regularization of the hierarchy construction on the torus. We note that the derivatives have to be written as a product of single particle translation operators $\prod_i^{N_e} t_{m_i,n_i}^{(i)}$. However, in order to preserve the q-fold degeneracy, we can not form any product but must restrict ourselves to combinations on the form $T_{m,n}^{(\alpha)} = \prod_{i_\alpha}^{N_\alpha} t_{m,n}^{(i_\alpha)}$. In this way all particles in the same group are translated rigidly. We have shown that, due to modular covariance, the physical generalized derivative $\mathbb{D}$ is a sum over all possible $T_{m,n}^{(\alpha)}$. The relative weights, and especially phases of $T_{m,n}^{(\alpha)}$ have been calculated from the principle of modular covariance.

As an application of the generalized derivative, we have constructed a trial wave function for the $\nu = \frac{2}{5}$ state. This wave function has excellent agreement with the Coulomb ground state in the entire τ-plane. Good agreement can be obtained with as little as a single $T_{m,n}$-term, provided it is chosen appropriately. This result is especially impressive as the requirement of modular covariance fixes the form of $\lambda_{m,n}$ up to a relative minus-sign between some terms. Further we have calculated the viscosity of the trial wave function numerically, and found that it coincides well with the values retrieved from exact diagonalization of the Coulomb potential.

Finally we have computed the TT-limit correction to the CFT normalization $\mathcal{N}(\tau)$. We numerically demonstrated that the viscosity exponentially approaches $\bar{s} = \frac{1}{2}$ in the TT-limit. This illustrates that the many-body correlation effect

present in the physical regime $\tau \approx \imath$ is not present in the TT-regime. This result is of course to be expected since the state reduces to a single Slater determinant. A Slater determinant has the same viscosity as the contributing single particle orbitals.

Several extensions can be made to the work presented in **Paper II** and **Paper III** especially. The first such extension is to generalize the CFT construction to also include quasi-hole condensations in the Hierarchy picture. The quasi-hole condensates produce K-matrices with negative eigenvalues and so they can not be computed directly in the framework of (5.5) and (5.6). The extension is however straight forward as the K-matrix is split into a holomorphic and an anti-holomorphic piece $K = \kappa - \bar{\kappa}$, where both κ and $\bar{\kappa}$ has positive eigenvalues. A state that falls into this category is the $\nu = \frac{2}{3}$ state, the particle hole conjugate of $\nu = \frac{1}{3}$, where the K-matrix is $K = \begin{pmatrix} 1 & 2 \\ 2 & 1 \end{pmatrix} = \begin{pmatrix} 3 & 2 \\ 2 & 3 \end{pmatrix} - \begin{pmatrix} 2 & 0 \\ 0 & 2 \end{pmatrix}$. Such work has already begun through a project together with the group headed by Joost Slingerland at Maynooth University.

The non-chiral nature of the $\nu = \frac{2}{3}$ state has a direct consequence for the CFT wave function: The $K = \kappa - \bar{\kappa}$ construction will not be restricted to lay only in the LLL. The CFT wave function is the best pictured as as a wave function in the guiding centre coordinates of coherent states rather than as a wave function in electron coordinates. Integrating over these coherent states then becomes the same as projecting to the LLL and hence for the chiral states – such as the Laughlin states – nothing happens. However if the Landau orbitals would be non-isotropic, then the coherent states would also be different. A convolution with these alternative coherent states would produce a different, non-isotropic Laughlin wave function. This type of analysis ties into the work of Haldane, who explores the possibility of writing the FQHE in a geometry where the Landau orbitals have a different shape than the ones usually considered[Hal11].

Further research could investigate how to practically perform the coherent state projection. One way would be to numerically perform the CS integration to obtain a numerical wave function. Such an approach has been stated by the Slingerland group. Another interesting possibility based on the Z_n expansion from **Paper IV** is to analytically perform the integration by formulating the projected wave function directly in a Fock basis. The integrals that appear are tractable to perform and yields a wave function in the LLL. However, the analytical form of this function is horrendously complicated and there is no obvious way to reformulate it as a sum of Slater determinant. The question remains whether this type of wave function can still be evaluated efficiently.

Another direct generalisation would be to also include quasi-particles and quasi-holes into the wave functions. This should be fairly straight forward to implement since the machinery to evaluate the CFT correlation functions is already in place.

Appendix A

Jacobi Theta Functions and some Relations

All LLL wave functions can be written as a Gaussian part and a holomorphic function. On the torus, which is quasi two-dimensional, an natural set of functions suitable for this purpose are the Jacobi ϑ-functions. In this appendix, we summarize the main properties of these functions that will be used throughout the main text. The generalized Jacobi ϑ-function is defined as

$$\vartheta\left[\begin{array}{c} a \\ b \end{array}\right](z|\tau) = \sum_{k=-\infty}^{\infty} e^{\imath\pi\tau(k+a)^2} e^{\imath 2\pi(k+a)(z+b)} \tag{A.1}$$

where $\Im(\tau) > 0$ for convergence. The zeros of (A.1) are located at

$$z = \frac{1}{2} + m - b + \left(\frac{1}{2} + n - a\right)\tau. \tag{A.2}$$

The ϑ-function has two real parameters a and b that fulfil

$$\vartheta\left[\begin{array}{c} a+1 \\ b \end{array}\right](z|\tau) = \vartheta\left[\begin{array}{c} a \\ b \end{array}\right](z|\tau) \tag{A.3}$$

and

$$\vartheta\left[\begin{array}{c} a \\ b+c \end{array}\right](z|\tau) = \vartheta\left[\begin{array}{c} a \\ b \end{array}\right](z+c|\tau) \tag{A.4}$$

The two main periodic properties are

$$\vartheta\left[\begin{array}{c} a \\ b \end{array}\right](z+n|\tau) = e^{\imath 2\pi a n}\vartheta\left[\begin{array}{c} a \\ b \end{array}\right](z|\tau) \tag{A.5}$$

where $n \in \mathbb{Z}$ and

$$\vartheta\left[\begin{array}{c} a \\ b \end{array}\right](z+c\tau|\tau) = e^{-\imath 2\pi c(z+b)} e^{-\imath\pi\tau c^2}\vartheta\left[\begin{array}{c} a+c \\ b \end{array}\right](z|\tau) \tag{A.6}$$

where $c \in \mathbb{R}$. Under transformations of the lattice parameter τ the relations are

$$\vartheta\left[\begin{array}{c} a \\ b \end{array}\right](z|\tau+n) = e^{-\imath\pi a(1+a)n}\vartheta\left[\begin{array}{c} a \\ an+\frac{n}{2}+b \end{array}\right](z|\tau) \tag{A.7}$$

where $n \in \mathbb{Z}$. Using the Poisson summation formula

$$\sum_{n\in\mathbb{Z}} e^{-\pi an^2+bn} = \frac{1}{\sqrt{a}}\sum_{k\in\mathbb{Z}} e^{\frac{(b+2\pi\imath k)^2}{4\pi a}} \tag{A.8}$$

we find that under inversion of the lattice parameter $\tau \to -\frac{1}{\tau}$, the transformation is

$$\vartheta\left[\begin{array}{c} a \\ b \end{array}\right]\left(z\middle|-\frac{1}{\tau}\right) = \sqrt{-\imath\tau}e^{\imath\tau\pi z^2}e^{\imath 2\pi ba}\vartheta\left[\begin{array}{c} b \\ -a \end{array}\right](\tau z|\tau) \tag{A.9}$$

There is a simple summation rule under Fourier sums

$$\sum_{r=1}^{N} e^{\imath\frac{2\pi}{N}rs}\vartheta\left[\begin{array}{c} a+\frac{r}{N} \\ b \end{array}\right](z|\tau) = e^{-\imath 2\pi as}\vartheta\left[\begin{array}{c} Na \\ \frac{b+s}{N} \end{array}\right]\left(\frac{z}{N}\middle|\frac{\tau}{N^2}\right) \tag{A.10}$$

We can define four special cases of the parameters a and b that have symmetry properties under $z \to -z$. These functions are

$$\vartheta_1(z|\tau) = \vartheta\left[\begin{array}{c} \frac{1}{2} \\ \frac{1}{2} \end{array}\right](z|\tau) \tag{A.11}$$

$$\vartheta_2(z|\tau) = \vartheta\left[\begin{array}{c} \frac{1}{2} \\ 0 \end{array}\right](z|\tau) \tag{A.12}$$

$$\vartheta_3(z|\tau) = \vartheta\left[\begin{array}{c} 0 \\ 0 \end{array}\right](z|\tau) \tag{A.13}$$

$$\vartheta_4(z|\tau) = \vartheta\left[\begin{array}{c} 0 \\ \frac{1}{2} \end{array}\right](z|\tau) \tag{A.14}$$

where $\vartheta_1(z|\tau)$ is odd and $\vartheta_{2,3,4}(z|\tau)$ are even.

Appendix B

Different Coordinates and Gauges

This Appendix lists the basic linear relations between the complex coordinates z and $\bar{z}$, the Cartesian coordinates $\tilde{x}$ and $\tilde{y}$ as well as the τ-coordinates x and y.

B.1 Coordinate relations

The complex coordinates are defined in terms of the Cartesian coordinates as

$$\begin{aligned} z &= \tilde{x} + \imath\tilde{y} \\ \bar{z} &= \tilde{x} - \imath\tilde{y}, \end{aligned} \tag{B.1}$$

and in terms of the τ-coordinates as

$$\begin{aligned} z &= L_x\,(x + \tau y) \\ \bar{z} &= L_x\,(x + \bar{\tau} y)\,. \end{aligned} \tag{B.2}$$

The inverted relations are then

$$\begin{aligned} \tilde{x} &= \frac{1}{2}\,(z + \bar{z}) \\ \tilde{y} &= \frac{1}{2\imath}\,(z - \bar{z})\,, \end{aligned} \tag{B.3}$$

and

$$\begin{aligned} x &= \frac{1}{L_x}\frac{\tau\bar{z} - \bar{\tau}z}{\tau - \bar{\tau}} \\ y &= \frac{1}{L_x}\frac{z - \bar{z}}{\tau - \bar{\tau}}. \end{aligned} \tag{B.4}$$

We can also construct the relations between the Cartesian coordinates and the τ-coordinates as

$$\begin{aligned} \tilde{x} &= L_x (x + \tau_1 y) \\ \tilde{y} &= L_x \tau_2 y, \end{aligned} \tag{B.5}$$

with the inverse relation

$$\begin{aligned} x &= \frac{1}{\tau_2 L_x} (\tau_2 \tilde{x} - \tau_1 \tilde{y}) \\ y &= \frac{\tilde{y}}{L_x \tau_2}. \end{aligned} \tag{B.6}$$

B.2 Derivative relations

The coordinates relations above can also be recast in the form of relations between the different derivatives

$$\begin{aligned} \partial_z &= \frac{1}{2} (\partial_{\tilde{x}} - \imath \partial_{\tilde{y}}) \\ \partial_{\bar{z}} &= \frac{1}{2} (\partial_{\tilde{x}} + \imath \partial_{\tilde{y}}), \end{aligned} \tag{B.7}$$

with the inverted relations

$$\begin{aligned} \partial_{\tilde{x}} &= \partial_z + \partial_{\bar{z}} \\ \partial_{\tilde{y}} &= \imath \partial_z - \imath \partial_{\bar{z}}, \end{aligned} \tag{B.8}$$

The connection to the τ-coordinates are

$$\begin{aligned} \partial_z &= \frac{1}{L_x (\tau - \bar{\tau})} (-\bar{\tau} \partial_x + \partial_y) \\ \partial_{\bar{z}} &= \frac{1}{L_x (\tau - \bar{\tau})} (\tau \partial_x - \partial_y), \end{aligned} \tag{B.9}$$

and

$$\partial_x = L_x (\partial_z + \partial_{\bar{z}}) \qquad \partial_y = L_x (\tau \partial_z + \bar{\tau} \partial_{\bar{z}}). \tag{B.10}$$

We can also construct the relations between the Cartesian derivatives and the τ-coordinates derivatives as

$$\begin{aligned} \partial_{\tilde{x}} &= \frac{1}{L_x} \partial_x \\ \partial_{\tilde{y}} &= \frac{1}{\tau_2 L_x} (-\tau_1 \partial_x + \partial_y), \end{aligned} \tag{B.11}$$

with the inverse relation

$$\begin{aligned} \partial_x &= L_x \partial_{\tilde{x}} \\ \partial_y &= L_x (\tau_1 \partial_{\tilde{x}} + \tau_2 \partial_{\tilde{y}}). \end{aligned} \tag{B.12}$$

Appendix C

The Covariant Derivative

In the main text we have been analysing the construction (3.8) where the ∂_z does not act on the exponential part $e^{-\frac{1}{4}|z|^2}$. This is a rather convenient way of writing on the plane, but the relevant operator to consider is the version of ∂_z that acts also on the exponential part. It is this operator that is generalizable to other gauge choices. It is easy enough to pull the derivative back to the left and find the operator in the symmetric gauge to be

$$D_S = \partial_z + \frac{1}{4}\bar{z}.$$

To compute the commutator with the generators of periodic boundary conditions $t(L_x)$ and $t(\tau L_x)$, we need to write these operators in the same gauge. Here we choose to write D_S in the τ-gauge by transforming it first to the Landau gauge with exponential $e^{-\frac{1}{2}\tilde{y}^2}$ as a middle step. The unitary operators that perform this transformation and the one from Landau gauge to τ-gauge are

$$\begin{aligned} O_{S\to L} &= \exp\left(-\imath\frac{1}{2}\tilde{x}\tilde{y}\right) = \exp\left(\frac{1}{8}\left(\bar{z}^2 - z^2\right)\right) \\ O_{L\to\tau} &= \exp\left(\imath\frac{1}{2}\frac{\tau_1}{\tau_2}\tilde{y}^2\right) = \exp\left(\imath\tau_1\pi N_s y^2\right), \end{aligned}$$

such that

$$D_L = O_{S\to L} D_S O_{S\to L}^\dagger = \partial_z + \frac{1}{2}\tilde{x}$$

and

$$D_\tau = O_{L\to\tau} D_L O_{L\to\tau}^\dagger = \partial_z + \frac{L_x}{2}x.$$

From (4.9) we find the generators of boundary conditions to be $t(L_x) = e^{\partial_x}$ and $t(\tau L_x) = e^{\partial_y + \imath 2\pi N_s x}$ and the commutations relations with these are

$$\begin{aligned} \left[t\left(L_x\right), D_\tau\right] &= \frac{L_x}{2} t\left(L_x\right) \\ \left[t(\tau L_x), D_\tau\right] &= \frac{\bar{\tau}L_x}{2} t(\tau L_x). \end{aligned}$$

Since these commutators are not zero, we can casually state that "∂_z does not commute with the boundary conditions". From a qualitative point of view, this is a reasonable statement, since D_τ does not commute with the boundary conditions either. In fact, it is straight forward to show that for a generic translation $t(\omega)$, then

$$[t(\omega)\,, D_\tau] = \bar{\omega} t(\omega)\,, \tag{C.1}$$

which means that there exists no translation direction that commutes with the derivative operator.

In hindsight we can understand why (C.1) looks the way it does. We know that D_τ is the projection of $\bar{z}$ such that

$$D_\tau f_{LLL}(z) = \mathcal{P}_{\mathrm{LLL}} \bar{z} f_{LLL}(z)\,,$$

where f_{LLL} is a LLL wave function. Since the translation operators commute with the projection operator $[t(\omega)\,, \mathcal{P}_{\mathrm{LLL}}] = 0$, the commutation relation $[t(\omega)\,, \bar{z}]$ will be preserved during the projection. Indeed, we find that $[t(\omega)\,, \bar{z}] = \bar{\omega} t(\omega)$, which is the same as (C.1).

Bibliography

[ASW84] D. Arovas, J. R. Schrieffer, and F. Wilczek. Fractional statistics and the quantum hall effect. *Phys. Rev. Lett.*, 53:722, 1984.

[ASZ95] J. E. Avron, R. Seiler, and P. G. Zograf. Viscosity of quantum hall fluids. *Phys. Rev. Lett.*, 75:697–700, 1995.

[Ber84] M. Berry. Quantal phase factors accompanying adiabatic changes. *Proc. R. Soc. Lond. A*, (392):45–57, 1984.

[BGN11] P. Bonderson, V. Gurarie, and C. Nayak. Plasma analogy and non-abelian statistics for ising-type quantum hall states. *Phys. Rev. B*, 83:075303, 2011.

[BH08] B. Andrei Bernevig and F. D. M. Haldane. Model fractional quantum hall states and jack polynomials. *Phys. Rev. Lett.*, 100:246802, 2008.

[BK06] E. J. Bergholtz and A. Karlhede. 'one-dimensional' theory of the quantum hall system. *J. Stat. Mech.-Theory E.*, 2006(04):L04001, 2006.

[BK08] E. J. Bergholtz and A. Karlhede. Quantum hall system in tao-thouless limit. *Phys. Rev. B*, 77:155308, 2008.

[FHS14] M. Fremling, T. H. Hansson, and J. Suorsa. Hall viscosity of hierarchical quantum hall states. *Phys. Rev. B*, 89:125303, 2014.

[Fre13a] M. Fremling. Coherent state wave functions on a torus with a constant magnetic field. *J. Phys. A*, 46:275302, 2013.

[Fre13b] Mikael Fremling. *Coherent State Wave Functions on the Torus.* Licentiate thesis, Stockholm University, May 2013.

[GJ84] S. M. Girvin and T. Jach. Formalism for the quantum hall effect: Hilbert space of analytic functions. *Phys. Rev. B*, 29:5617, 1984.

[Hal79] E. H. Hall. On a new action of the magnet on electric currents. *Am. J. Math.*, 2:287, 1879.

[Hal83a] F. D. M. Haldane. Fractional quantization of the hall effect: A hierarchy of incompressible quantum fluid states. *Phys. Rev. Lett.*, 51:605, 1983.

[Hal83b] B. I. Halperin. Theory of the quantized hall conductance. *Helv. Phys. Acta*, 56:75, 1983.

[Hal85] F. D. M. Haldane. Many-particle translational symmetries of two-dimensional electrons at rational landau-level filling. *Phys. Rev. Lett.*, 55:2095, 1985.

[Hal91] F. D. M. Haldane. "fractional statistics" in arbitrary dimensions: A generalization of the pauli principle. *Phys. Rev. Lett.*, 67:937–940, 1991.

[Hal11] F. D. M. Haldane. Geometrical description of the fractional quantum hall effect. *Phys. Rev. Lett.*, 107:116801, 2011.

[HHV09] T. H. Hansson, M. Hermanns, and S. Viefers. Quantum hall quasi-electron operators in conformal field theory. *Phys. Rev. B*, 80:165330, 2009.

[HR85] F. D. M. Haldane and E. H. Rezayi. Periodic laughlin-jastrow wave functions for the fractional quantized hall effect. *Phys. Rev. B*, 31(4):2529, 1985.

[HSB+08] M. Hermanns, J. Suorsa, E. J. Bergholtz, T. H. Hansson, and A. Karlhede. Quantum hall wave functions on the torus. *Phys. Rev. B*, 77(12):125321, 2008.

[Jai07] J. K. Jain. *Composite Fermions*. Cambridge University Press, 2007.

[KDP80] K. v. Klitzing, G. Dorda, and M. Pepper. New method for high-accuracy determination of the fine-structure constant based on quantized hall resistance. *Phys. Rev. Lett.*, 45:494, 1980.

[Kit03] A. Yu. Kitaev. Fault-tolerant quantum computation by anyons. *Annals of Physics*, 303(1):2 – 30, 2003.

[Kit09] A. Kitaev. Periodic table for topological insulators and superconductors. In V. Lebedev and M. Feigel'Man, editors, *American Institute of Physics Conference Series*, volume 1134 of *American Institute of Physics Conference Series*, pages 22–30, 2009.

[KM05] C. L. Kane and E. J. Mele. Quantum spin hall effect in graphene. *Phys. Rev. Lett.*, 95:226801, 2005.

[Kvo13] T. Kvorning. Quantum hall hierarchy in a spherical geometry. *Phys. Rev. B*, 87:195131, 2013.

[KWB+07] M. König, S. Wiedmann, C. Brüne, A. Roth, Ha. Buhmann, L. W. Molenkamp, X.-L. Qi, and S.-C. Zhang. Quantum spin hall insulator state in hgte quantum wells. *Science*, 318(5851):766–770, 2007.

[Lan30] L. Landau. Diamagnetismus der metalle. *Z. Phys.*, 64:629, 1930.

[Lau81] R. B. Laughlin. Quantized hall conductivity in two dimensions. *Phys. Rev. B*, 23:5632, 1981.

[Lau83] R. B. Laughlin. Anomalous quantum hall effect: An incompressible quantum fluid with fractionally charged excitations. *Phys. Rev. Lett.*, 50:1395, 1983.

[LLM00] L. Lapointe, A. Lascoux, and J. Morse. Determinantal expression and recursion for jack polynomials. *electron. J. Comb.*, 7(2):N1–N1, 2000.

[MR91] G. Moore and N. Read. Nonabelions in the fractional quantum hall effect. *Nucl. Phys. B*, 360(2-3):362, 1991.

[NGM+05] K. S. Novoselov, A. K. Geim, S. V. Morozov, D. Jiang, M. I. Katsnelson, I. V. Grigorieva, S. V. Dubonos, and A. A. Firsov. Two-dimensional gas of massless dirac fermions in graphene. *Nature*, 438(7065):197, 2005.

[NJZ+07] K. S. Novoselov, Z. Jiang, Y. Zhang, S. V. Morozov, H. L. Stormer, U. Zeitler, J. C. Maan, G. S. Boebinger, P. Kim, and A. K. Geim. Room-temperature quantum hall effect in graphene. *Science*, 315(5817):1379, 2007.

[oWM14] "General Conference on Weights and Measures". Resolution 1 of the 25th cgpm, 2014.

[RB11] N. Regnault and B. A. Bernevig. Fractional chern insulator. *Phys. Rev. X*, 1:021014, 2011.

[Rea89] N. Read. Order parameter and ginzburg-landau theory for the fractional quantum hall effect. *Phys. Rev. Lett.*, 62:86–89, 1989.

[Rea09] N. Read. Non-abelian adiabatic statistics and hall viscosity in quantum hall states and $p_x + ip_y$ paired superfluids. *Phys. Rev. B*, 79:045308, 2009.

[RGJ08] N. Regnault, M. O. Goerbig, and Th. Jolicoeur. Bridge between abelian and non-abelian fractional quantum hall states. *Phys. Rev. Lett.*, 101:066803, 2008.

[RR11] N. Read and E. H. Rezayi. Hall viscosity, orbital spin, and geometry: Paired superfluids and quantum hall systems. *Phys. Rev. B*, 84:085316, 2011.

[SRCB07] S. H. Simon, E. H. Rezayi, N. R. Cooper, and I. Berdnikov. Construction of a paired wave function for spinless electrons at filling fraction $\nu = 2/5$. *Phys. Rev. B*, 75:075317, 2007.

[SS81] W. P. Su and J. R. Schrieffer. Fractionally charged excitations in charge-density-wave systems with commensurability 3. *Phys. Rev. Lett.*, 46:738–741, 1981.

[Sto92] H.L. Stormer. Two-dimensional electron correlation in high magnetic fields. *Physica B*, 177(1-4):401 – 408, 1992.

[SVH11a] J. Suorsa, S. Viefers, and T. H. Hansson. A general approach to quantum hall hierarchies. *New J. Phys.*, 13(7):075006, 2011.

[SVH11b] J. Suorsa, S. Viefers, and T. H. Hansson. Quasihole condensates in quantum hall liquids. *Phys. Rev. B*, 83:235130, 2011.

[TLAK+10] A. Tzalenchuk, S. Lara-Avila, A. Kalaboukhov, S. Paolillo, M. Syväjärvi, R. Yakimova, O. Kazakova, T. J. B. M. Janssen, V. Fal'Ko, and S. Kubatkin. Towards a quantum resistance standard based on epitaxial graphene. *Nat. Nanotechnol.*, 5:186–189, 2010.

[TSG82] D. C. Tsui, H. L. Stormer, and A. C. Gossard. Two-dimensional magnetotransport in the extreme quantum limit. *Phys. Rev. Lett.*, 48:1559, 1982.

[TT83] R. Tao and D. J. Thouless. Fractional quantization of hall conductance. *Phys. Rev. B*, 28:1142–1144, 1983.

[Wen95] X.-G. Wen. Topological orders and edge excitations in fractional quantum hall states. *Adv. Phys*, 44(5):405, 1995.

[Wik12] E. Wikberg. Nontrivial ground-state degeneracies and generalized fractional excitations in the 1d lattice. *ArXiv e-prints*, October 2012.

[Wit89] E. Witten. Quantum field theory and the jones polynomial. *Commun. Math. Phys.*, 121:351, 1989. 10.1007/BF01217730.

[WPW10] R. L. Willett, L. N. Pfeiffer, and K. W. West. Alternation and interchange of e/4 and e/2 period interference oscillations consistent with filling factor 5/2 non-abelian quasiparticles. *Phys. Rev. B*, 82:205301, 2010.

[WZ91] X. G. Wen and A. Zee. Topological structures, universality classes, and statistics screening in the anyon superfluid. *Phys. Rev. B*, 44:274–284, 1991.

[ZHK89] S. C. Zhang, T. H. Hansson, and S. Kivelson. Effective-field-theory model for the fractional quantum hall effect. *Phys. Rev. Lett.*, 62:82–85, 1989.